GEOLOGICAL SURVEY OF CANADA

OPEN FILE 3787

Wellbore temperature measurements and preliminary interpretation in terms of groundwater movement in the Oak Ridges Moraine, Ontario

A. Taylor, V. Allen, M. Burgees, J. Naufal

1999

Natural Resources Canada Ressources naturelles Canada

Canada

GEOLOGICAL SURVEY OF CANADA

OPEN FILE 3787

Wellbore temperature measurements and preliminary interpretation in terms of groundwater movement in the Oak Ridges Moraine, Ontario

A. Taylor[1], V. Allen[2], M. Burgees[3], J. Naufal[3]

[1]9379 Maryland Drive,
Sidney, BC
V8L 2R5

[2]19617 Somerset Drive,
Pitt Meadows, BC
V3Y 2L4

[3]Terrain Sciences Division,
Geological Survey of Canada,
601 Booth Street,
Ottawa, ON
K1A 0E8

A contribution to the Oak Ridges Hydrogeology Program, Geological Survey of Canada

1999

CONTENTS

Preface

Ground temperatures have been used extensively at the research level to detect sub-surface water flow along faults, vertical water flow between aquifers and rates of percolation and recharge at the surface, etc. Temperature analyses have also been invoked in practical applications such as the detection of water circulation in geothermal resource areas, locating permeable zones in well injection operations, detecting seepage through dams, or to demonstrate degree of groundwater exchange in possible waste landfill. The scales involved in these various projects are local, regional or continental.

This report examines the extent to which precision temperatures might contribute to a multidisciplinary study of the geology and hydrogeology of the Oak Ridges Moraine, an important source of potable water for the northern Greater Toronto Area, Ontario. As a pilot study, precision temperatures were measured in some 38 wells in the Oak Ridges Moraine and examined for some of the classical signatures of groundwater advection and fracture flow, recharge and wellbore flow. There are numerous theoretical, analytic models of such phenomena in the literature, and appropriate theoretical equations were fitted to the observed temperatures to illustrate the level of agreement, and in some cases, to derive directions and rates of flow. These interpretations could be made without knowledge of parameters, such as head or permeability, so are very complementary to traditional hydrogeologic techniques.

Summary

The Oak Ridges Moraine Project is an initiative of the Geological Survey of Canada (GSC) to study the hydrogeology of the Oak Ridges Moraine, a geological structure traversing the north side of Greater Toronto Area used extensively as a source of water for the regions of Peel, York and Durham. From 1993 to 1995, the GSC made some 51 temperature logs on 31 community water level monitoring wells and 7 science holes in the Oak Ridges Moraine to ascertain the contribution that ground temperatures could make to the hydrogeology (Fig. 1.0, Table 1). Ground temperatures have been used extensively at the research level to detect water flow along faults, vertical water flow between aquifers and rates of percolation at the surface, etc. (Appendix C surveys some of the research applications and provides a short bibliography). In this report, the geothermal program is briefly described and the data are provided in graphical form, with some preliminary interpretation and modelling of particular features observed.

The GSC and the Ontario Geological Survey (OGS) drilled several carefully located science holes for multidisciplinary studies, and temperatures in these holes exhibit features that have been mathematically modelled in terms of groundwater movement. In the Region of York, GSC hole 1MC has small steps in the temperature-depth profile (Fig. 1.1) that are characteristic of water flow into a wellbore and up (or down) the wellbore. Modelling of the 1993 data (Figs. 1.2, 1.3) suggests some 12 litres/hour is entering near the bottom of this well, flowing up the wellbore and exiting some 15 metres above (Fig. 1.4). A smaller inflow occurs around the 66 m depth and flows down, leaving the wellbore at 74 m; piezometers located above and below this latter zone give heads that are consistent with this flow direction. At GSC hole 1VD, a small flow moves downward through the wellbore around 107 m, and this is also consistent in direction with piezometer heads. GSC hole

2MC shows evidence of down flow within the wellbore between 123-134 m, also consistent with piezometer heads. At OGS 9315, a pronounced peak in temperatures (Fig. 2.1) has been modelled in terms of a subhorizontal fracture or permeable zone that carries water of surface origin on a seasonal basis. A similar, smaller peak on the 1993 log that is absent on subsequent logs suggests a zone where drilling fluid was absorbed in the drilling of the well. This illustrates how a temperature log taken shortly after drilling can identify fractured or porous zones through this temporary thermal storage effect. All logs on OGS 9316 exhibit a bow-shaped feature extending over a 50-m interval in the temperature profile (Fig. 3.1), a portion of which fits the mathematical model of upwards water movement within the formation at a rate of about 0.6 m/year (Figs. 3.2, 3.5). However, heads from piezometers some 3 km distant suggest downward flow. Figures 3.6 and 3.7 show that temperatures do not fit a model of flow within the borehole (as at 1MC), and the interpretation of the OGS 9316 profile is a local effect.

Despite the success in using community water monitoring wells for such purposes elsewhere, this study found that water wells available to us in the Oak Ridges Moraine area were disturbed by close proximity (metres to tens of metres) to community pumping wells and generally no interpretation of the regional character of the hydrogeology could be attempted. This is unfortunate, since monitoring wells are numerous, widespread and available without cost.

1.0 Introduction

The effect of groundwater flow on the subsurface geothermal regime has long been recognized (see Appendix C and references therein). While not a routine measurement in hydrogeology, ground temperatures have been used extensively at the research level to detect water flow along faults, vertical water flow between aquifers and rates of percolation at the surface, effects of pumping and injection, calculation of aquifer properties, and thermal pollution of groundwater due to discharge of waste heat (or heat pumps) in the ground or lakes. Subsurface temperatures may be used as a tracer for detecting groundwater movement, because heat in the subsurface is transported not only by conduction but also by water movement. Unlike standard hydrological techniques in wells and use of chemical tracers, temperatures of the formations can be measured in cased holes with no direct communication to the aquifer. Temperature measurements have detected regional groundwater flow that would be difficult to detect (or rates too low to measure) by other methods; such very low rates can be calculated solely because precise temperatures can be measured over large depth intervals.

The thermal signature of subsurface water movement is achieved because of the large amount of heat carried by water. The specific heat and thermal capacity of water is large, approximately five times that of rock. If water migrates at rates more than a few millimetres per year over distances of kilometres, it becomes a significant process in thermal transport of heat and is measurable in subsurface temperatures (e.g. Andrews-Speed et al., 1984).

This report contains all the temperature logs measured over 3 seasons (1993-95) on holes in the Regions of York, Peel and Durham, southern Ontario (Fig. 1.0, Table 1), as part of the Geological Survey of Canada's Oak Ridges Hydrogeology Project (Sharpe et al., 1996). Thermal modelling of anomalous thermal features observed in these logs is undertaken for several holes and general comments are tabulated for the others. Appendix B contains examples from the literature of a variety of temperature profiles where anomalies are attributed to hydrological effects. This suggests a variety of applications of ground temperature measurements in hydrogeology, but is not meant to be complete.

1.1 The Oak Ridges Geothermal Program

In 1993-1995, temperature logs were taken in some 37 wells in the Peel, York and Durham region, Ontario (Fig. 1.0). Most wells were holes of opportunity, abandoned test wells drilled in the course of water surveys, but a few were drilled specifically for scientific purposes by the Ontario Geological Survey (OGS) and the Geological Survey of Canada (GSC; Pullan et al., 1994; Sharpe et al., 1994; 1996). In general, the former wells were located in the vicinity of active pumping wells used for community water service, and the temperatures were generally not useful for regional perspectives.

Wells were logged for temperature with in-house equipment. Quasi-continuous logs, that is with measurement depth-intervals of a few centimetres, were run in most holes. In 1993 and 1994, the temperature probe was a digital, self-contained temperature data logger (Brancker Research XL series) with resolutions of 0.006 K (some 1993 logs had less resolution) and a time constant of 2 or 3 seconds; this probe was not designed originally for continuous temperature logging. In 1995, most logs were undertaken with an digital IFG, Inc. logging system, with a resolution less than 0.001 K. Logs were taken as the probe was lowered down the wellbore at a rate of 1.5 m/minute or less. Some logs (e.g. all wells in the Peel region, and logs in York and Durham that have a coarse depth interval) were taken using a manual winch system for which an older style analogue probe was stopped for a minute at about 1-metre intervals and the temperature recorded. This was necessary when the access hole to the well was smaller than the 6 cm diameter XL or 3 cm IFG probes, or for initial logs on a hole of unknown possible obstructions.

Table 1 lists the wells logged by region. Appendix A describes features observed in the temperature profiles that might be attributed to hydrogeological effects. Appendix B contains graphs of the corresponding temperature logs.

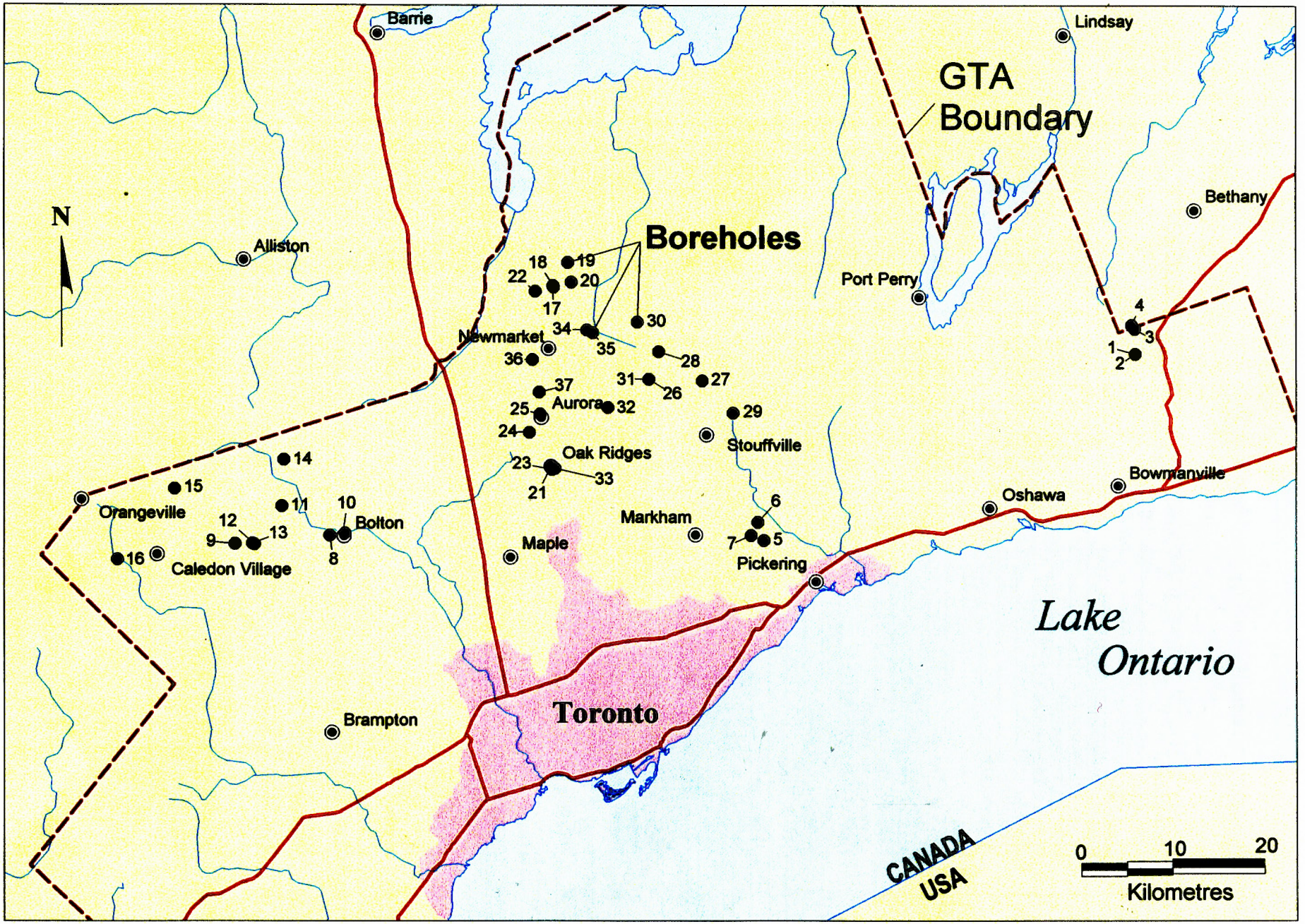

Fig. 1.0 Location of wells logged in Peel, York, and Durham regions, 1993-1995

Table 1. Location and details of wells logged in this study.

Item Number	Name / Number	UTM zone	Northing	Easting	Depth logged (m)	Date
	DURHAM					
1	Ministry of Environment (MOE) W-1	17	4878940	687880	40	11/03/94
2	Ministry of Environment (MOE) W-2	17	4878940	687880	152.1	11/03/94
3	Ministry of Environment (MOE) W-8	17	4881680	687860	195	11/03/94
4	Ministry of Environment (MOE) W-10	17	4882100	687500	195	11/03/94
5	Whitevale P1-16D	17	4858464	647295	58.1	05/15/95
6	Whitevale P1-26D	17	4860433	646626	68.8	05/17/95
7	Whitevale P1-29B	17	4858975	645890	54.6	05/16/95
	PEEL					
8	Bolton #6 - TW1-88	17	4859005	599825	104	08/03/94
9	Caledon East #1 - Granite Stones	17	4858075	589455	56.6	03/08/94
10	Bolton #4 - TW2-72	17	4859250	601455	51.6	08/04/94
11	Centreville - Holly Park	17	4862200	594550	41	08/05/94
12	Caledon East #3 - TW4-77	17	4858020	591545	44.9	08/04/94
13	Caledon East #3 - TW1-77b	17	4858100	591355	39.4	08/04/94
14	Palgrave #2 - TW6-72	17	4867300	594750	46.2	08/04/94
15	Mono Mills #6 - TW2-90	17	4864095	582850	47.6	08/05/94
16	Caledon Well #4	17	4856360	576625	58.7	08/05/94
	YORK					
17	Queensville #8 - Test Well 10A/82	17	4886250	624250	104.8	07/26/94
18	Queensville #7 - Test Well 9-88	17	4886400	624210	104.9	07/26/94
19	Queensville #5 - Test Well 8/88	17	4888930	625800	74.8	07/26/94
20	Queensville #6 - Test Well 2/88	17	4886785	626175	66	07/26/94
21	Oak Ridges Test Well #3	17	4866530	623940	109.1	07/27/94
22	Queensville #9 - Test Well 1/91	17	4885775	622250	105	07/28/94
23	Mitchell	17	4866210	624050	120.1	07/27/94
24	Henderson Road	17	4870300	621600	126.9	07/27/94
					128.4	08/24/93
25	Collis	17	4872350	622750	78.6	07/28/94
26	OGS 93-16	17	4876150	634650	88.6	03/22/95
					91	07/25/94
					89.6	07/16/94
					89.6	09/16/93
27	OGS 93-17	17	4876000	640500	86.5	03/23/95
					89.8	07/13/94
					89.8	09/14/93
28	OGS 93-15	17	4979200	635700	84.8	03/24/95
					83.6	07/11/94
					83.6	09/14/93
29	OGS 93-19	17	4872450	643900	88.7	03/23/95
					89.9	07/12/94
					87.7	09/15/93
30	1MC - McCowan Road (GSC-BH-MSR-01)	17	4882400	633400	107.8	03/22/95
					107.1	07/14/94
31	2MC - McCowan Road (GSC-BH-BAL-01)	17	4876150	634650	155.4	03/22/95
					157	10/13/94
32	1VD - Vandorf Side Road (GSC-BH-VSR-01)	17	4873050	630150	123.9	07/12/94
33	Ozark	17	4866330	624400	92.5	07/13/94
					87.4	09/15/93
34	Bales Road North	17	4881550	627900	55.6	08/24/93
35	Bales Road South	17	4881250	628500	55.1	08/23/93
36	Newmarket Well #2	17	4878320	621920	66.8	08/24/93
37	Aurora #5	17	4874755	622655	93.1	08/26/93

2.0 Models of some temperature profile anomalies that imply groundwater movement

Several temperature-depth profiles were modelled in terms of the effect of water advection within the formation, flow along zones or faults, flow within the wellbore, and storage effects due to drilling. In this section, these temperature profiles are analyzed using simple analytic models found in the literature. Wells drilled in the proving of community water supplies showed thermal features that are probably due to more massive hydrologic effects, i.e. pumping from nearby wells. Numerical hydrogeologic models that include the temperature field might be used on this latter data set, but generally inferences would be of local, rather than regional perspective.

Seven wells are discussed in detail in this section, with graphs illustrating the modelling done. Refer to Appendix B for graphs showing all the logs done on the particular well.

2.1 1MC McCowan Road (GSC-BH-MSR-01)

This 15 cm diameter borehole was instrumented with two access tubes, one of which is 7.5 cm in diameter and extends to near the total depth, and is screened between 90-93 m. The 15 cm borehole was backfilled with sand, with bentonite plugs sealing off the screened interval above and below. Another piezometer tube monitored the head at 44-47 m. The temperature logs were run in the 7.5 cm access tube in summer 1994 and spring 1995. Features common to both logs below 80 m appear to be displaced by about 1.5 m, suggesting some slippage occurred on one log or different ground "zero" points were used (see Appendix B). Both temperature logs show distinct signatures of wellbore flow within two intervals, and possibly of recent warming of the ground surface at the wellhead (Fig. 1.1).

A temperature-depth gradient of 12 mK/m fits the general trend of temperatures at mid-depths, suggesting a lithology of fairly high thermal conductivity; this is consistent with the general sandy lithologic description. The linearity of the profile in this section (except for the wellbore flow features to be discussed below) suggests that the thermal properties of the sands, silty clays and diamicton are nearly identical. A gradient of 32 mK/m is established in the bottom few metres of the hole, suggesting a lower formation of fairly low thermal conductivity. The step-like departures from this slope may be attributed to water entering the wellbore at one level, flowing within the borehole, and out at another. Only the anomalous features in the 1994 log will be discussed in detail.

103 - 89 m: it appears that water flows into the wellbore from the formation near 102 m, and flows up the borehole with further inflow from the formation at 101 and 97 m. Water flows out of the borehole into the formation around 89 m (Fig. 1.1). The shape of the temperature profile between an inflow and another inflow (or an outflow) is directly related to the rate of heat transfer between the moving fluid and the formation surrounding the wellbore. Water comes into the borehole at the temperature of the formation, and the borehole provides a conduit.

Ramey (1962; or see eq. 14 in Mansure and Reiter, 1979) provides an expression for the disturbance to the temperature profile due to water flow within a borehole. This equation has been fitted to the temperatures in the 3 intervals A, B and C (Fig. 1.4) to calculate the wellbore flow in each section. The fitting procedure is demonstrated for interval C (Fig. 1.2); the step-in-temperature nature of the 1994 data results from the limited resolution of the probe (0.007 K). The solid curve is Ramey's equation for the borehole flow giving the best fit ($3.3 \times 10^{-6} m^3/s$). The fit just above the inflow might be improved by specification of a slightly lower formation (inflow) temperature. When the water reaches 89 m, the borehole water still has a temperature in excess of the formation temperature at this point, and since wellbore temperatures return abruptly to near formation temperatures just above 89 m, the flow must exit at this point through the screen. The mathematical model shows that hypothesizing a higher rate of borehole flow (short dashed curve) would result in too large a departure from formation temperatures, while a lower rate (long dashed curve) would create less disturbance than observed.

For the above fit, a thermal conductivity of 3.5 W/mK was specified. No conductivity measurements were made, but this value is typical of silty sands and was estimated by dividing the terrestrial heat flow for the region (40 mWm^{-2}; Jessop et al., 1984) by the geothermal gradient in this section (12 mK/m). Figure 1.3 indicates the sensitivity of the fit, for the same flow rate, to specification of formation thermal conductivity: 2 and 5 W/mK are typical of silty or sandy clays and quartz-rich sands, respectively. Lower conductivity formations would result in less cooling of the wellbore fluid as it moves up the borehole, and hence higher wellbore temperatures, than are observed.

Fits to the wellbore temperatures in intervals A and B are made similarly; by subtraction we can infer the water inflow at intermediate points (Fig. 1.4). In all, about 12 litres per hour is flowing out of the hole near 89 m into the sand aquifer. It appears that no or very little water is flowing within the borehole just above 89 m, since the gradient is undisturbed; this suggests that the upper bentonite plug (about 75-82 m) provides a seal, whereas the lower plug (around 100 m) clearly does not. Also,

3 distinct flows into the well appear below the bottom of the screened interval, suggesting the bottom plug of the access tube and lower joint may leak, or that there is flow within the sand-filled annulus.

The calculated flow rates may vary by 50% depending on the value of thermal diffusivity chosen (see discussion for OGS 9315). Also, Ramey's theory is for unobstructed flow in a single hole. This hole contains access tubes surrounded by sand, so the geometry and possible flow paths through the sand are considerably different from Ramey's model.

66 - 74 m: water flows into the hole near 66 m from the sand aquifer, lowering temperatures slightly, flows down the borehole, and leaves the borehole around 73 m (top of the bentonite plug) at the silty clay/diamicton interface, where there is a small, sharp increase in temperature to the background gradient (Fig. 1.1). The 1995 log does not indicate this flow (Appendix B). Because of the limited temperature resolution, this borehole flow has not been modelled, however, it is less than the upward flow detected in the deeper interval. Notice that the temperature signature for flow down the wellbore is the opposite of that for flow up the borehole.

Piezometers were installed at 91 m and 45 m. The total heads measured at four dates in 1994 are 6 m greater at 45 m than at 90 m, suggesting a downward flow between these depths. Note that this is consistent with the geothermal interpretation of downward flow between 66-74 m. The upward wellbore flow between 103-89 m occurs deeper than the lower piezometer installed at 90 m, so there is no relative head information to confirm this interpretation.

10 m to 55+ m: the temperature profile in this interval represents two temperature inversions that probably arose from recent changes in ground surface temperature (Fig. 1.1). In the July 1994 temperature log, the variation to 10 m below the water table is recording the past winter and preceding summer air temperatures that have diffused downwards from the surface. The temperature inversion between 55 m and about 30 m may result from an increase in ground surface temperature around 1988 (clearing of site?).

FIGURE CAPTIONS for 1MC

Fig. 1.1 1MC, McCowan Road, July 1994 log with lithology. Geothermal gradient lines reflect temperature gradients appropriate to the lithology and serve to show

temperature departures caused by water flow into and out of the borehole, as indicated.

Fig. 1.2 1MC, fit of Ramey's (1962) model for upward flow of water within the borehole, and sensitivity to hypothesized higher and lower rates of borehole flow. At depths above 97 m, temperatures measured in the wellbore are higher than the formation because of the movement of water up the borehole. Best fit suggests a flow rate of $3.3 \times 10^{-6} m^3/s$ (12 litres per hour).

Fig. 1.3 1MC, sensitivity of Ramey's model to choice of thermal conductivity, assuming the same flow rate. This shows that temperatures measured in this interval would be even higher in a clay or shale lithology because of the reduced capacity of low conductivity formations to conduct away the excess heat being carried upwards by the water.

Fig. 1.4 1MC, summary of the wellbore flow regime below 89 m. Flows into the wellbore 103-89 m accumulate and exit the wellbore just below 89 m. The upper bentonite seal is at 78-82 m.

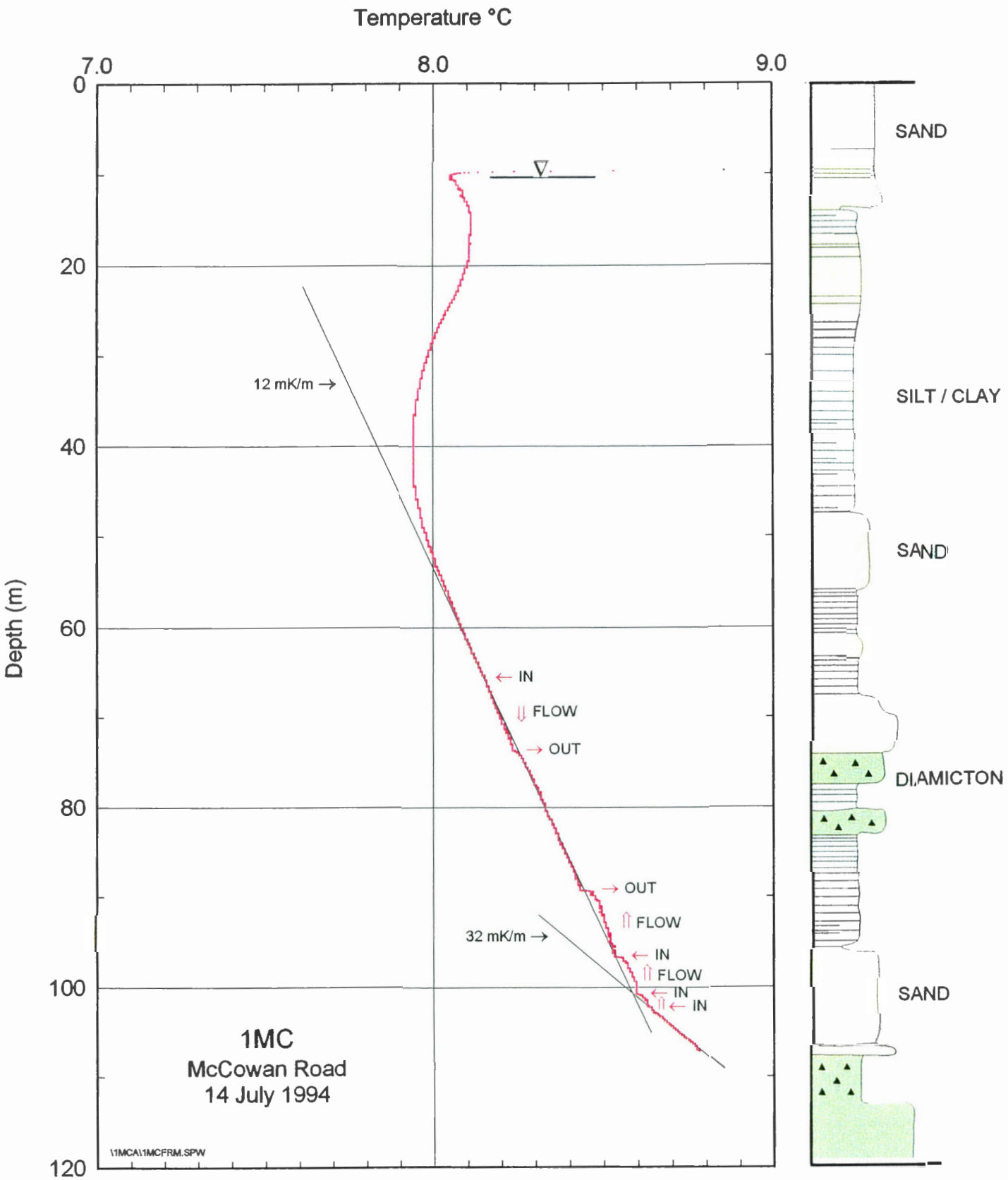
Temperature °C
7.0
8.0
9.0
0
20
40
60
80
100
120
Depth (m)
12 mK/m →
32 mK/m →
← IN
⇓ FLOW
→ OUT
→ OUT
⇑ FLOW
← IN
⇑ FLOW
← IN
⇑ ← IN
1MC
McCowan Road
14 July 1994
\1MCA\1MCFRM.SPW
SAND
SILT / CLAY
SAND
DIAMICTON
SAND

FIG. 1.1

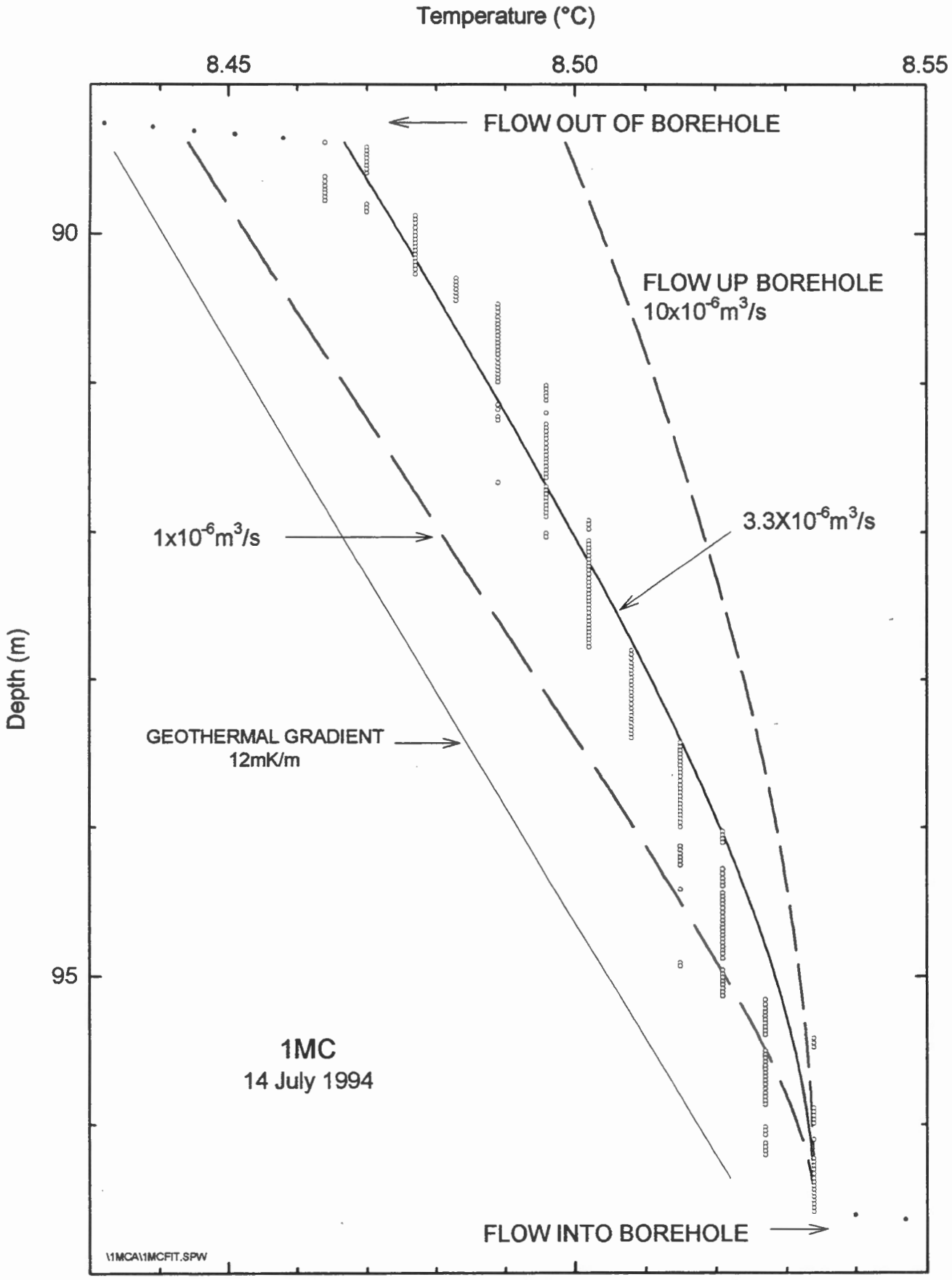
Temperature (°C)
8.45
8.50
8.55
FLOW OUT OF BOREHOLE
90
FLOW UP BOREHOLE
10x10-6m3/s
1x10-6m3/s
3.3X10-6m3/s
Depth (m)
GEOTHERMAL GRADIENT
12mK/m
95
1MC
14 July 1994
FLOW INTO BOREHOLE
\1MCA\1MCFIT.SPW

FIG. 1.2

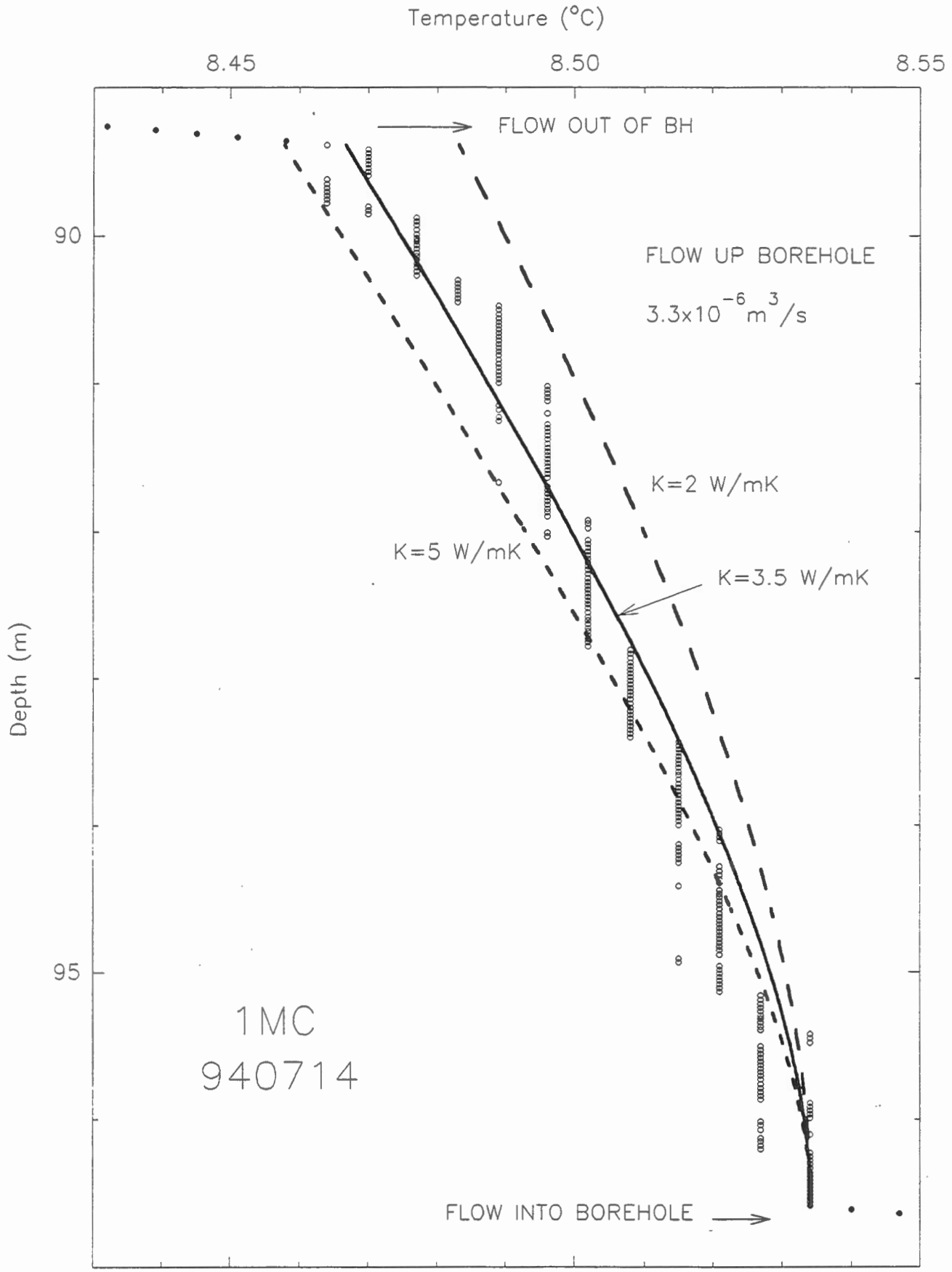

FIG 1.3

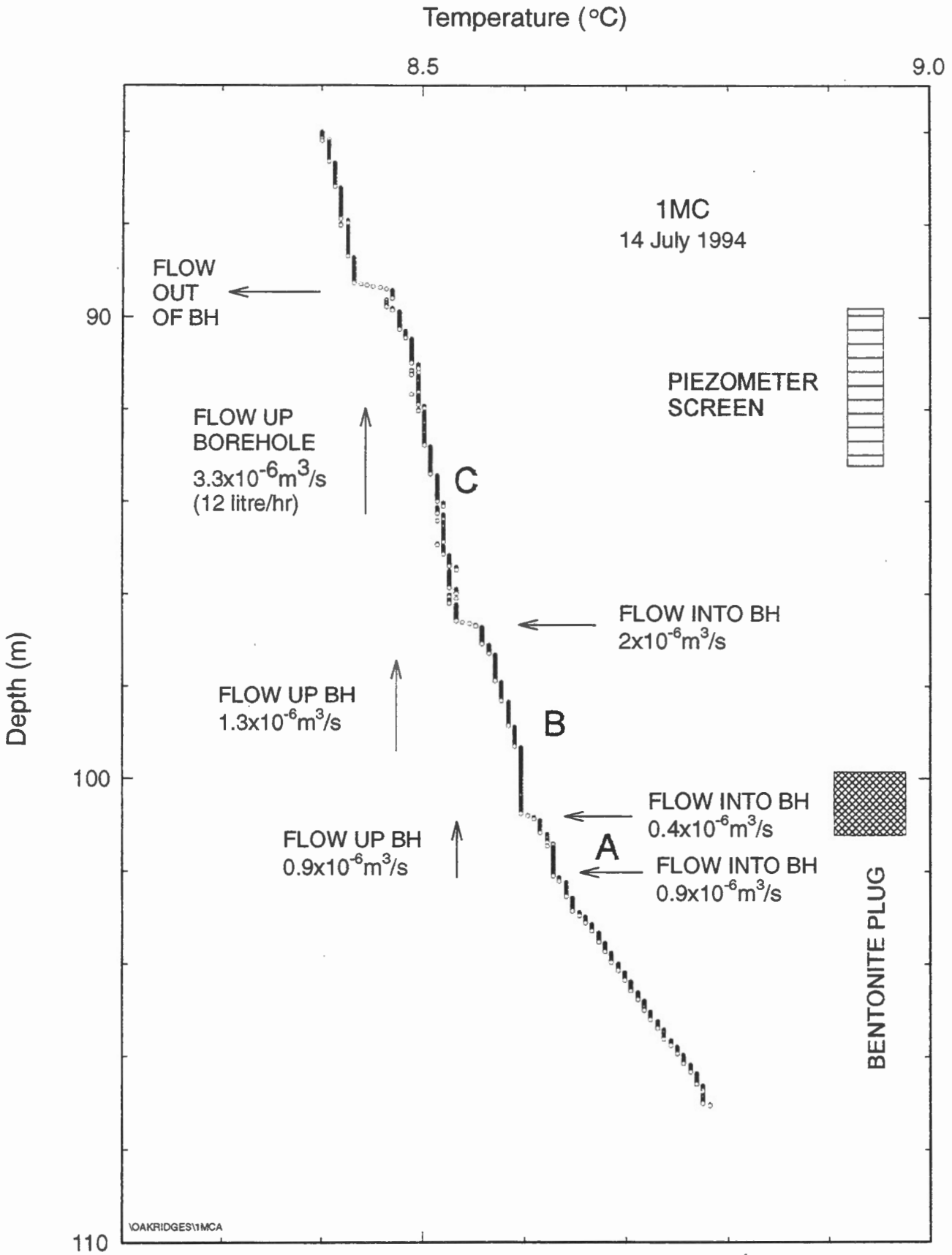
Temperature (°C)
8.5
9.0
1MC
14 July 1994
FLOW OUT OF BH
FLOW UP BOREHOLE
3.3x10-6m3/s
(12 litre/hr)
C
PIEZOMETER SCREEN
FLOW INTO BH
2x10-6m3/s
FLOW UP BH
1.3x10-6m3/s
B
FLOW INTO BH
0.4x10-6m3/s
FLOW UP BH
0.9x10-6m3/s
A
FLOW INTO BH
0.9x10-6m3/s
BENTONITE PLUG
Depth (m)
90
100
110
\OAKRIDGES\1MCA

FIG. 1.4

2.2 OGS9315

Four logs were taken on this well between 1993 and 1995 (Pullan et al., 1994; see Appendix A, one log is not shown). Figure 2.1 shows the four logs offset from one another for clarity. The coarse digital resolution of temperature (0.02 K) for the 1993 and the July 1994 logs results from the particular probe used; the other two logs were taken with probes having resolutions 5-10 times better than this. Below 40 m, the four temperature logs are very similar, with a temperature-depth gradient of 8.2 mK/m, which persists to the bottom of the hole. If we assume that this is the geothermal gradient, then for a regional terrestrial heat flow of approximately 40 mWm^{-2} (Jessop et al., 1984), this gradient implies a moderately high thermal conductivity (5 W/mK) for the silty, sandy diamicton encountered below 43 m.

The temperature logs on this hole (and those at OGS9317 and OGS9319, some 5.2 km and 9 km to the southeast, respectively, see Appendix B) show features that might be attributed (a) to transient flow along a geological contact or (b) to the transient storage of heat in a porous zone following drilling.

Anomaly around 17 m: this major feature appears as a temperature peak and occurs in a silty, very fine sand interval (16 m at OGS9317 and OGS9319), and temperatures decrease both above and below this peak (Fig. 2.1). At about 40 m, temperatures approach asymptotically the geothermal gradient.

The character of this anomalous feature suggests onset of flow of water along a thin subhorizontal permeable zone. Following the theory developed by Bodvarsson (1973, eq. 2-4), initiation of a flow introduces a temperature anomaly which gradually diffuses vertically into the formation above and below, increasing the width with time but maintaining the amplitude of the peak.

For this data, the width appears to vary little from one log to another, but the amplitude is slightly smaller on the spring logs, and the contrast to the sharper summer peaks suggests that the causative event is repeated seasonally (Fig. 2.1). The amplitude on the summer logs is about 0.35 K above the geothermal gradient extrapolated from the deeper temperatures.

Two modelling strategies were tested on the 1993 profile. (1) a thermal diffusivity of $1x10^{-6}$ m^2/s, generally typical of rock, was used with Bodvarsson's theory to model for the curvature below the

peak. Modelling the September 1993 profile suggests the flow started about 1.7 years before the measurement (i.e. early 1992, Fig. 2.2). The curved section of profile above 17 m might be analyzed similarly, but the proximity to the water table results in seasonal effects extending into the zone of interest; Ziagos and Blackwell (1981) give a more refined theory for this portion due to its proximity to the surface. Modelling the July 1994 log taken a year later yielded a similar time (1.75 years), suggesting the originating event occurred in early 1993 (not 1992). This presents a causal conundrum if a single event associated with drilling the well is assumed, but confirms the visual impression that there is little difference between the spring/summer curve sets for the two years and that a seasonal cause is more likely. (2) a thermal diffusivity of 2×10^{-6} m^2/s is used in the theory: this is somewhat higher than expected for geologic material but consistent with a convective contribution to heat transfer that might be induced by the higher temperature gradient (22 mK/m) within the peak region. This yielded an onset time for the flow of about 0.8 years before the logs were measured, a time that is acceptable to a seasonal event. The fit and bracketing times for this model are shown in Fig. 2.3.

The geological interpretation is that some water (the theory does not provide the magnitude) flows along a permeable horizon and repeats annually, increasing in temperature in the spring to create a (maximum?) peak each summer. We might conjecture that every fall the peak dissipates. Peak temperatures are greater than the geotherm, suggesting a surface origin for the water.

The geophysical logs provide some support (Pullan et al., 1994). In OGS9315, -17 and -19, the peak of the temperature anomaly occurs in a local minimum in the density log, and in OGS9315 and -19, the peak lies in a low electrical conductivity zone. These log responses suggest a porous zone that might allow fluid flow in a sub-horizontal sense.

Anomaly at 21 and 30 m: the small temperature anomalies ("spikes" towards lower temperatures) in 1993 are somewhat larger in 1994 and absent in 1995 (Appendix B, and Fig. 2.1). Possibly a seasonal flow effect, similar to the major anomaly at 17 m.

Anomaly at 37 m: Amplitude is 0.1 K in 1993 log, but anomaly has disappeared by 1994 (Fig. 2.1). This suggests the thermal storage of drilling fluid. Drilling fluid at a temperature different from the formation temperature may have invaded a porous zone at 37 m while drilling the hole, and the excess temperature dissipates with time. For this scenario, the form of the anomaly expected from theory is a spike, the amplitude of which decreases with time and the width increases with time; the

peak would disappear eventually. The analysis is different from that used at 17 m and requires estimates of the duration of drilling times, fluid temperatures and the quantity of fluid that invaded the fractured or porous zone (e.g. Drury et al., 1984); it will not be attempted here because of lack of estimates of these parameters.

This feature occurs in a very fine to fine sand unit; the geophysical logs show no particular signatures that correlate with this temperature anomaly. This example illustrates how temperature logs shortly after a hole is drilled may detect unusually permeable, porous or fractured zones through storage of a drilling fluid at a temperature different from the formation; such zones may not be detected otherwise if they are not transporting groundwater.

FIGURE CAPTIONS for OGS9315

Fig. 2.1 OGS9315, summer and following spring logs, two successive years; logs are offset from one another for clarity. Difference in temperature resolution arises from the probes used. Geothermal gradient line extrapolated from deeper temperatures (for 930914) shows temperature anomaly attributed to either thermal storage initiated during drilling or recent initiation of flow along a thin permeable zone.

Fig. 2.2 OGS9315, models of the thermal effect of subhorizontal water flow along the horizon "A", after Bodvarsson (1973). A thermal diffusivity value of $1x10^{-6}m^2s^{-1}$, typical of rock, was used in the calculations shown here, which gave onset times that are too large considering similar features on the later logs.

Fig. 2.3 As above, but models using a thermal diffusivity value of $2x10^{-6}m^2s^{-1}$ that would imply some thermal convection as well as conduction. A higher thermal diffusivity value is required to force a "seasonal" fit (see text).

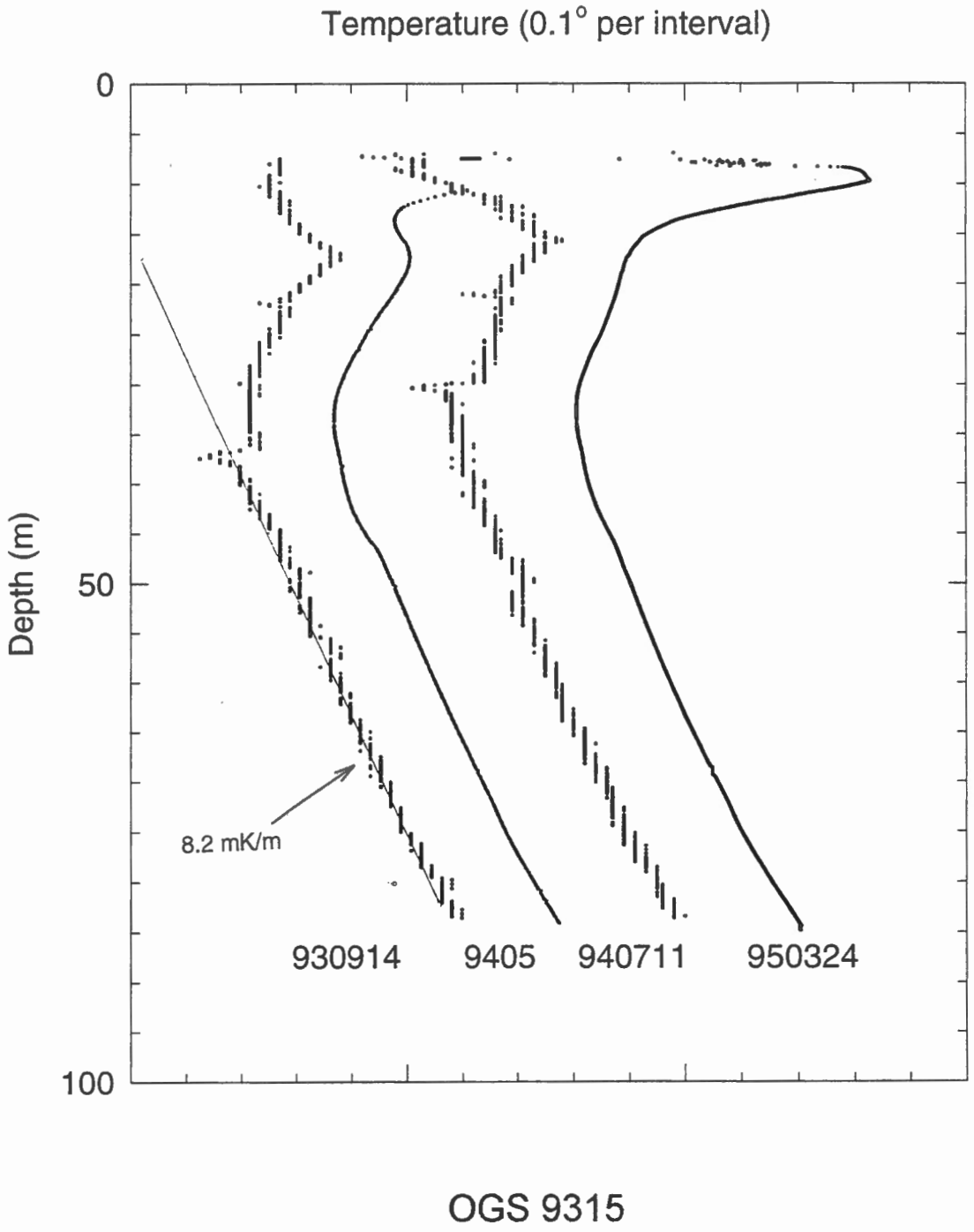

OGS 9315

\YORK\9315RPT.SPW

FIG. 2.1

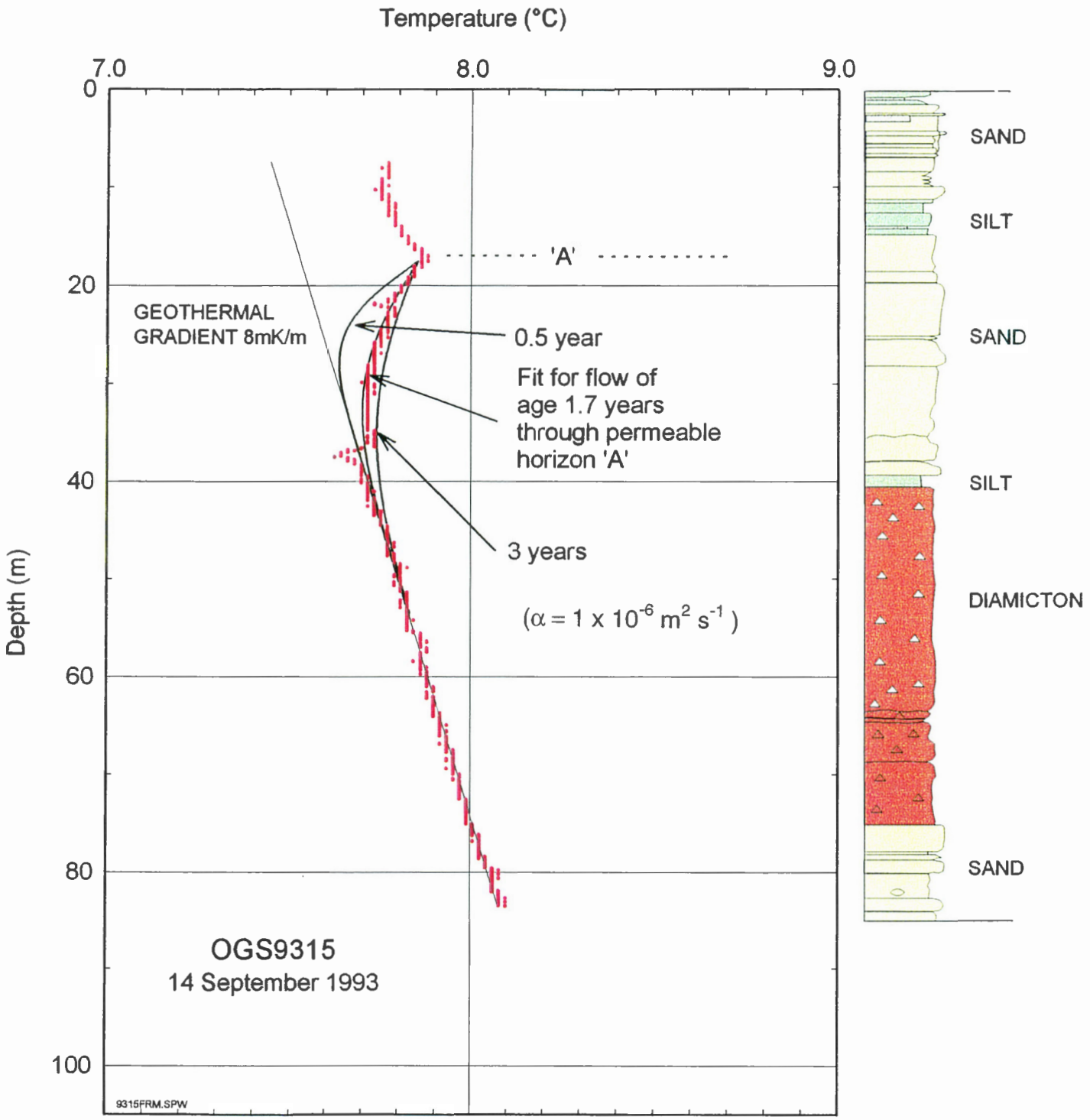
Temperature (°C)
7.0
8.0
9.0
0
20
40
60
80
100
Depth (m)
'A'
GEOTHERMAL
GRADIENT 8mK/m
0.5 year
Fit for flow of
age 1.7 years
through permeable
horizon 'A'
3 years
(α = 1 x 10-6 m2 s-1)
OGS9315
14 September 1993
9315FRM.SPW
SAND
SILT
SAND
SILT
DIAMICTON
SAND

FIG. 2.2

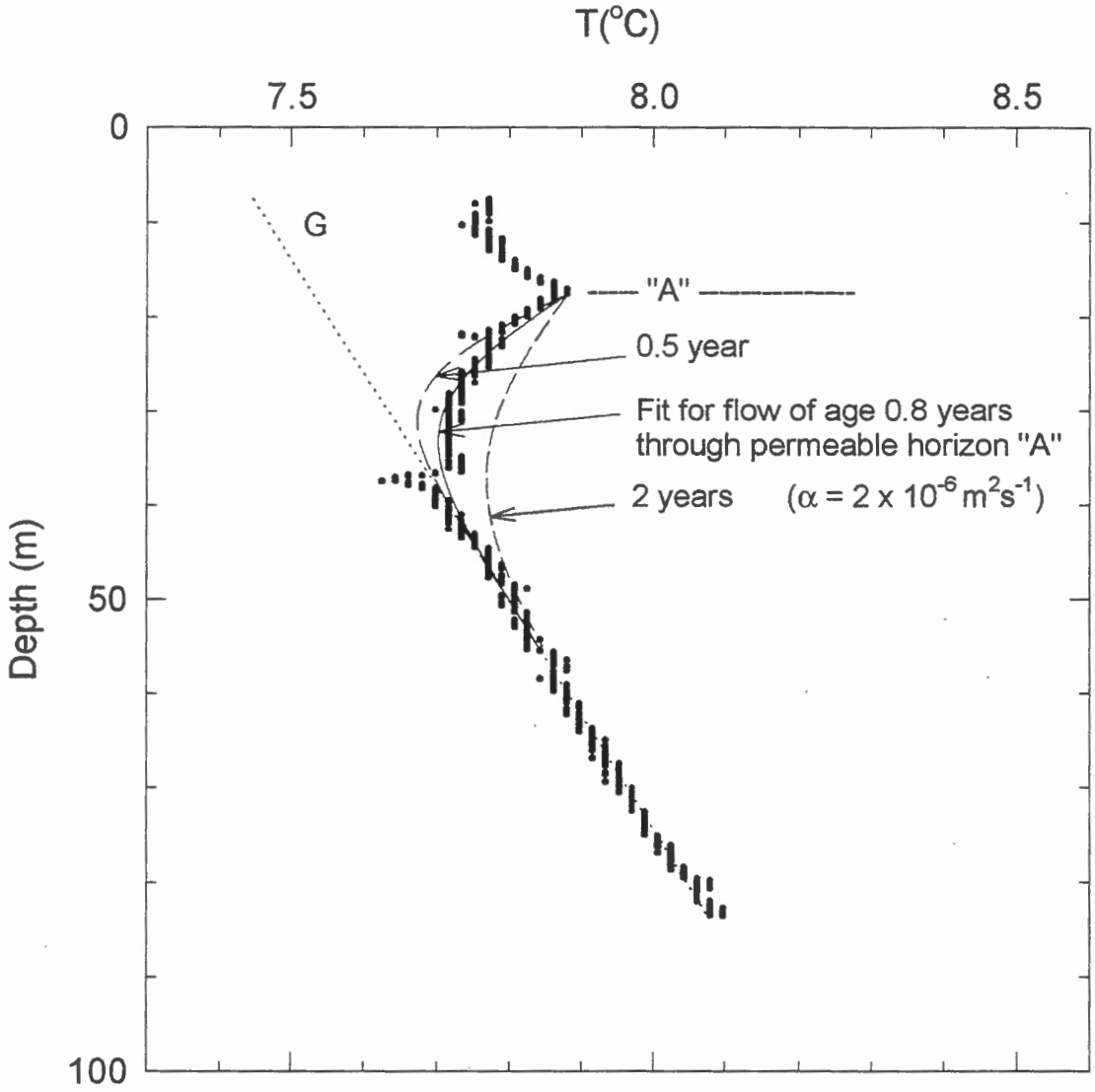

Temperature models for flow in fracture
OGS 9315 - 930914

\oakridgs.rpt\york\9315c spw

FIG. 2.3

2.3 OGS9316

Four logs were taken on this hole (Pullan et al., 1994; Appendix B); small differences in temperature from one log to another probably arise from variability in the absolute calibration of the temperature probes used. Except for near-surface seasonal variations, temperatures above 20 m and below 75 m have a common linear trend that is interpreted as the geothermal gradient (13 mK/m; Fig. 3.1). The thermal conductivity implied from the assumed value of terrestrial heat flux (40 mWm^{-2}, Jessop et al., 1984) is 3 W/mK, typical of the medium to fine sands reported.

Bow-shaped anomaly, 20-77 m. Bredehoeft and Papadopulos (1965) developed a theory that attributed such curvature to the upward movement of groundwater through a semi-confining layer separating aquifers. The effect is such that at a particular depth, temperatures are higher than expected, based on the geothermal gradient (downward flow would lower the temperatures and create a concave-upwards bow feature in the temperature profile). Where such a formation flow exists, the theory indicates that a plot of temperature-depth gradient versus temperature is linear, with a slope proportional to the rate of water movement (e.g. Mansure and Reiter, 1979, eq. 5). In Figure 3.2, such a plot is linear between 6.6°C and 7.2°C (about 20-60 m) and non-linear outside this interval; an upward flow of 0.6 m/year is calculated from the slope. Similar plots for the 1994 and 1995 logs also exhibit linear sections (Figs. 3.3, 3.4). Alternatively, the theoretical equation may be fitted directly to the measured temperatures (Fig. 3.5), showing an excellent fit to the data and giving a similar advection rate. Note that the calculation gives the vertical component of the flow through this zone; there probably is a horizontal component, but this is unlikely to show up thermally (see the two-dimensional theory developed by Lu and Ge, 1996).

The theoretical model indicates that the anomalous temperatures develop due to flow from one aquifer to another, through a less pervious lithology. In this well, the lithology of the bow interval consists of silty very fine sand to very fine sand rhythmite sets and clay caps; massive, loose very fine sand lies above it (<32 m) and a silty clay unit lies below (>60 m). Fine to medium sand with heavy mineral laminations lies deeper (>75 m). Qualitatively, the silty very fine sand rhythmites of the bow interval may be less pervious than the loose very fine to medium sands lying above and the silty clay unit below, creating a semi-confining layer separating two aquifers.

According to this model, the temperature anomaly implies that the head in the lower aquifer below 61 m is higher than in the upper aquifer above 31 m, such that water is forced upwards through the

semi-confining zone. However, piezometers were installed in hole 2MC at 37 m and 92 m (adjacent to OGS9316), and the head is lower at the greater depth, requiring a net downwards flow contrary to the geothermal interpretation at OGS9316. This discrepancy remains unexplained; however, we look for alternate explanations of the bow-shaped feature.

Effect of thermal conductivity variation: The bow-shaped section reflects a monotonic decrease of temperature gradient with depth that might be attributed to an increase in thermal conductivity. Measurements of thermal properties were not made. However, the average temperature gradients between 20-30 m (20 mK/m) and 60-70 m (9.5 mK/m) imply conductivity values of about 2 and 4.2 W/mK, respectively, opposite in sense to that typical of the described lithology: i.e., the upper sand would be expected to have a higher thermal conductivity than the lower silty clay and silt. Hence, it is unlikely the bow-shape arises from a gradual variation in thermal conductivity. If conductivity data were available, the previous analysis could be normalized for the effect of conductivity variations by considering a thermal depth rather than depth (e.g. Jessop, 1990) or by using the plot of apparent heat flow (temperature gradient x thermal conductivity) versus temperature (Reiter et al., 1989).

Upward flow of water within the wellbore: There are two difficulties with this hypothesis to explain the bow-shape. First, there is no visible signature on the temperature logs of water flow into (or out of) the well (see discussion on 1MC, above). Second, the shape of the bow nowhere approximates that expected for flow up the wellbore, based on Ramey's (1962) theory. Assuming an inflow at the base of the bow section, for instance, theory predicts wellbore temperatures that do not match the temperatures measured (Fig. 3.6-3.7).

FIGURE CAPTIONS for OGS9316

Fig. 3.1 OGS9316, four temperature logs offset for clarity. Geothermal line reflects a temperature gradient appropriate to the silts and silty-sand lithology, and serves to show the temperature departure (bow shaped feature) that is attributed to upward flow of water through the formation.

Fig. 3.2 OGS9316, temperature-depth gradient versus temperature, 1993 log. The section of the hole where the plot is linear is a signature of vertical flow within this section, of

a magnitude proportional to the slope, with a negative slope implying flow upwards (after Mansure and Reiter, 1979).

Fig. 3.3 As above, 1994 log.

Fig. 3.4 As above, 1995 log.

Fig. 3.5 OGS 9316. Mathematical fit (solid line) of Bredehoeft and Papadopoulos (1965) theory for vertical advection of groundwater through a semi-confining layer between two aquifers to the data (points).

Fig. 3.6 OGS 9316. Ramey's (1962) theory for flow of water upwards within the wellbore, at 3 rates, to show lack of fit of such wellbore flow to the data.

Fig. 3.7 As above, detail of the lack of model fit to the data.

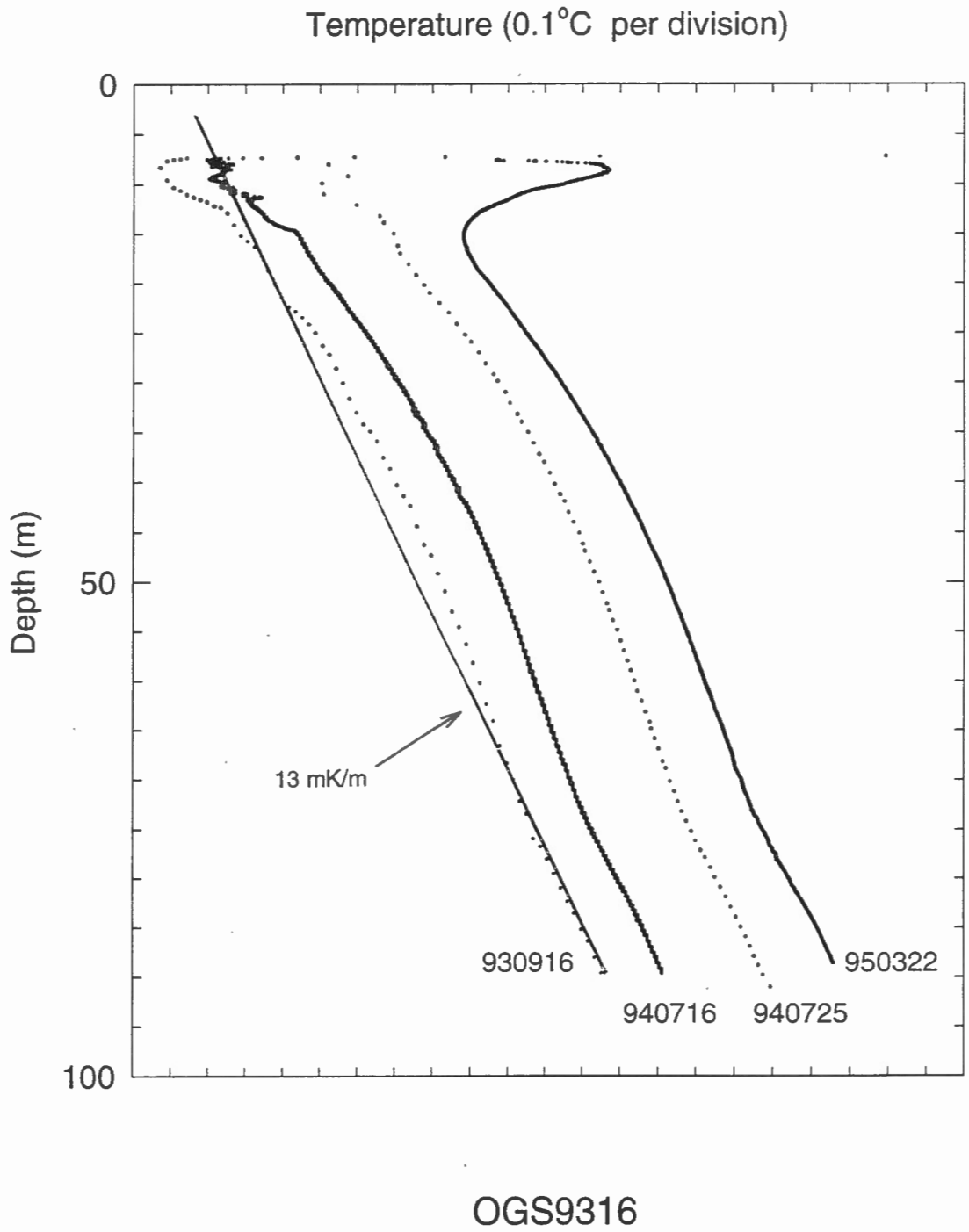

\OAKRDG\9316RPT2.SPW

FIG. 3.1

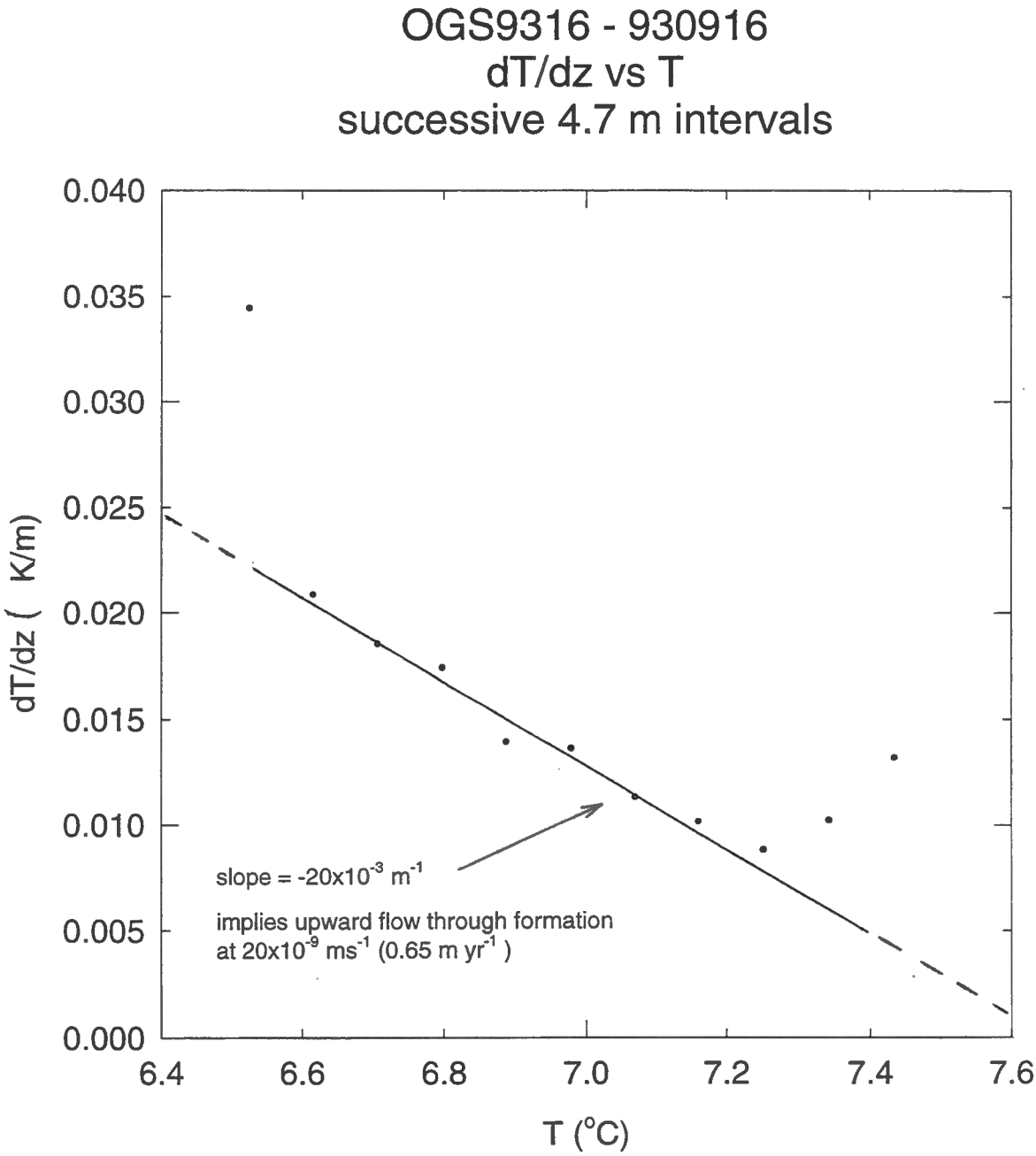

\OAKRIDGS\9316RPT2.SPW

FIG. 3.2

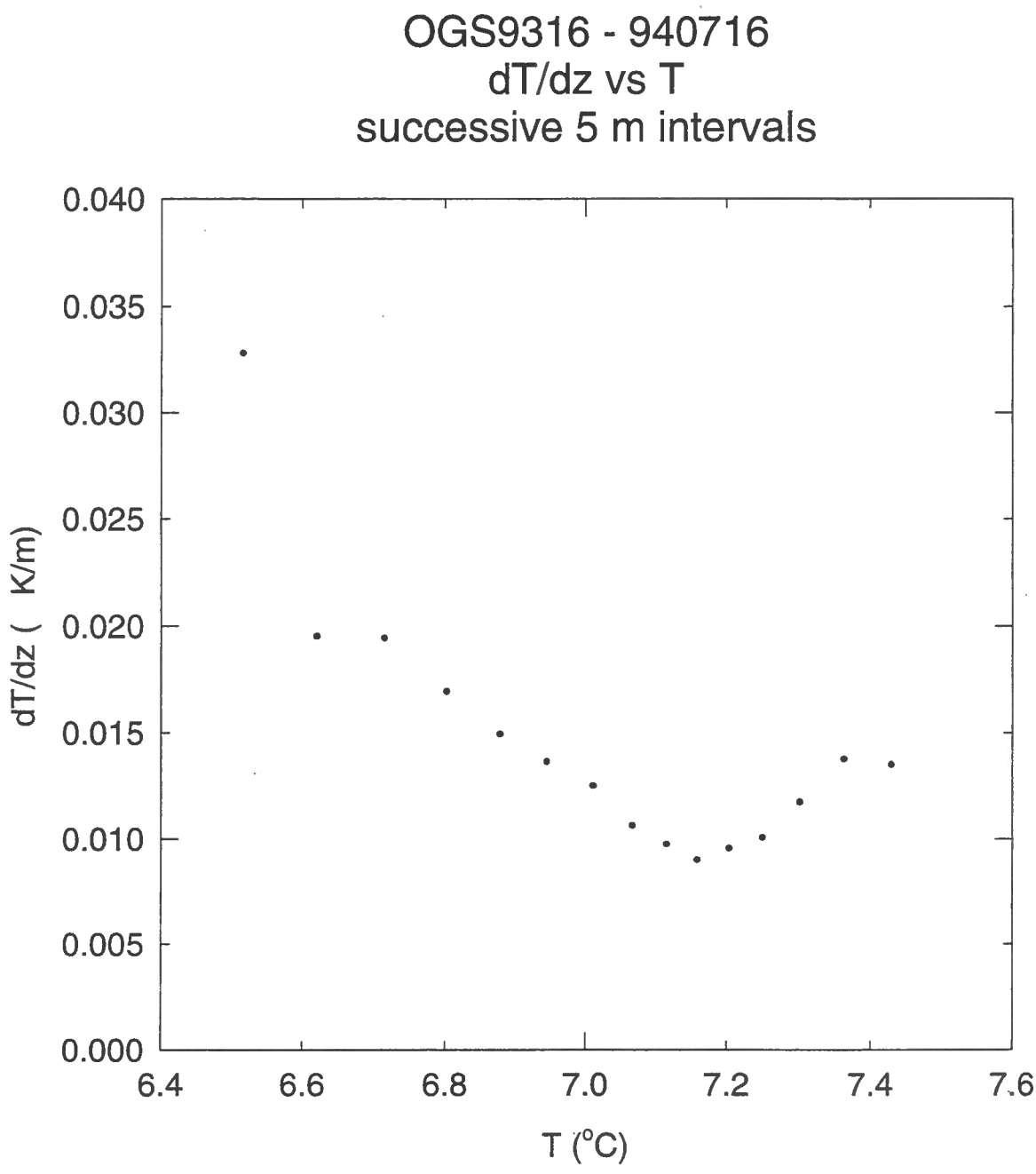

\OAKRIDGS\9316RPT2.SPW

FIG. 3.3

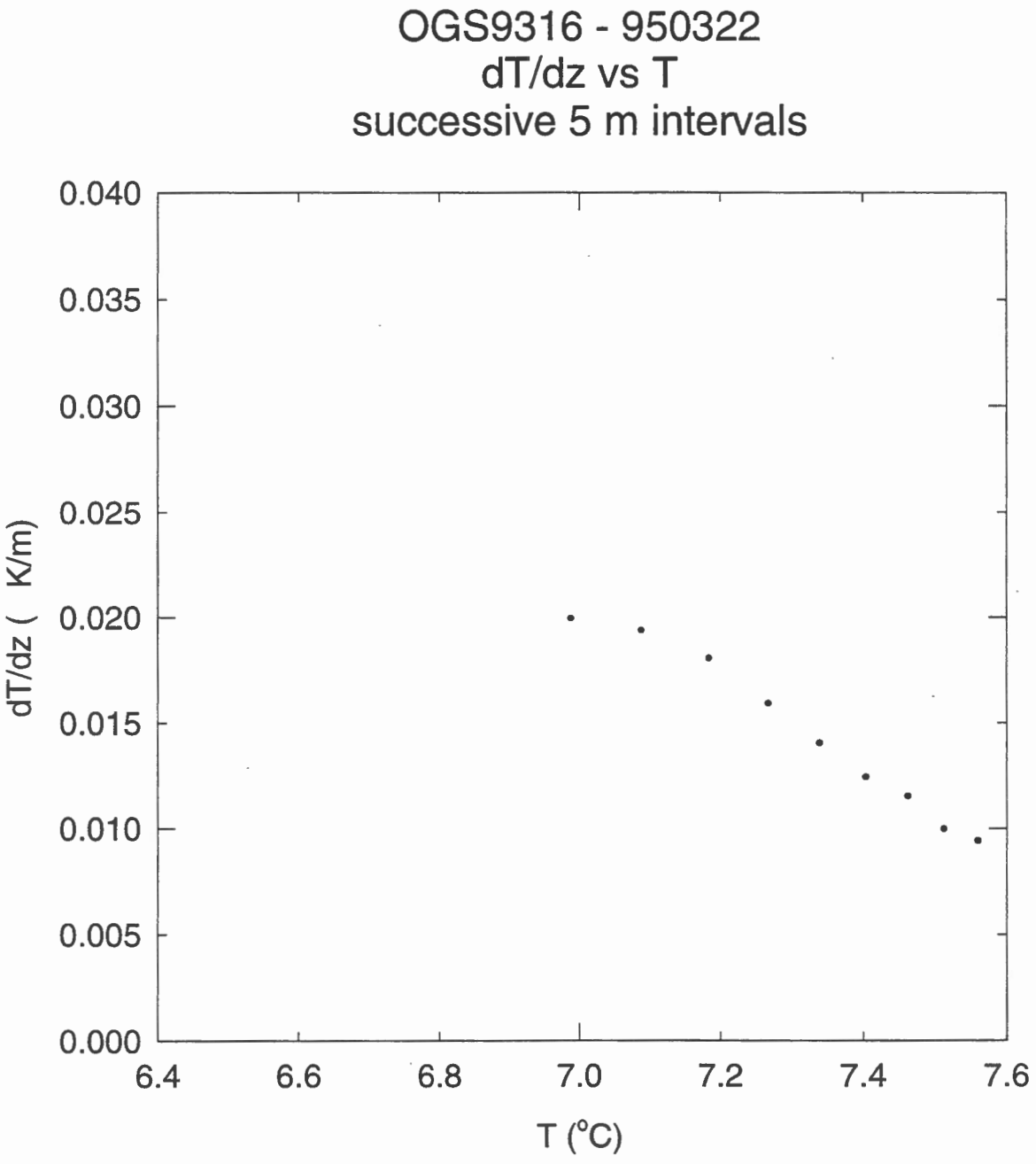

\OAKRIDGS\9316RPT2.SPW

FIG. 3.4

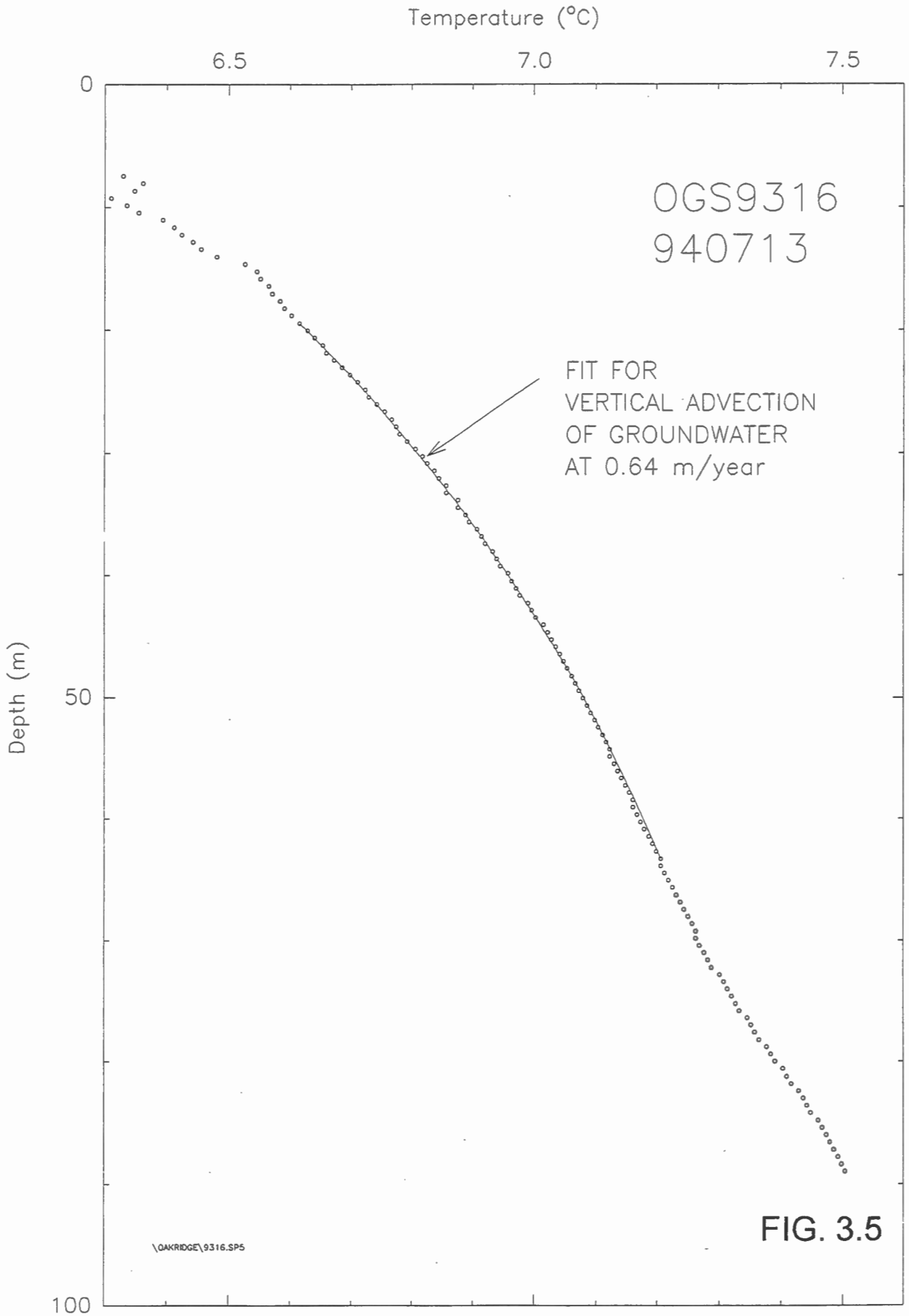
Temperature (°C)
6.5
7.0
7.5
0
50
100
Depth (m)
OGS9316
940713
FIT FOR
VERTICAL ADVECTION
OF GROUNDWATER
AT 0.64 m/year
\OAKRIDGE\9316.SP5

FIG. 3.5

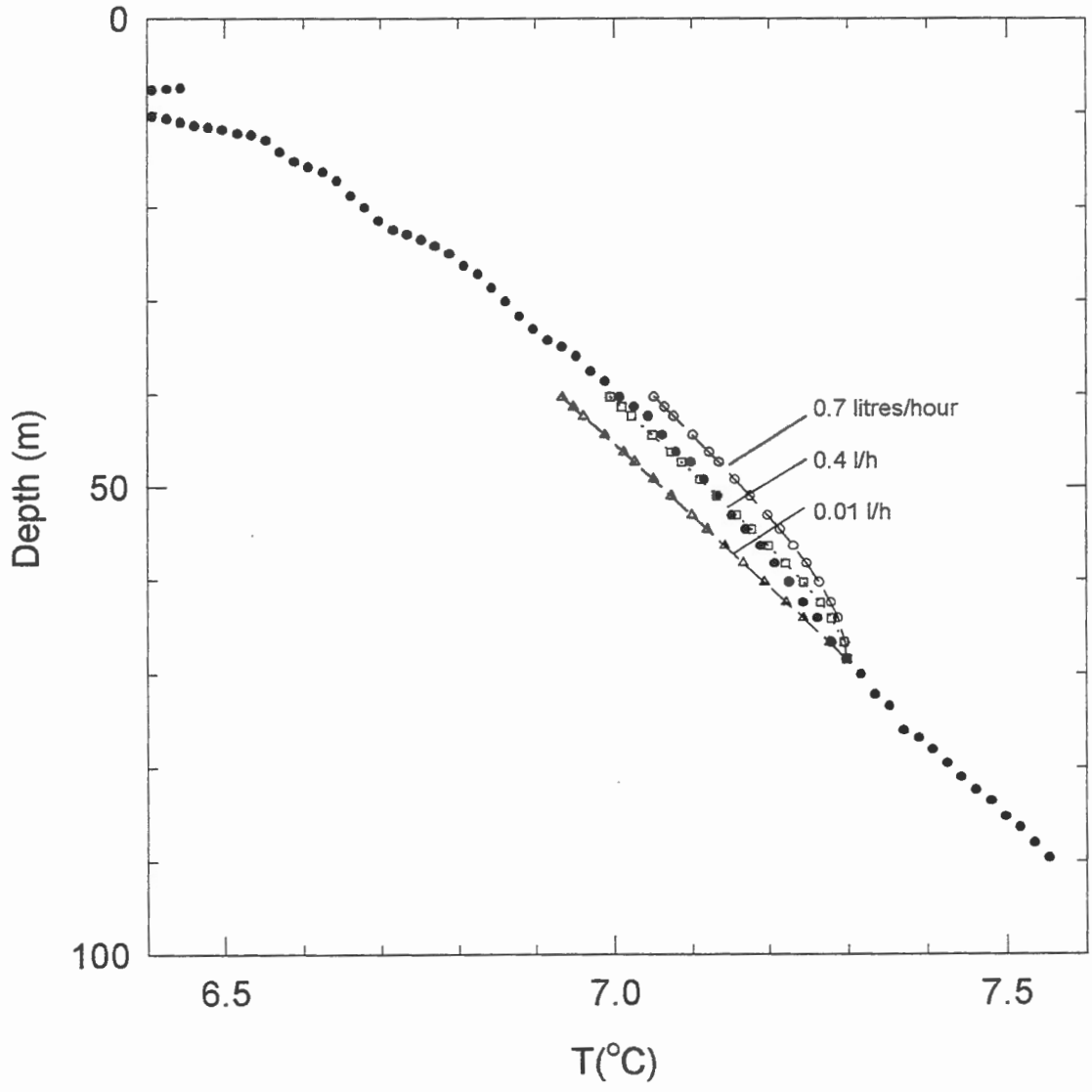

\OAKRIDGS\9316RPT2.SPW

FIG. 3.6

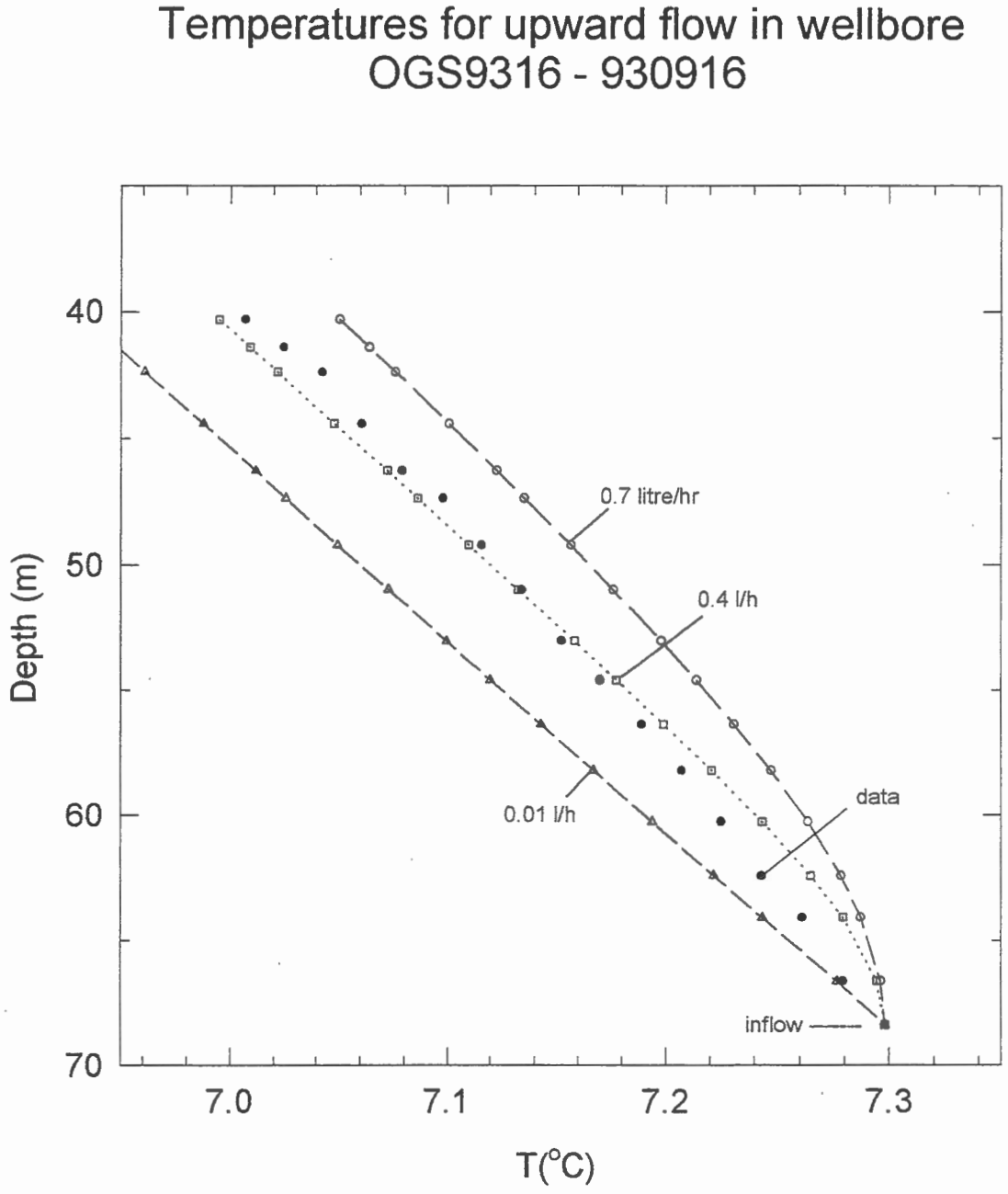

\OAKRIDGS\9316RPT2.SPW

FIG. 3.7

2.4 2MC McCowan Road (GSC-BH-BAL-01)

Two temperature logs are available (fall 1994 and spring 1995, Appendix B). The water level in the borehole is at about 50 m depth. The hole is air-filled above this and temperature data from 0 to 50 m depth in the October 1994 log are thus air temperatures, not those of the adjacent formations. A section of down wellbore flow (125-134 m) is evident in the 1995 log (compare 66 m-74 m at 1MC, Fig. 1.1), but not the 1994 log; possibly a seal deteriorated during the interim 7 months. Piezometer readings in both 1994 and 1995 at 40 m, 94 m and 132-135 m indicate a tendency for downward flow. This hole is nearby OGS 9316, but the logs do not show the bow-shaped feature (at 20-77 m) described above; also, a plot of temperature gradient versus temperature does not reveal a linear section (Fig. 4.1).

FIGURE CAPTION for 2MC

Fig. 4.1 2MC McCowan Road. Temperature gradient versus temperature (after Mansure and Reiter, 1979), to show lack of clear linear section that would suggest vertical movement of water in the formation.

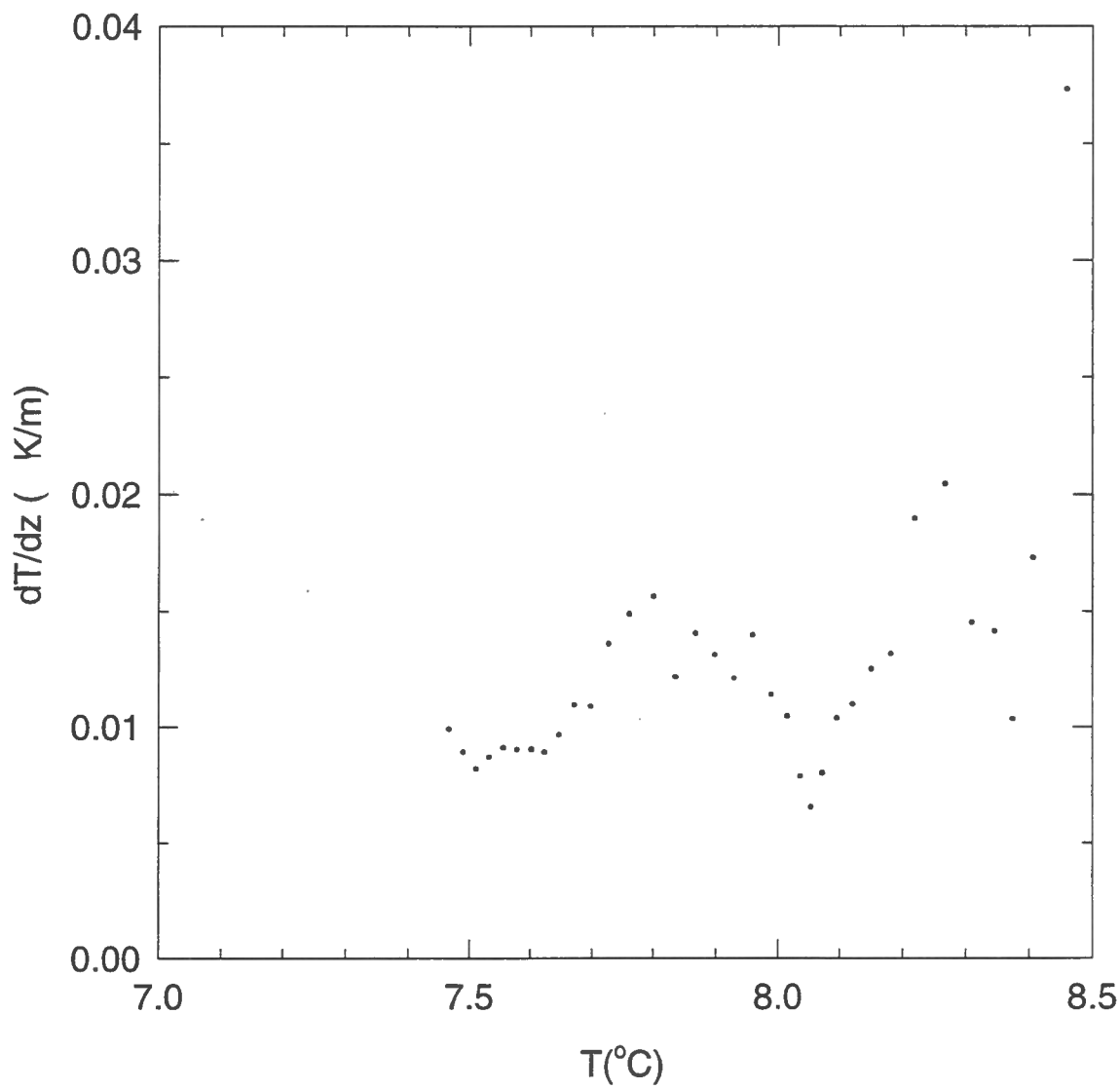
2MC - 950322
dT/dz vs T
successive 5 m intervals
0.04
0.03
0.02
0.01
0.00
dT/dz (K/m)
7.0
7.5
8.0
8.5
T(°C)

FIG. 4.1

2.5 1VD Vandorf Side Road (GSC-BH-VSR-01)

The temperature profile consists of a number of sections of distinct linear temperature-depth gradient, and a close correlation with the lithology can be seen (Fig. 5.1). The deepest segment has a gradient of 19 mK/m in sand, suggesting a thermal conductivity of about 2 W/mK, based on the terrestrial heat flow value for the region (40 mWm^{-2}; Jessop et al., 1984). The gradient in the upper sand (11 mK/m) implies a conductivity of 3.6 W/mK, more typical of sand. The deepest clay unit has a gradient of 24 mK/m (not shown in Fig. 5.1), implying a conductivity of 1.7 W/mK.

A short section (a few metres) of wellbore flow occurs below 100 m, leaving the wellbore around 107 m at the clay-sand to clay contact (compare 66-74 m at 1MC, Fig. 1.1). Piezometers are installed at 61 m and 123 m, and yield heads that give a downward tendency to water movement (L. Dyke, pers. commun., 1996), consistent with the geothermal interpretation.

FIGURE CAPTION for 1VD

Fig. 5.1 1VD Vandorf Side Road, July, 1994 log. Geothermal gradient sections correlate with the lithology. A short interval of flow down the wellbore is indicated around 107 m.

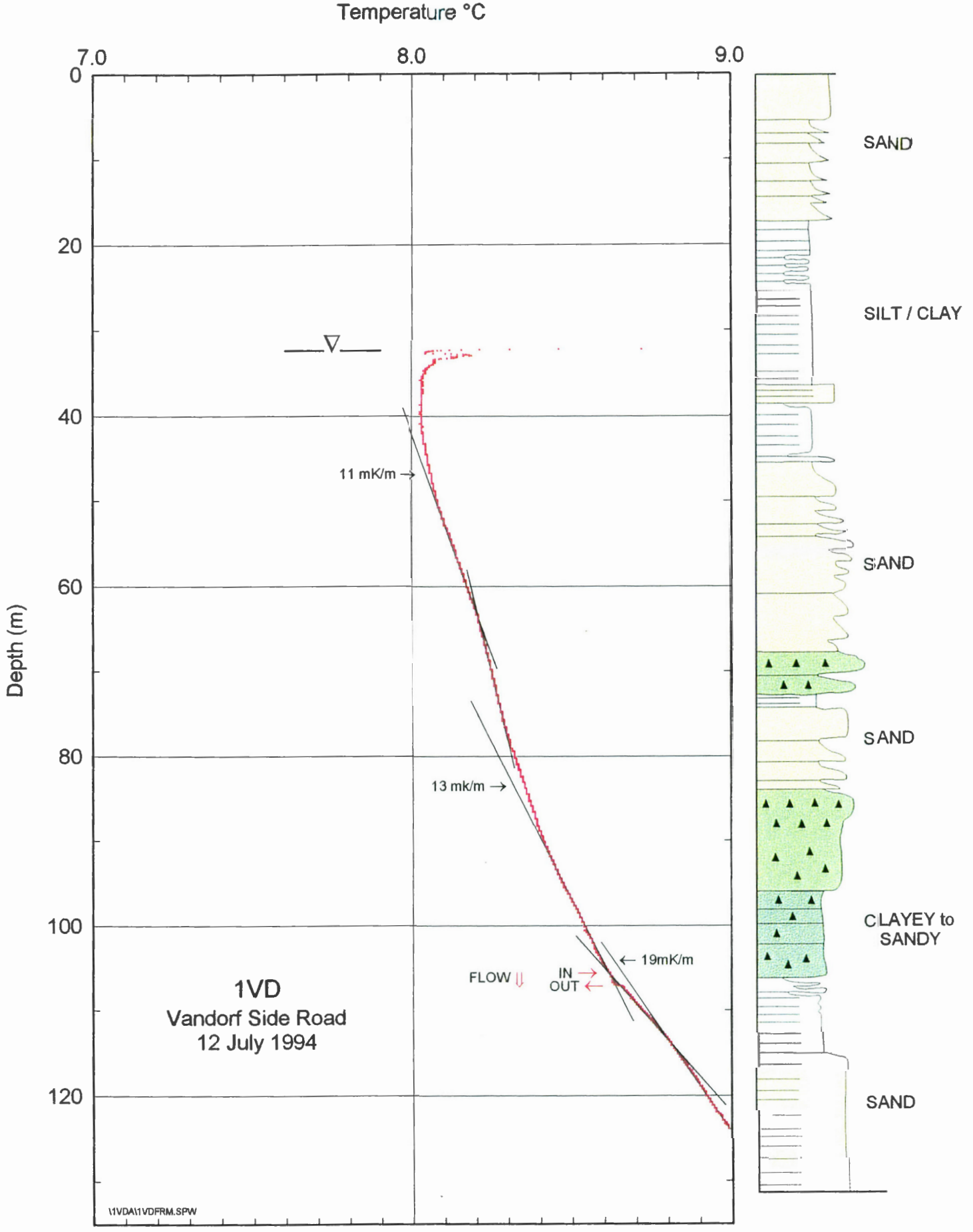
Temperature °C
7.0
8.0
9.0
0
20
40
60
80
100
120
Depth (m)
11 mK/m
13 mk/m
19mK/m
FLOW
IN
OUT
1VD
Vandorf Side Road
12 July 1994
\1VDA\1VDFRM.SPW
SAND
SILT / CLAY
SAND
SAND
CLAYEY to SANDY
SAND

FIG. 5.1

2.6 Bolton #6

One log was taken at this test well (Appendix B), situated some 30 m from a community well being actively pumped. The higher temperature gradient near the bottom of the well probably reflects the silty (some clay) lithology (Fig. 6.1). The upper hole is in silt, sand and some gravel. The temperature gradient versus temperature plot (after Mansure and Reiter, 1979) shows a linear section through this interval but interpretation is uncertain in this disturbed environment.

FIGURE CAPTION for Bolton #6

Fig. 6.1 Bolton #6. Temperature gradient versus temperature, to show linear section that suggests possible vertical movement of water in the formation.

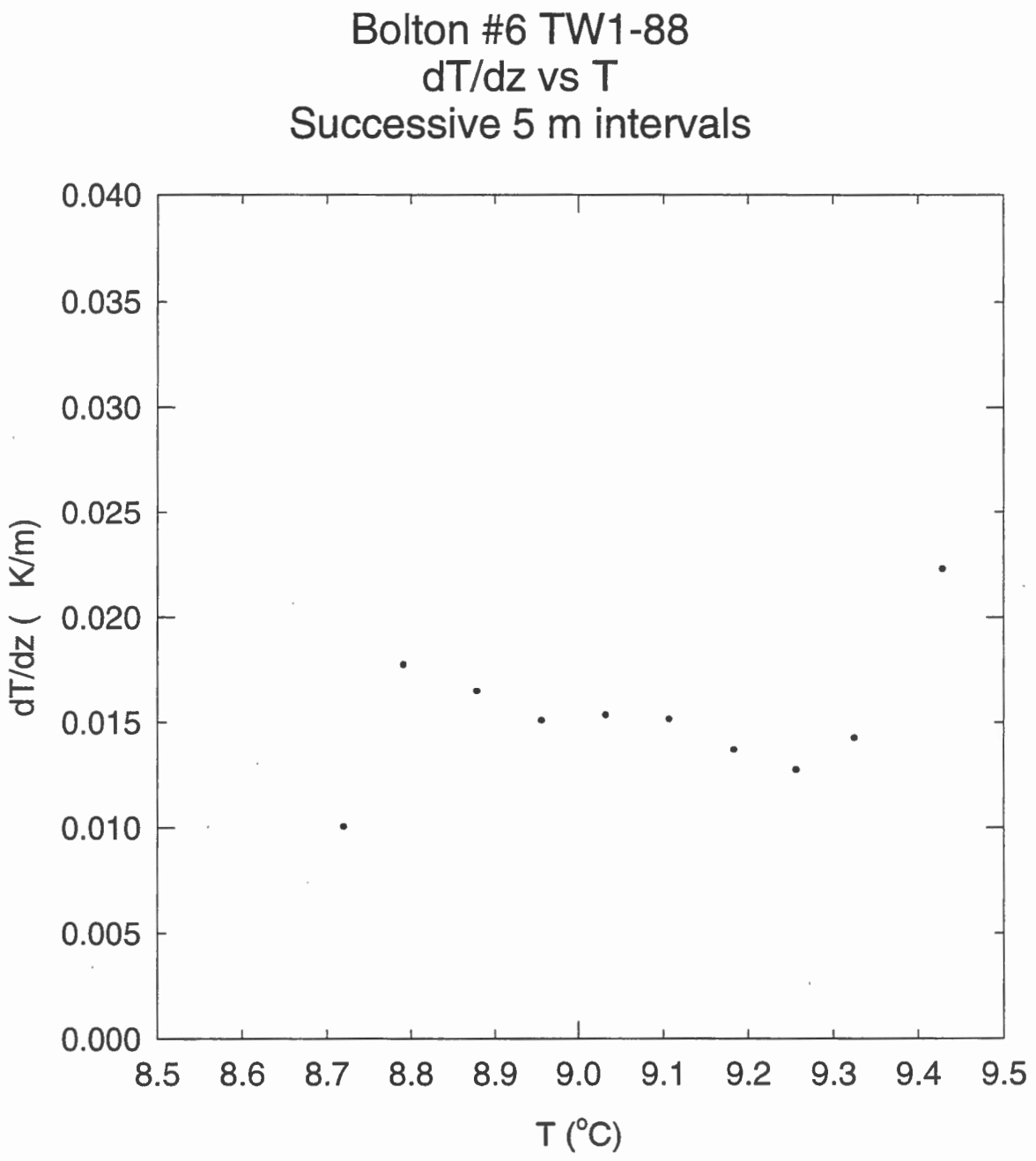

\PEEL\BLTN6RPT.SPW

FIG. 6.1

2.7 MOE W-8

One temperature log was run on this well in November, 1994. The temperature-depth gradient gradually increases with depth, creating a bow-shaped profile concave upwards (Appendix B). The temperature gradient versus temperature plot (after Mansure and Reiter, 1979) does not appear to have a linear trend and shows considerable scatter (Fig. 7.1). The bow-shaped nature of the log probably reflects the lithology (thermal conductivity effect due to coarsening upwards from clay till through silty sandy till through to gravels in the upper 80 m) other than an increase in surface temperature over the past few centuries.

FIGURE CAPTION for MOE W-8

Fig. 7.1 MOE W-8. Temperature gradient versus temperature, to show lack of clear linear section that would suggest vertical movement of water in the formation.

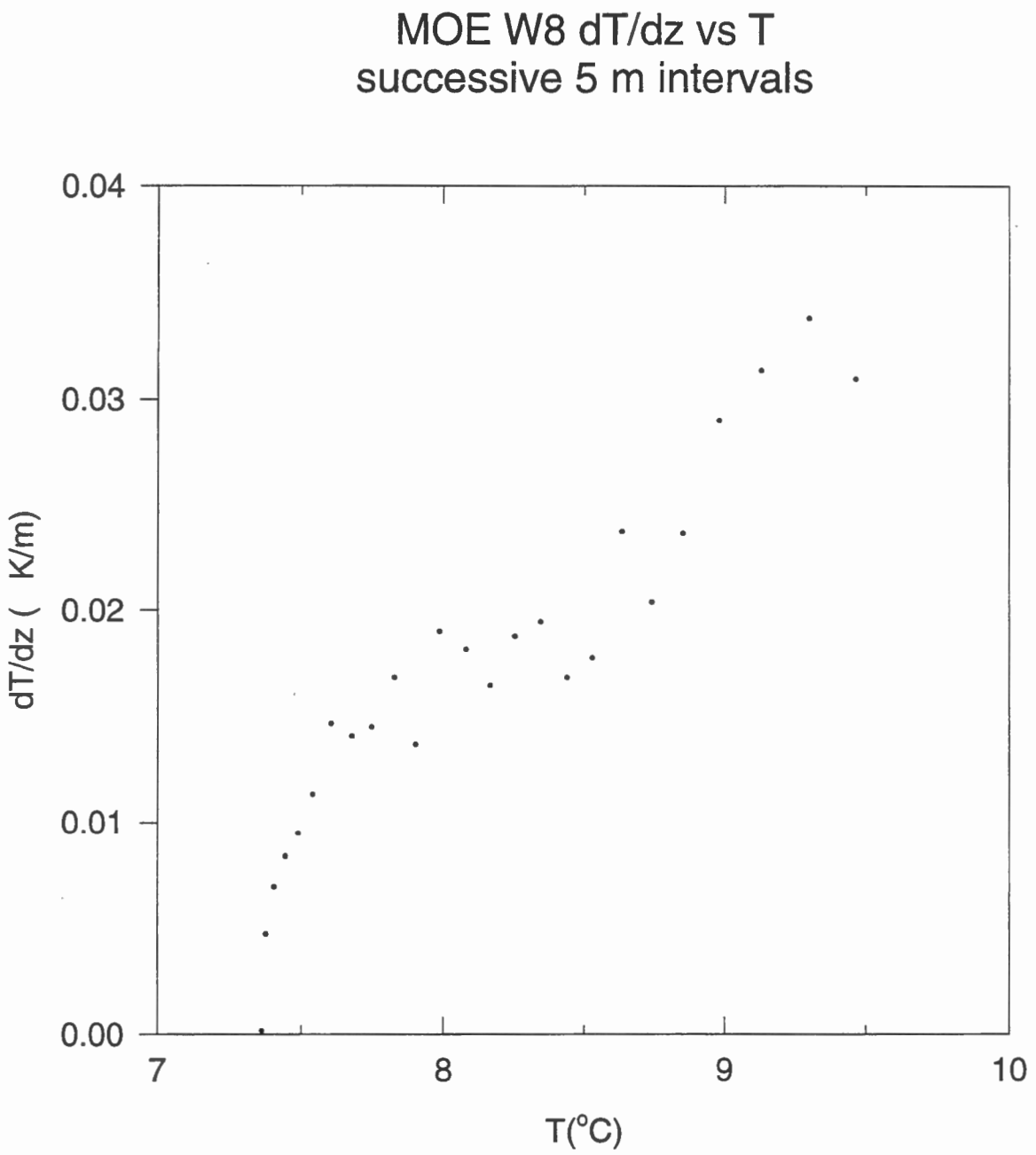
MOE W8 dT/dz vs T
successive 5 m intervals
0.04
0.03
0.02
0.01
0.00
dT/dz (K/m)
7
8
9
10
T(°C)

FIG. 7.1

3.0 Conclusions

Of the well temperature data examined in this study, only those from holes drilled specifically for scientific purposes yielded features that were interpreted in terms of regional subsurface flow. Wells drilled in the process of developing community water sources were within metres or tens of metres of pumping wells, and temperature profiles appeared to reflect this proximity.

The following styles of regional or local subsurface water flow are apparent in the interpretation of temperature profiles at the science holes:

1. Flow into a wellbore at one level, up or down the wellbore, and out of the well at another level. The rate of flow (about 12 litres/hour) was determined solely from interpretation of the temperature profile. Piezometer data were used to support the direction of flow interpreted from the temperature logs.
2. Flow along a sub-horizontal fracture or permeable zone that a wellbore intersects, showing evidence of the seasonal nature of the flow. The interpretation is supported by a local minimum in the downhole density log.
3. Flow forced into a porous zone during drilling. This occurred in a fine sandy unit, but there appears to be no supporting evidence in the logs.
4. Flow upward through a semi-confining layer separating aquifers. Fitting a theoretical analytic model of this flow to the temperature profile illustrated the excellent fit of the data to this interpretation and yielded a flow rate without knowledge of permeabilities (0.6 m/year). Logs suggest that the material in the anomalous temperature area is very fine sand rhythmite sets and clay caps, which may create a semi-confining layer. Piezometers at an adjacent hole do not support the interpreted direction of flow, so this discrepancy remains unexplained.

4.0 Acknowledgments

This project was financed through the Oak Ridges Hydrogeology Program of the Terrain Sciences Division, Geological Survey of Canada. Engineering and works departments of the regions of Peel, York and Durham enabled our access to log abandoned community water exploration wells. The authors thank Drs. David Sharpe, Larry Dyke and Susan Pullan for their support. Mr. Dan Desrochers logged some of the wells.

5.0 References

Andrews-Speed, C.P., Oxburgh, E.R., and Cooper, B.A. (1984). Temperatures and depth-dependent heat flow in western North Sea. American Association of Petroleum Geologists Bulletin, 68, p. 1764-1781.

Bodvarsson, G. (1973). Temperature inversions in geothermal systems. Geoexploration, 11, p. 141-149.

Bredehoeft, J.D. and Papadopulos, I.S. (1965). Rates of vertical groundwater movement estimated from the Earth's thermal profile. Water Resources Research, 1, p. 325-328.

Drury, M.J., Jessop, A.M., and Lewis, T.J. (1984). The detection of groundwater flow by precise temperature measurements in boreholes. Geothermics, 13, p. 163-174.

Jessop, A.M. (1990). Thermal Geophysics. Developments in Solid Earth Geophysics 17. Elsevier Science Publishers, 306 pp.

Jessop, A.M., Lewis, T.J., Judge, A.S., Taylor, A.E., and Drury, M.J. (1984). Terrestrial heat flow in Canada. Tectonophysics, 103, p. 239-261.

Lu, N. and Ge, S. (1996). Effect of horizontal heat and fluid flow on the vertical temperature distribution in a semiconfining layer. Water Resources Research, 32, p. 1449-1453.

Mansure, A.J. and Reiter, M. (1979). A vertical groundwater movement correction for heat flow. Journal of Geophysical Research, 84, p. 3490-3496.

Pullan, S.E., Pugin, A., Dyke, L.D., Hunter, J.A., Pilon, J.A., Todd, B.J., Allen, V.S., and Barnett, P.J. (1994). Shallow geophysics in a hydrogeological investigation of the Oak Ridges Moraine, Ontario. *in* Proceedings, Symposium on the application of geophysics to engineering and environmental problems. R.S. Bell and C.M. Lepper, eds. March 27-31, Boston, MA, V. 1, p. 143-161.

Ramey, H.J. (1962). Wellbore heat transmission. Journal of Petroleum Technology, 14, p. 427-435.

Reiter, M., Costain, J.K., and Minier, J. (1989). Heat flow data and vertical groundwater movement, examples from southwestern Virginia. Journal of Geophysical Research, 94, p. 12,423-12,431.

Sharpe, D.R., Barnett, P.J., Dyke, L.D., Howard, K.W.F., Hunter, G.T., Gerber, R.E., Paterson, J., and Pullan, S.E. (1994). Quaternary geology and hydrogeology of the Oak Ridges Moraine area. Geological Association of Canada-Mineralogical Association of Canada, Joint Annual Meeting, Waterloo. Field Trip A7: guidebook, 32 pp.

Sharpe, D.R., Dyke, L.D., Hinton, M.J., Pullan, S.E., Russell, H.A.J., Brennand, T.A., Barnett, P.J., and Pugin, A. (1996). Groundwater prospects in the Oak Ridges Moraine area, southern Ontario: application of regional geological models. *in* Current Research 1996-E, Geological Survey of Canada, p. 181-190.

Ziagos, J.P. and Blackwell, D.D. (1981). A model for the effect of horizontal fluid flow in a thin aquifer on temperature-depth profiles. Geothermal Resources Council, Transactions, 5, p. 221-223.

Appendix A

Summary of comments on borehole temperature logs

YORK REGION WELLS

HOLE #	undisturbed gradient (mK/m)	Description and comments
		OGS/GSC holes
1MC (GSC-BH-MSR-01)	12 & 32	66-74 m, flow into wellbore near 66 m from sand aquifer, leaves borehole near 74 m at silty clay/diamicton contact, consistent with piezometer record; 89-103 m, flow into well near 103 m at diamicton/bedrock contact and at two locations above; forced out of borehole at bentonite plug near 90 m. Modelling suggests 12 litres/hour leaves borehole.
2MC (GSC-BH-BAL-01)		30 m from road in 20 m high pine grove; adjacent to OGS9316, similar profile but no signature of upward flow in the formation. 125-134 m, indication of down wellbore flow (direction consistent with piezometer record).
1VD (GSC-BH-VSR-01)	11, 13, 24	Log date 940712: 105 m, flow into wellbore (compare 1MC); flow down wellbore to 107 m and out of borehole at till/silty clay contact.
OGS9315	8	Log data 930914 and 940711: 17 m, high temperature peak anomaly (0.35 K); 22 m, small low temperature peak; both possible seasonal water flows along thin beds. Log date 9405: anomaly at 37-46 m gives signature of downward borehole flow.

OGS9316	13	Log date 930916: 8-12 m, seasonal variation; 22-70 m, particularly 35-70 m, bow-shaped section, possible upward flow of groundwater at 0.5 m/a. Bow shape persists on later logs.
OGS9317	9	similar to OGS9315; 14 m, high temperature anomaly (0.76 K), persists on 1993 and 1994 logs and lower on spring, 1995 log, possibly seasonal effect; 34 m, small low temperature anomaly (1993) not visible on 1994 log, probably thermal storage effect.
OGS9319	8	similar to OGS9315; 17 m, high temperature anomaly (0.35 K, 1993) and about half magnitude (1994); 26 m, small low temperature anomaly (1993) not visible on 1994 log
		Community test wells
Aurora #5	23	45 m, small temperature peak to higher temperatures, possible flow along horizontal bed or subhorizontal fracture, or transient storage of heat from drilling
Bales Rd N.	13	40-50 m, possible flow of water down wellbore from around 40 m, out of wellbore at 50 m
Bales Rd S.	13	20-55 m, temperature inversion, probably downhole temperature effect of nearby road
Collis Leather		3 m from building; 23-80 m: possible recent increase in surface temperature due to placement of structure
Henderson Rd	14	3 m from paved road; 1993: high temperature peaks at 68-70 and 78 m, possible transient storage of warmer fluid in aquifers due to drilling; 1994: no peak at 68-

		70 m (heat dissipated), and less curvature 79-95 m than 1993, hence both peaks may be storage effects.
Mitchell	15	4 m from highway, 1 m from ditch; 50-90 m: possible downhole effect of adjacent highway
Newmarket #2		49-66 m: only record obtained; isothermal
Oak Ridges #3		30-60 m: warming effect of gravel pad and adjacent firehall
Ozark Park	13?	30-45 m partially seasonal effect in wellbore; 45-70 m, possibly recent surface temperature increase
Queensville #5		in soybean field; farmer had pumped nearby well previous day
Queensville #6		cornfield, 5 m from road; isothermal, farmer had pumped well previous day
Queensville #7		gravel pad, adjacent to production well
Queensville #8		7 m from gravel road, adjacent to large pond; slope breaks probably reflect lithologic changes
Queensville #9	16	10 m from paved road, grass surface on ridge top; approximately geothermal gradient for area
Rogers Park		46-66 m: only record obtained

PEEL REGION WELLS

HOLE #	undisturbed gradient (mK/m)	Description and comments
Bolton #4 (TW2-72)		few metres from producing well in town
Bolton #6 (TW1-88)	15, 24	ridge above Bolton, 30 m from producing well; approximates geothermal gradient, possible slight bow indicating upwards advection in formation
Caledon East #1 (Granite Stones)		10 m SE of producing well
Caledon East #3 (TW1-77B)		79 m NW of producing well, in playground
Caledon East #3 (TW4-77)		3 m SE of producing well
Caledon Well #4		12 m, flow out of wellbore; 12-20 m, 22-30 m and 32-60 m, flow up wellbore; inflow to wellbore at bottom, near 31 and 21 m
Centreville (Holly Park)		20 m from highway, 1 km from producing well in small valley
Mono Mills #6 (TW2-90)		100 m SE of producing wells; 10-25 m, bow shape suggesting upwards advection through limestone; 25 m, fracture, flow into well?; 29-48 m, possible upwards advection
Palgrave #2 (TW6-72)		several metres from road and producing well

DURHAM REGION WELLS

HOLE #	undisturbed gradient (mK/m)	Description and comments
MOE W-1		temperatures similar to MOE W-2; shallow hole no undisturbed gradients
MOE W-2	12-16	gradients 60-83 m, 12 mK/m, 83-107 m, 16 mK/m, 142-153 m, 15 mK/m.
MOE W-8	34 to 15	curvature 65-100 m; gradients of four deeper linear sections probably closely reflect lithology; 100-122 m, 15 mK/m, 122-160 m, 18 mK/m, 160-177 m, 22 mK/m and 177-195, 34 mK/m. Linearity suggests probably no vertical component of flow between 100-195 m.
MOE W-10	20-34	gradients 115-153 m, 20 mK/m; 175-190 m, 34 mK/m; 190-195, 22 mK/m
Whitevale P1-16D	6.6-8.2	gradients 25-45 m, 6.6 mK/m; 45-55 m, 8.2 mK/m
Whitevale P1-26D		gradients 32-41 m, 3.3 mK/m; 41-51 m, 7 mK/m; 51-68 m, 12.9 mK/m
Whitevale P1-29B	11	gradient 29-47 m, 11mK/m

Appendix B

Graphs of temperature-depth profiles

N.B. All plots have the same scale of depth and temperature intervals, for ease of comparison

The following temperature-depth graphs were taken during the summer/fall of 1993-95. Wells are grouped alphabetically by region, starting with York, followed by Peel and Durham. Wells may be located in Figure 1.0 and Table 1. A summary of largely qualitative interpretations is given in Table 2.

1. The upper few metres of most holes are air-filled and temperatures in that zone should be ignored. Also, the seasonal variation extends to about 10 m, or a few metres from the top of the water table.

2. Most profiles exhibit a linear section that may be interpreted as the undisturbed geothermal gradient, and this has been extrapolated to the ground surface to emphasize any departures that might be attributed to local or transient effects. This gradient (8 to 23 mK/m) when considered with the regional terrestrial heat flow (40 mWm^{-2}; Jessop et al., 1984) suggests that thermal conductivity of the materials lie in the range 5.0 to 1.7 W/mK. The higher thermal conductivity is typical of sands, gravel and sandstone, the lower of clays and clayey silts and shale. No attempt has been made to correlate the temperatures and thermal properties to the lithology at each hole, or to other geophysical logs at the present time.

3. Some wells may be influenced by nearby wells, pumping etc.; this has not been investigated at present.

YORK REGION WELLS

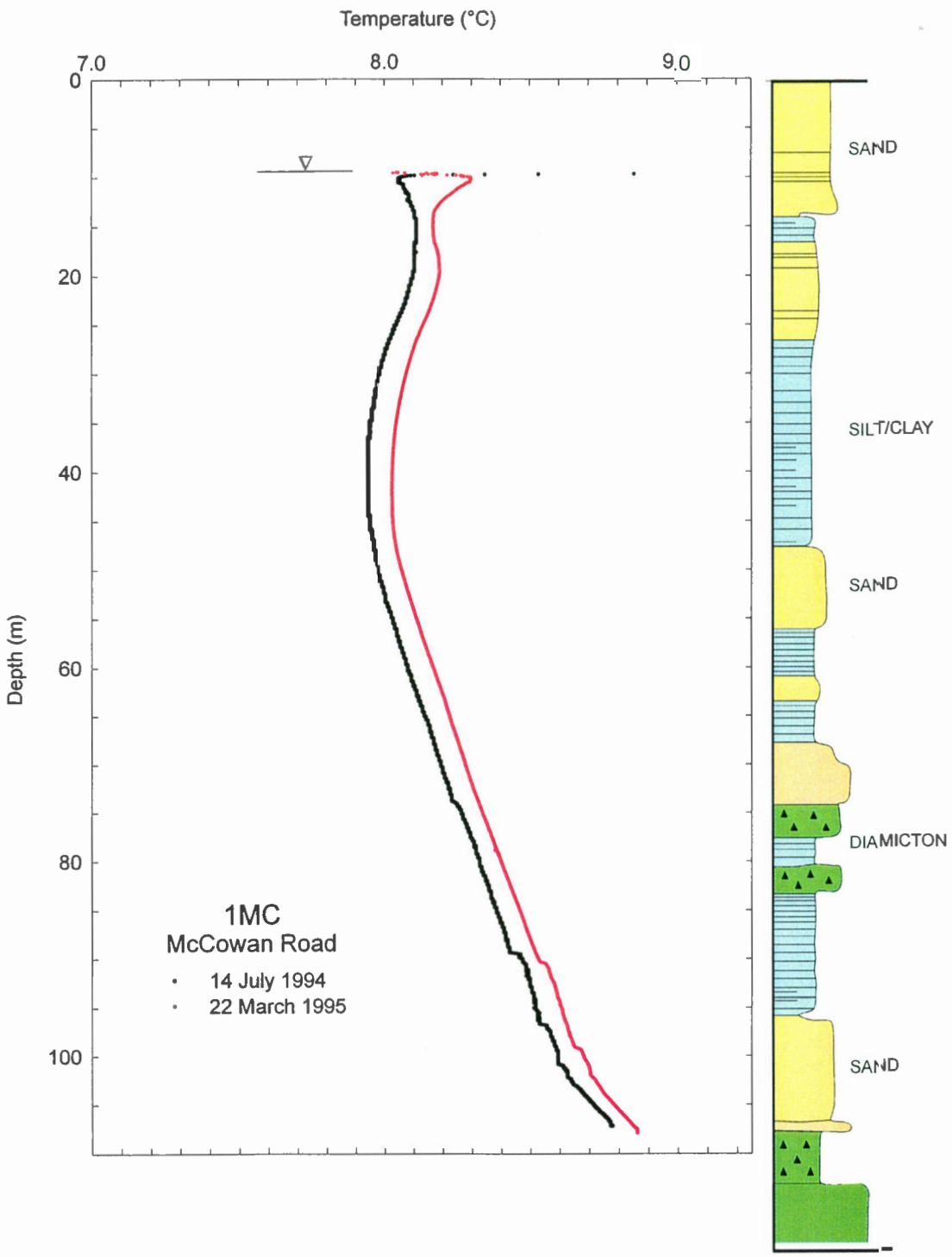
Temperature (°C)
7.0
8.0
9.0
0
20
40
60
80
100
Depth (m)
1MC
McCowan Road
14 July 1994
22 March 1995
SAND
SILT/CLAY
SAND
DIAMICTON
SAND

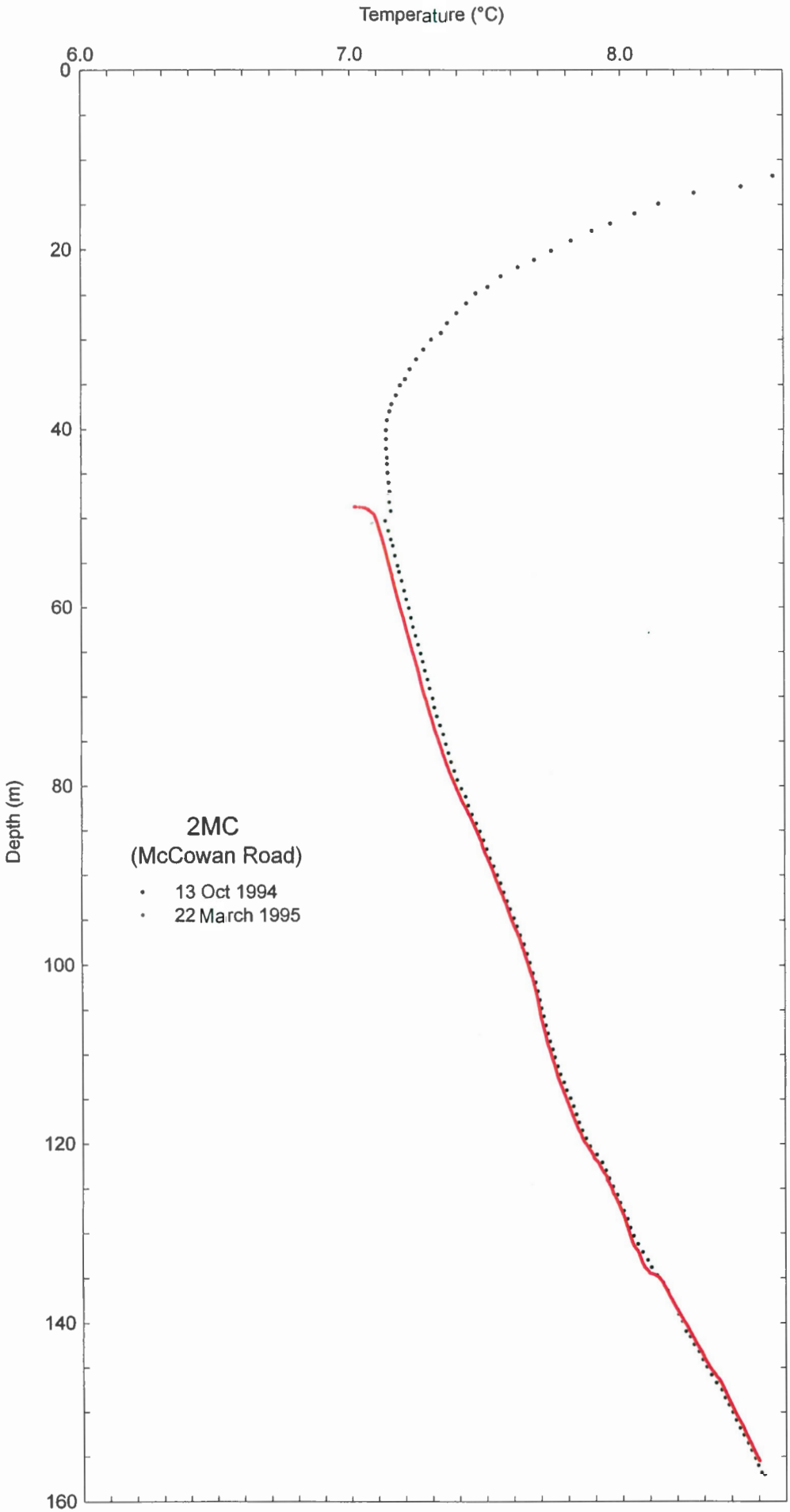
Temperature (°C)
6.0
7.0
8.0
0
20
40
60
80
100
120
140
160
Depth (m)
2MC
(McCowan Road)
13 Oct 1994
22 March 1995

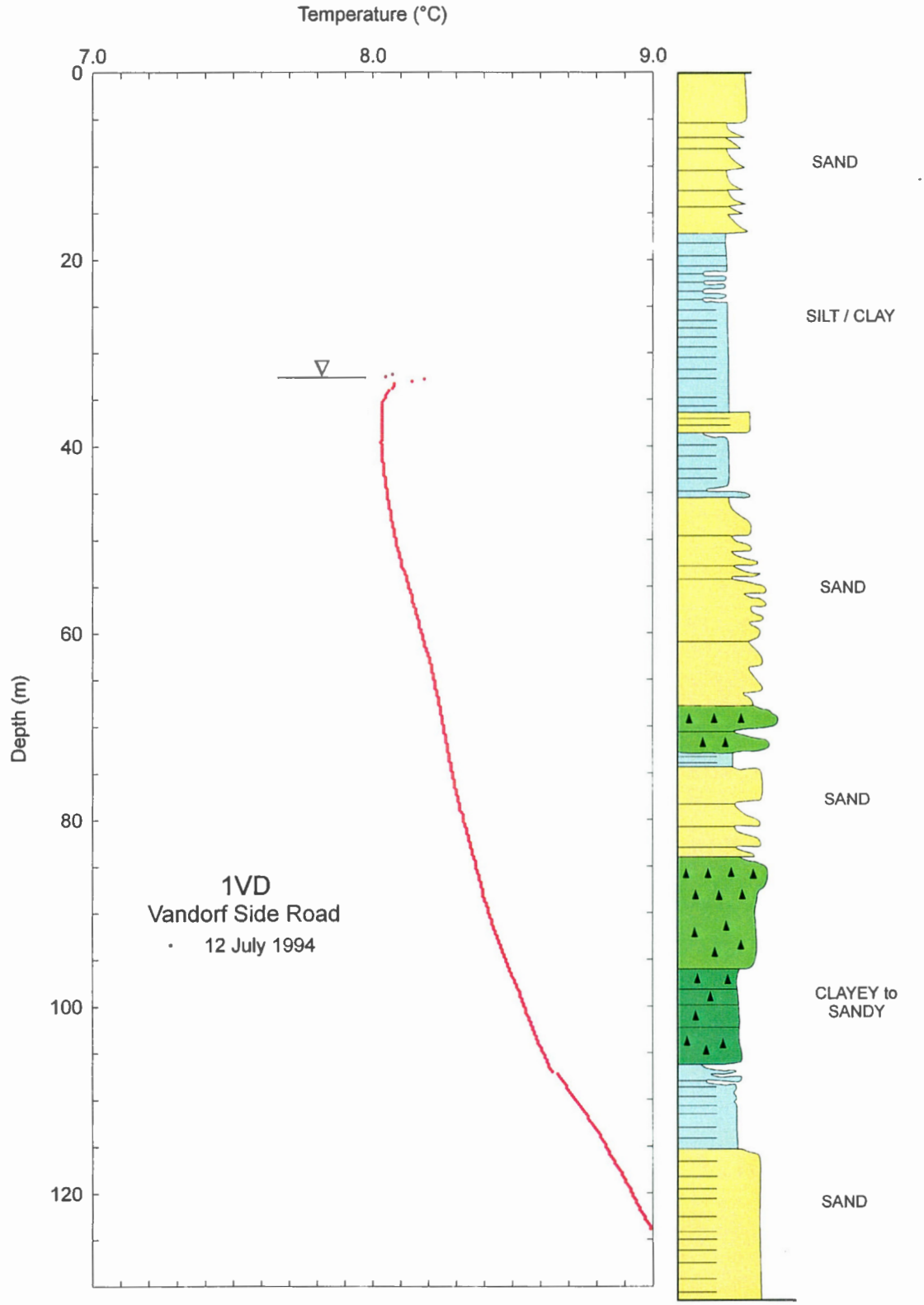
Temperature (°C)
7.0
8.0
9.0
0
20
40
60
80
100
120
Depth (m)
1VD
Vandorf Side Road
12 July 1994
SAND
SILT / CLAY
SAND
SAND
CLAYEY to SANDY
SAND

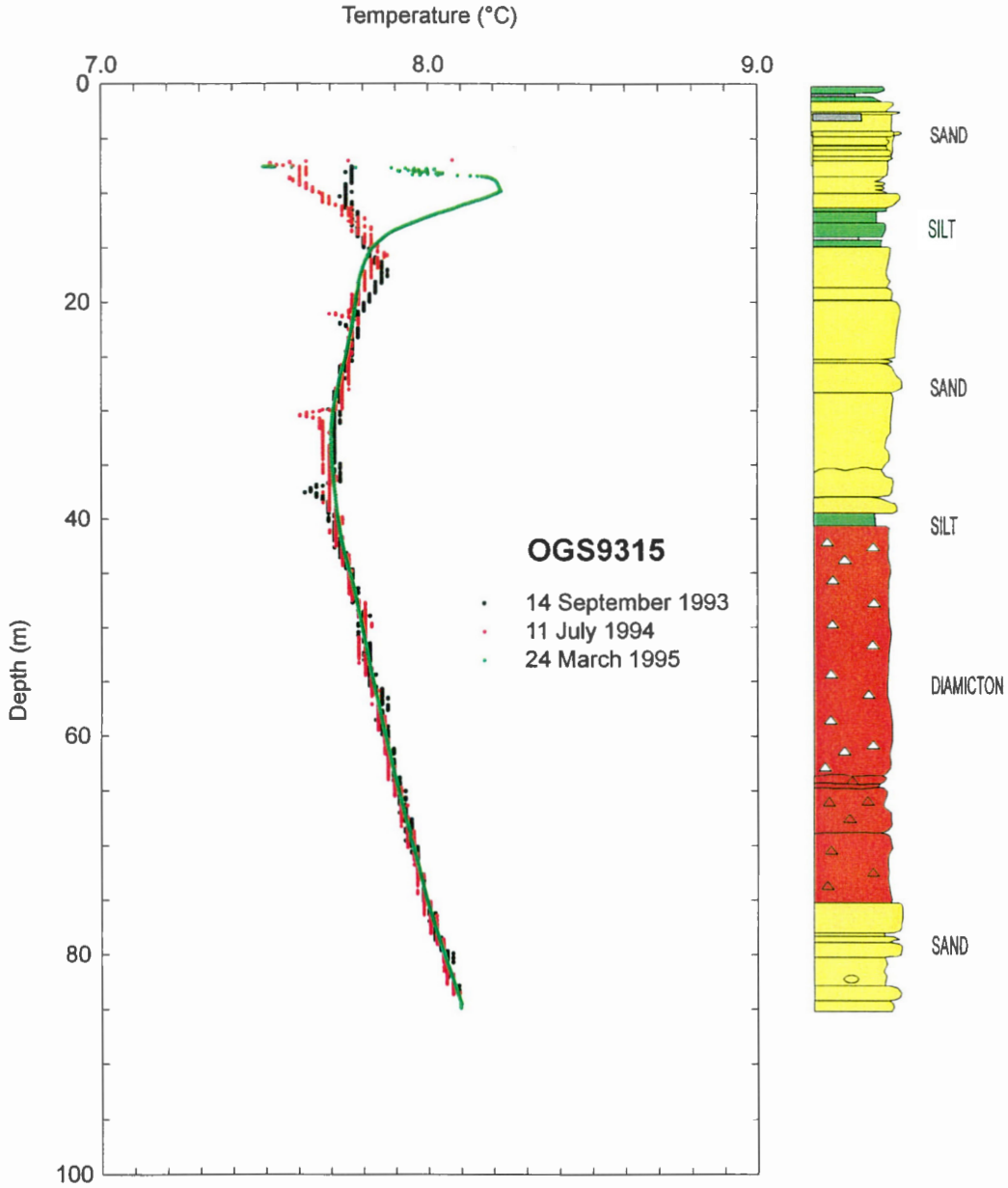
Temperature (°C)
7.0
8.0
9.0
0
20
40
60
80
100
Depth (m)
OGS9315
14 September 1993
11 July 1994
24 March 1995
SAND
SILT
SAND
SILT
DIAMICTON
SAND

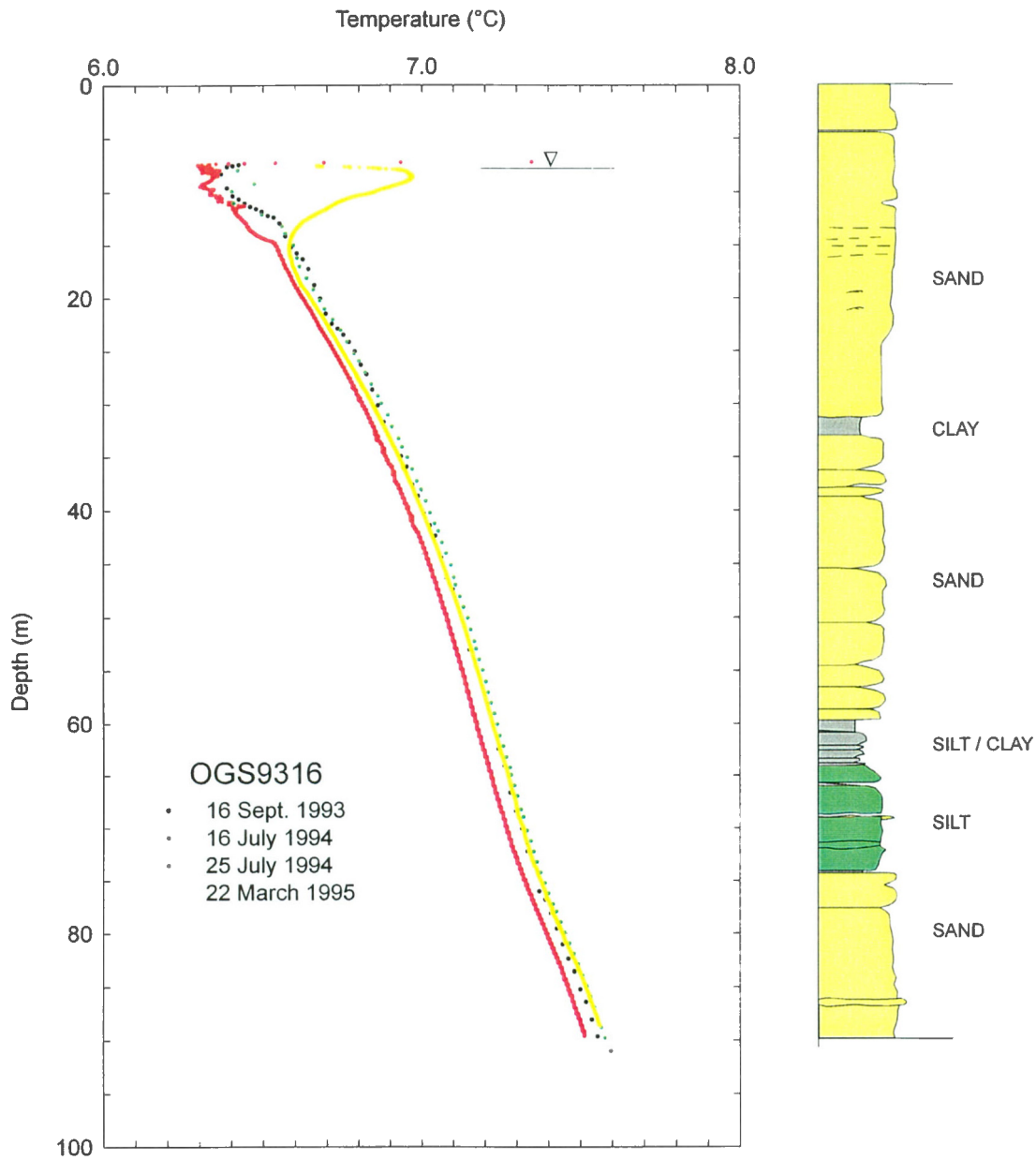
Temperature (°C)
6.0
7.0
8.0
0
20
40
60
80
100
Depth (m)
OGS9316
16 Sept. 1993
16 July 1994
25 July 1994
22 March 1995
SAND
CLAY
SAND
SILT / CLAY
SILT
SAND

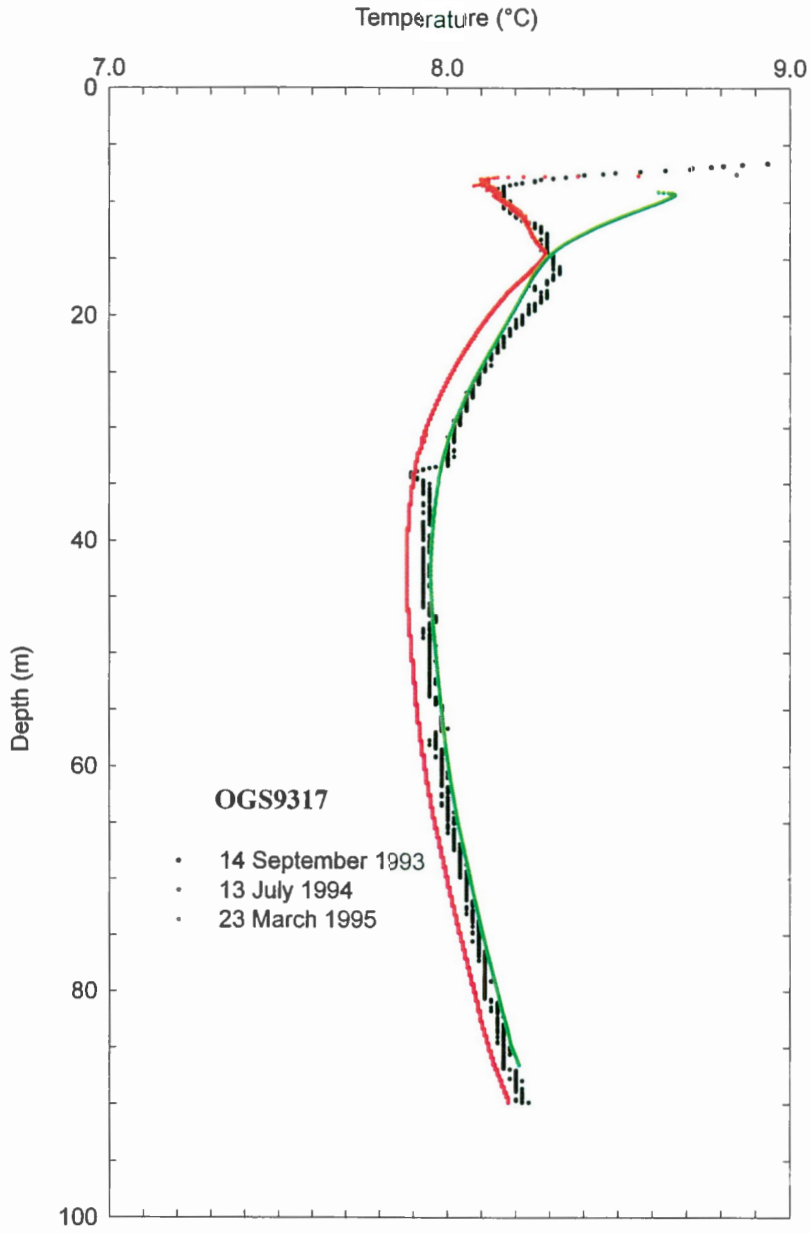
Temperature (°C)
7.0
8.0
9.0
0
20
40
60
80
100
Depth (m)
OGS9317
14 September 1993
13 July 1994
23 March 1995

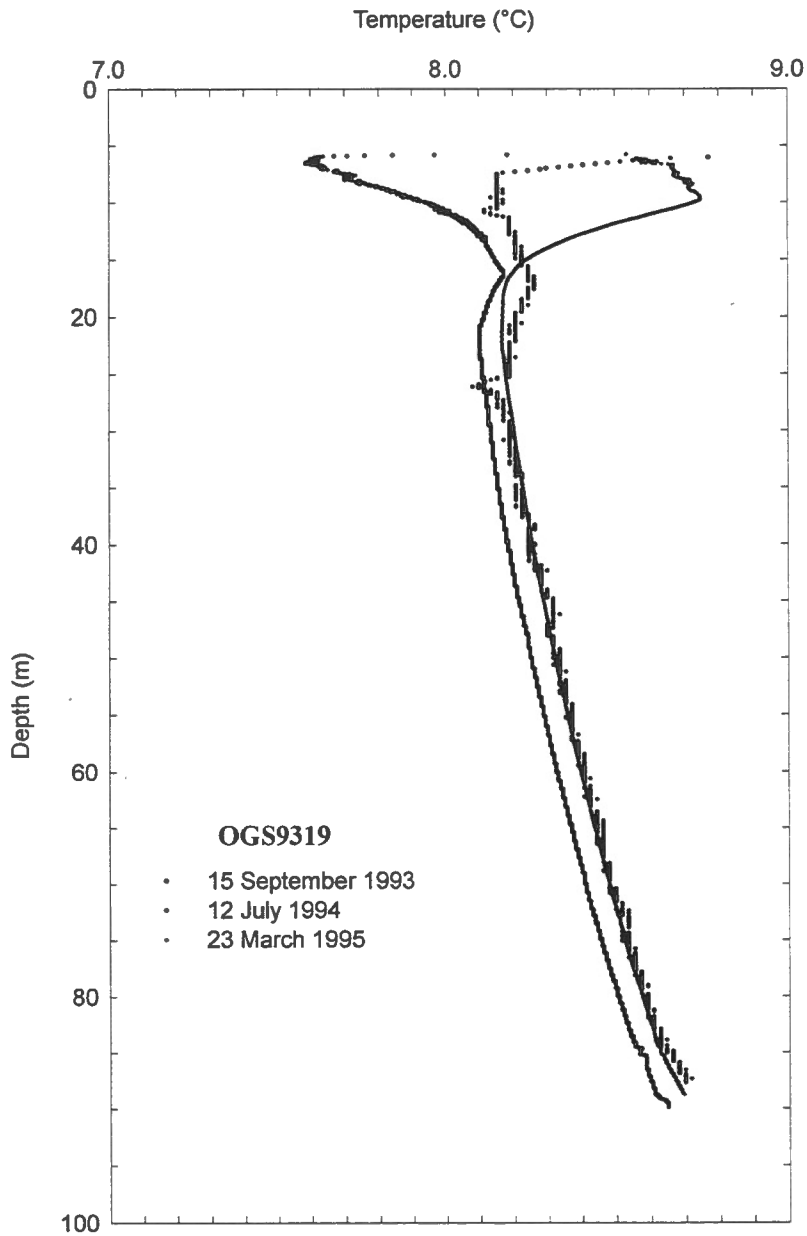
Temperature (°C)
7.0
8.0
9.0
0
20
40
60
80
100
Depth (m)
OGS9319
15 September 1993
12 July 1994
23 March 1995

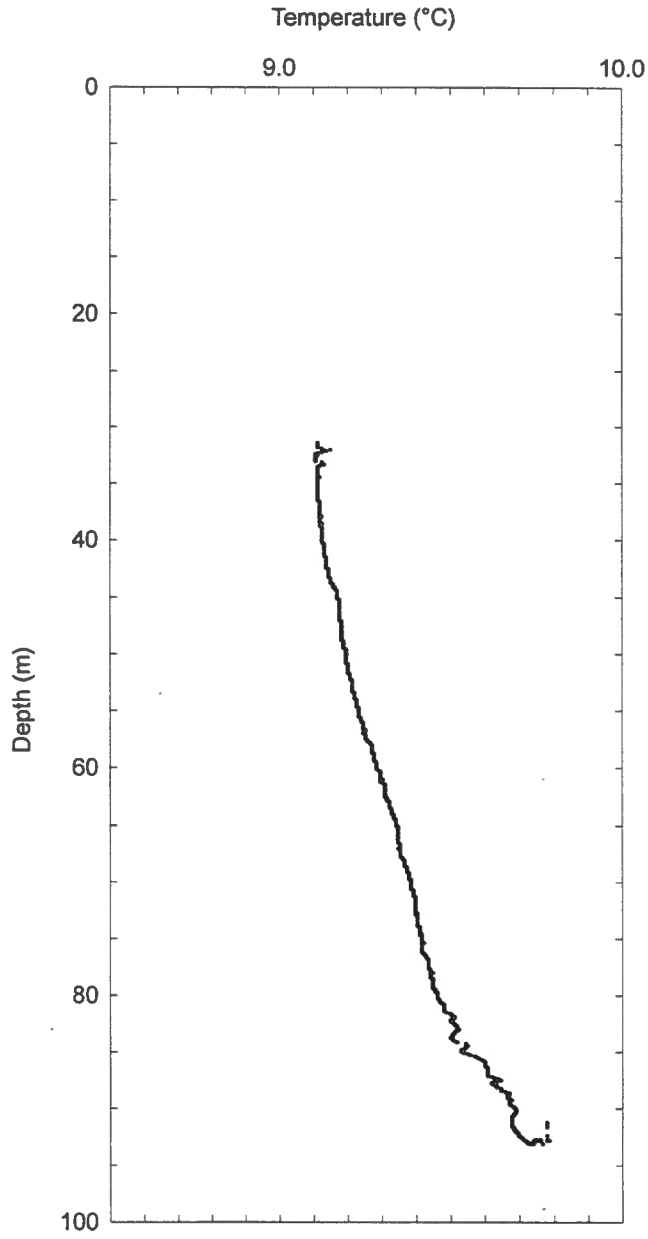

AURORA #5

- 26 August 1993

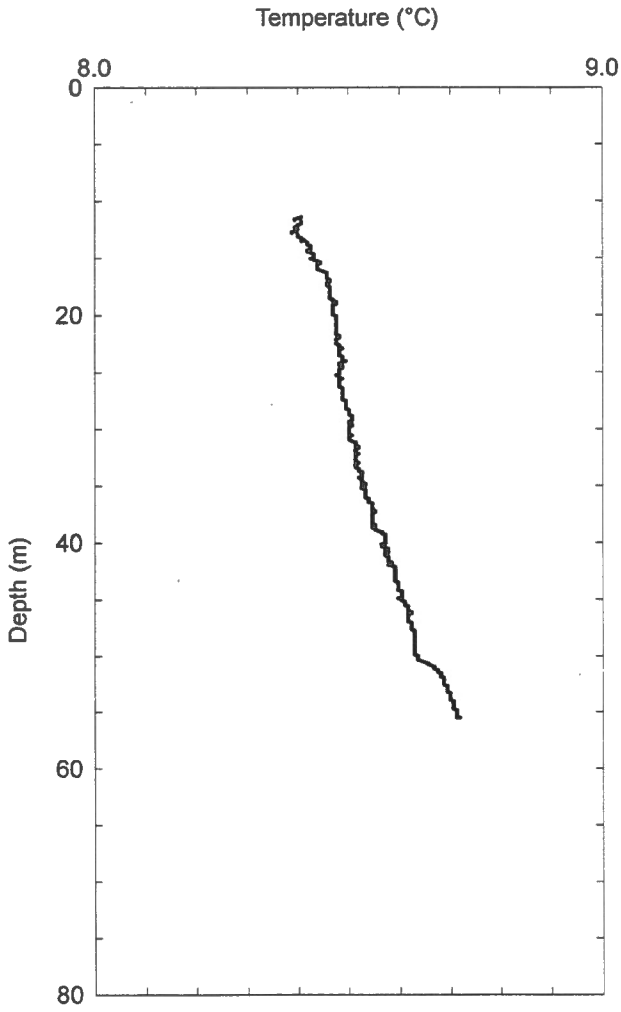

BALES ROAD NORTH

- 24 August 1993

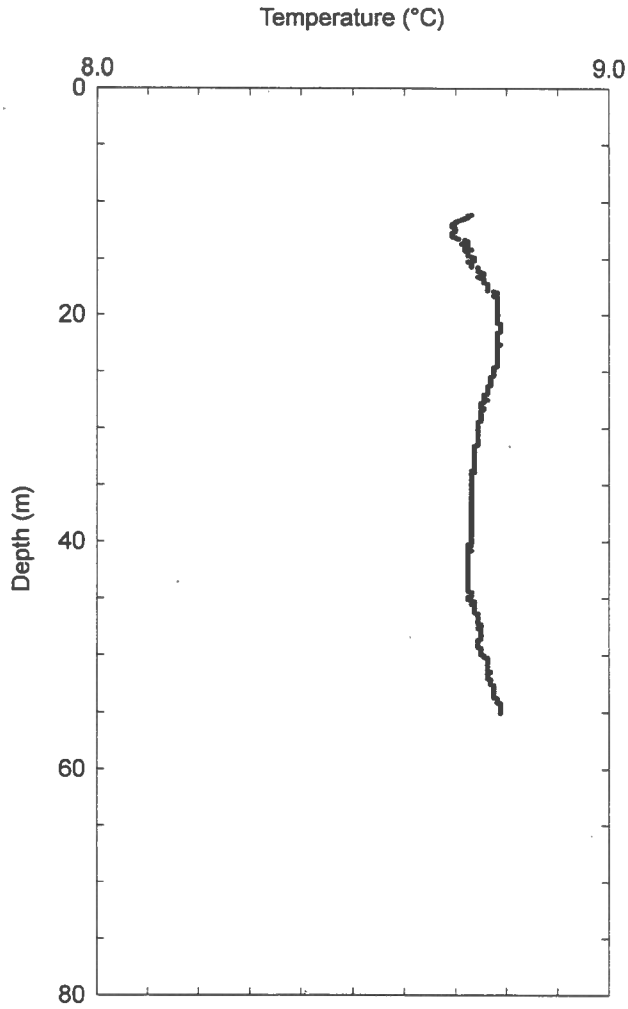

BALES ROAD SOUTH

- 23 August 1993

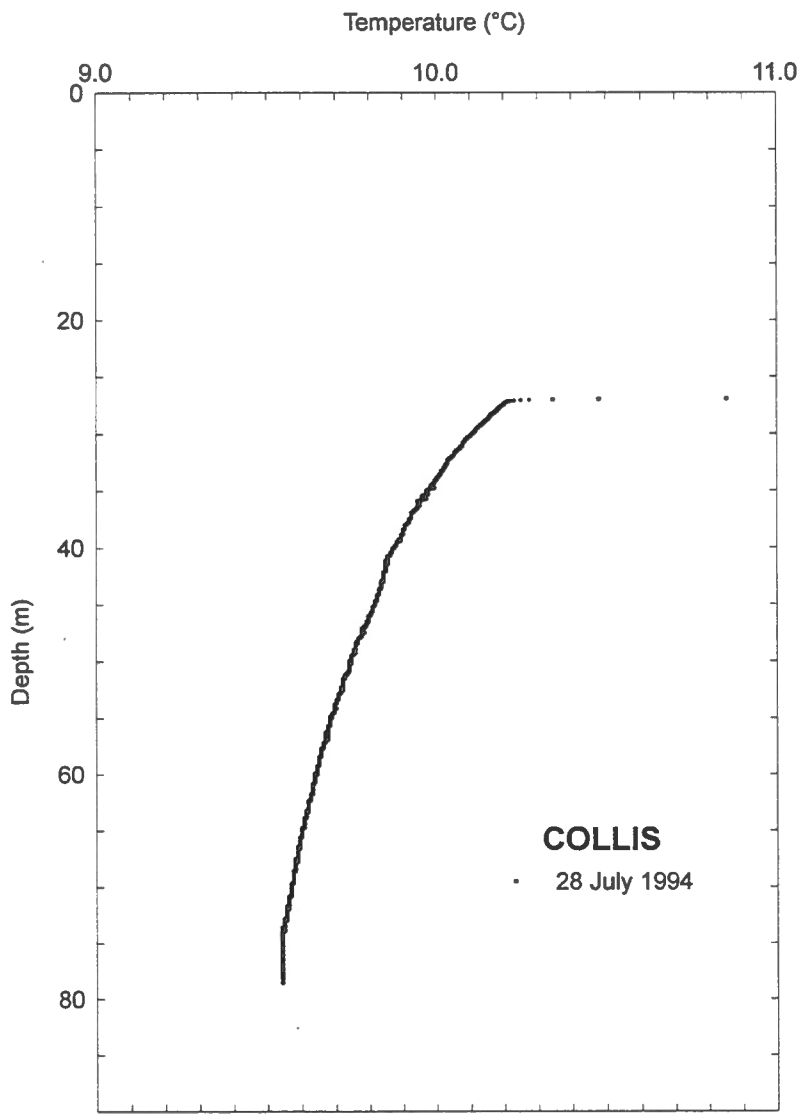
Temperature (°C)
9.0
10.0
11.0
0
20
40
60
80
Depth (m)
COLLIS
28 July 1994

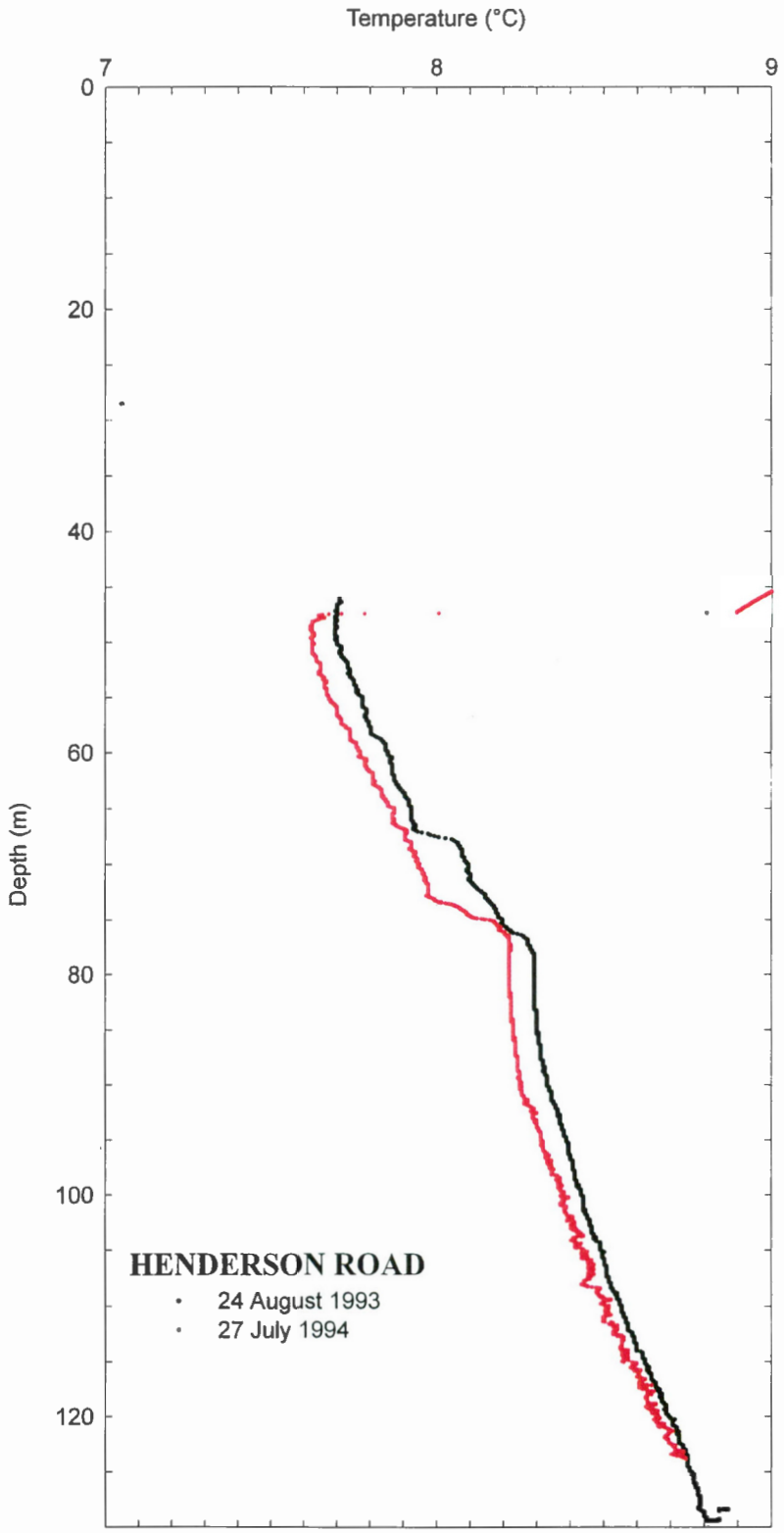
Temperature (°C)
7
8
9
0
20
40
60
80
100
120
Depth (m)
HENDERSON ROAD
24 August 1993
27 July 1994

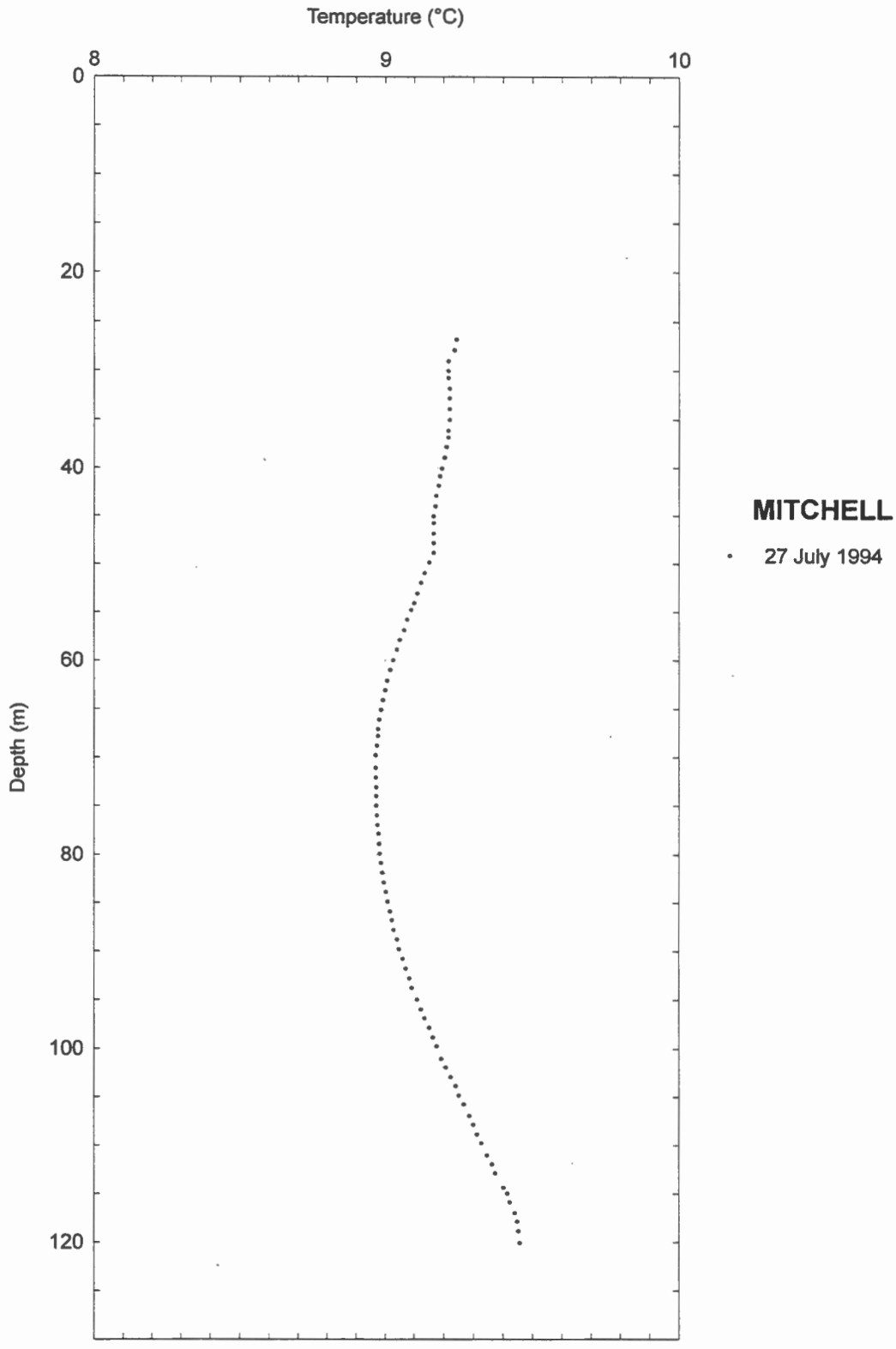
Temperature (°C)
8
9
10
0
20
40
60
80
100
120
Depth (m)
MITCHELL
27 July 1994

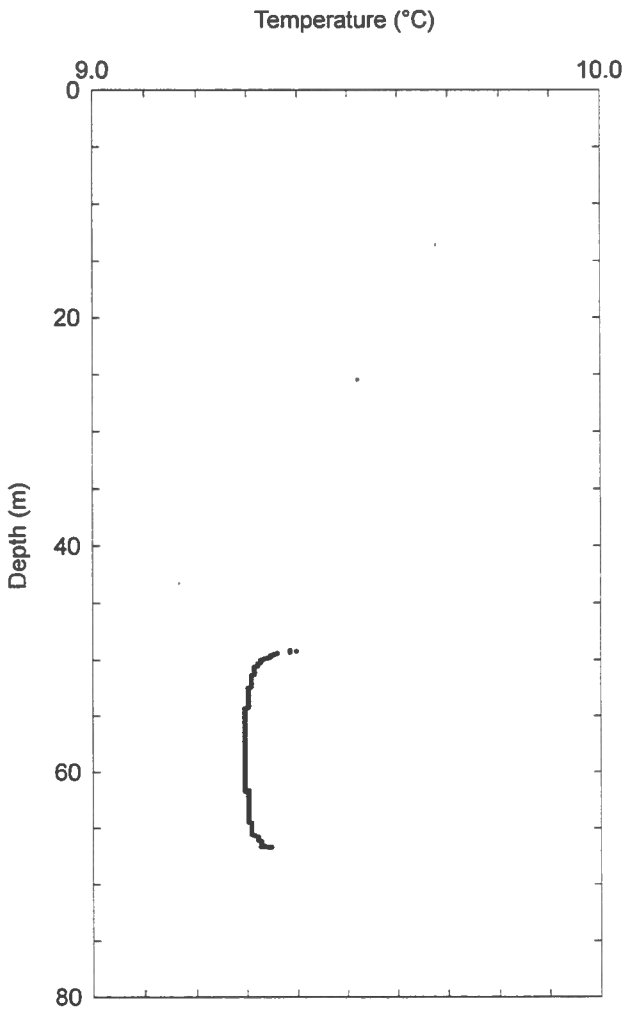

NEWMARKET WELL #2

- 24 August 1993

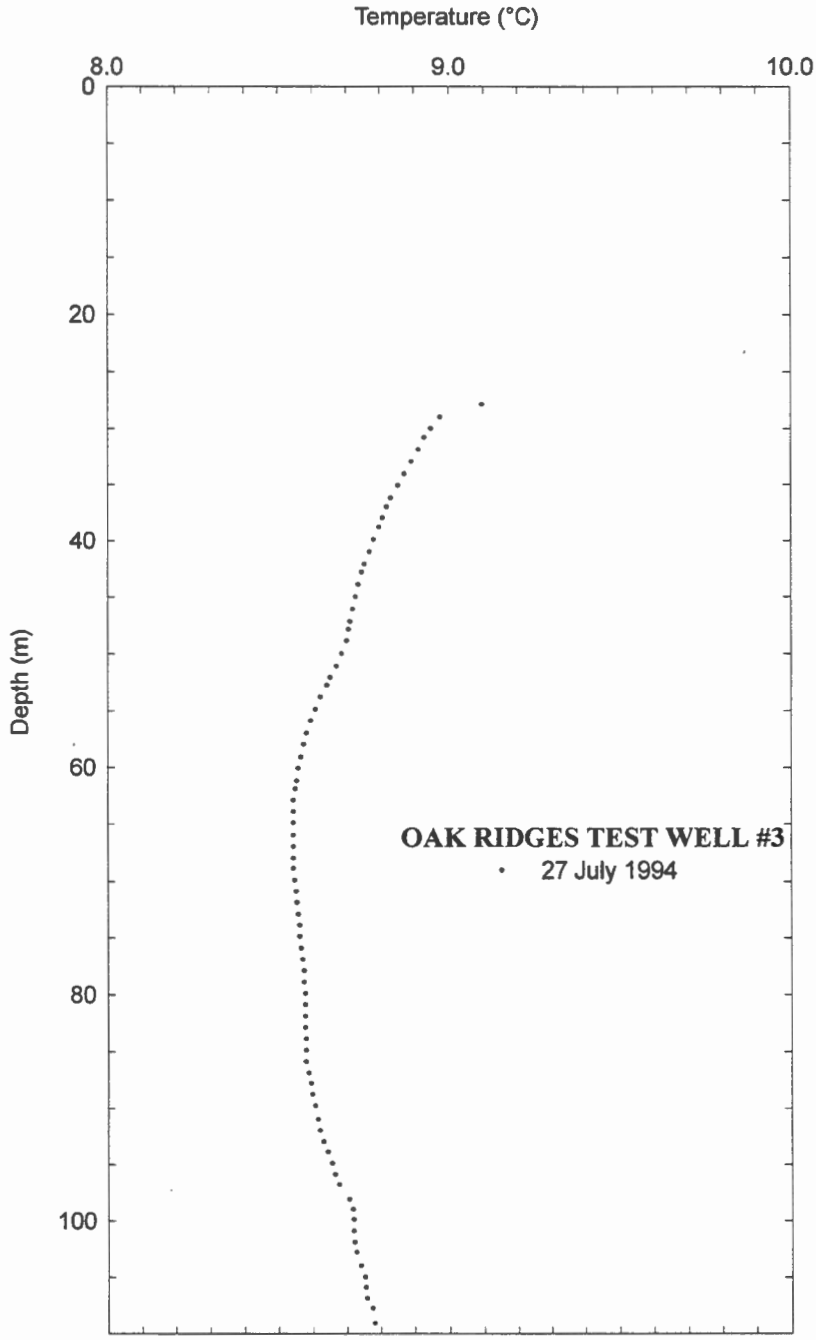
Temperature (°C)
8.0
9.0
10.0
0
20
40
60
80
100
Depth (m)
OAK RIDGES TEST WELL #3
27 July 1994

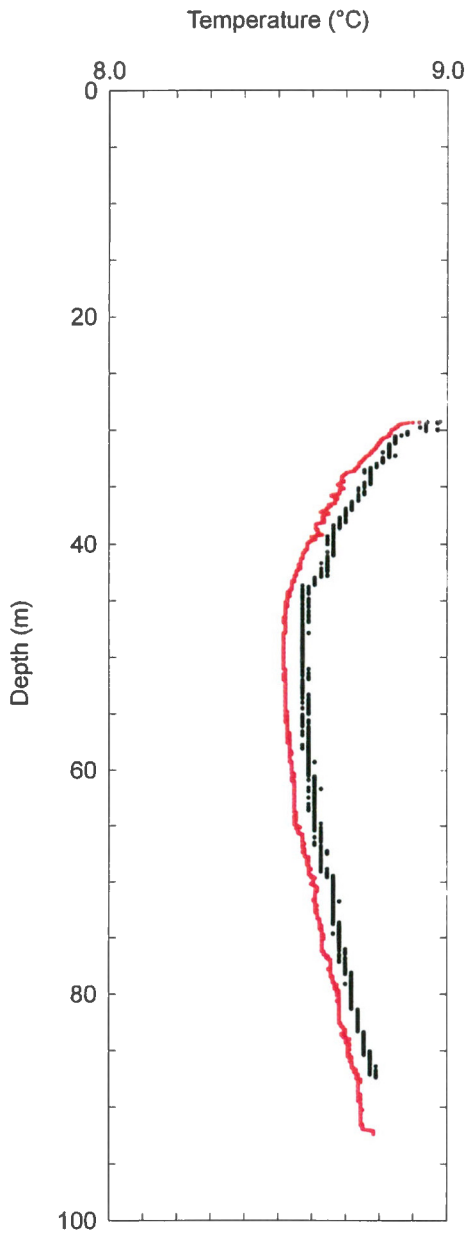

OZARK

- 15 September 1993
- 13 July 1994

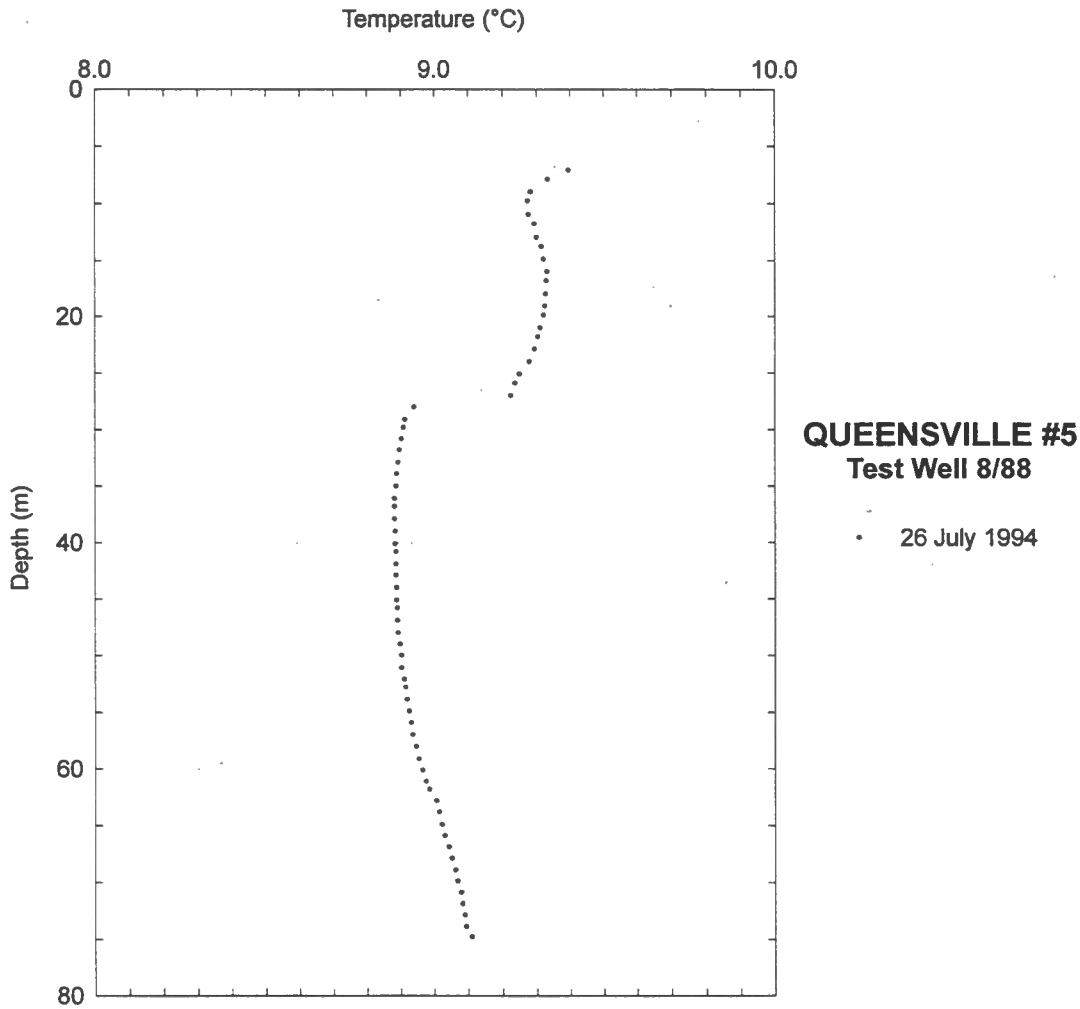
Temperature (°C)
8.0
9.0
10.0
0
20
40
60
80
Depth (m)
QUEENSVILLE #5
Test Well 8/88
26 July 1994

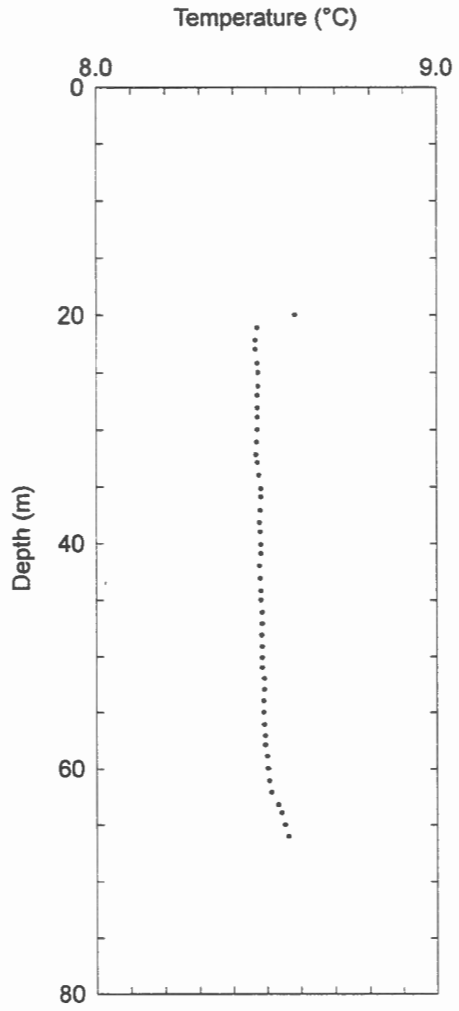

QUEENSVILLE #6
Test Well 2/88

• 26 July 1994

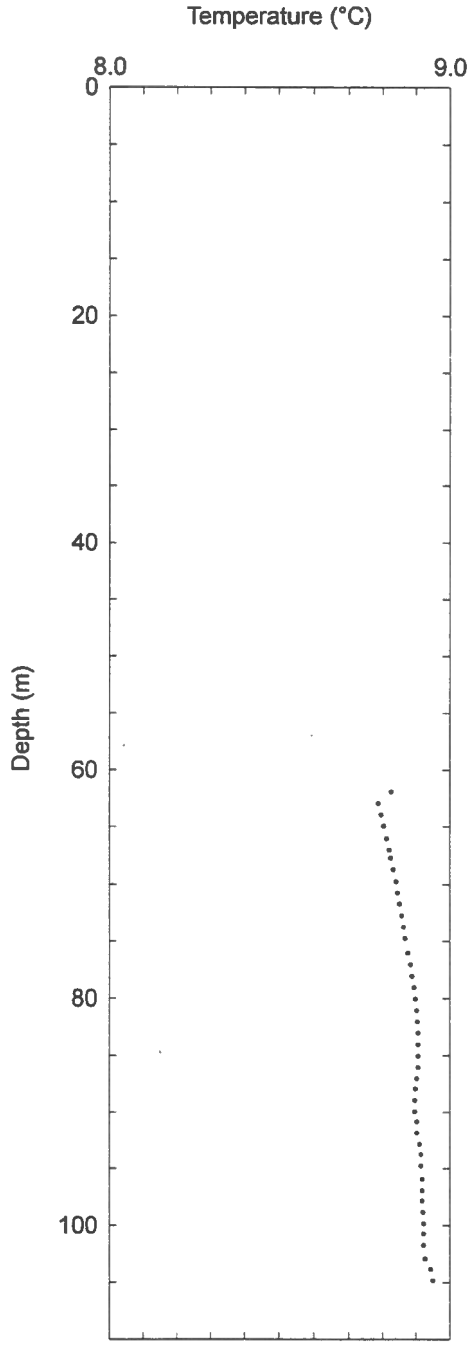

QUEENSVILLE #7
Test Well 9-88

- 26 July 1994

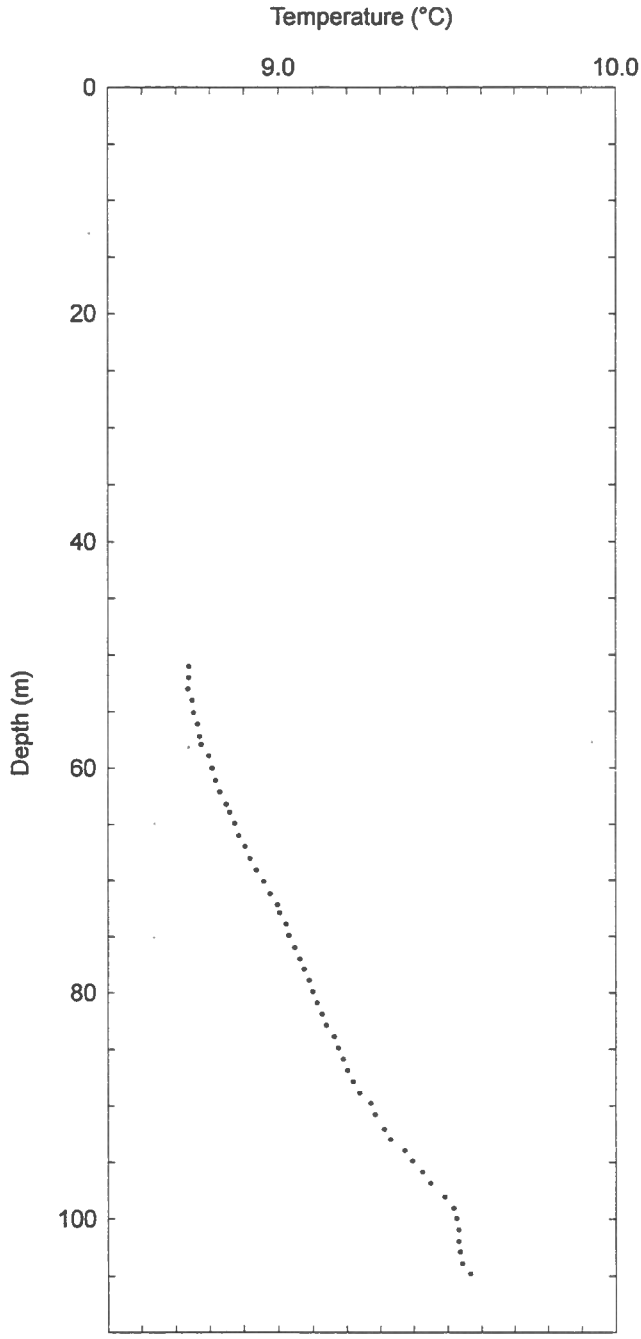

QUEENSVILLE #8
Test Well 10A/82

• 26 July 1994

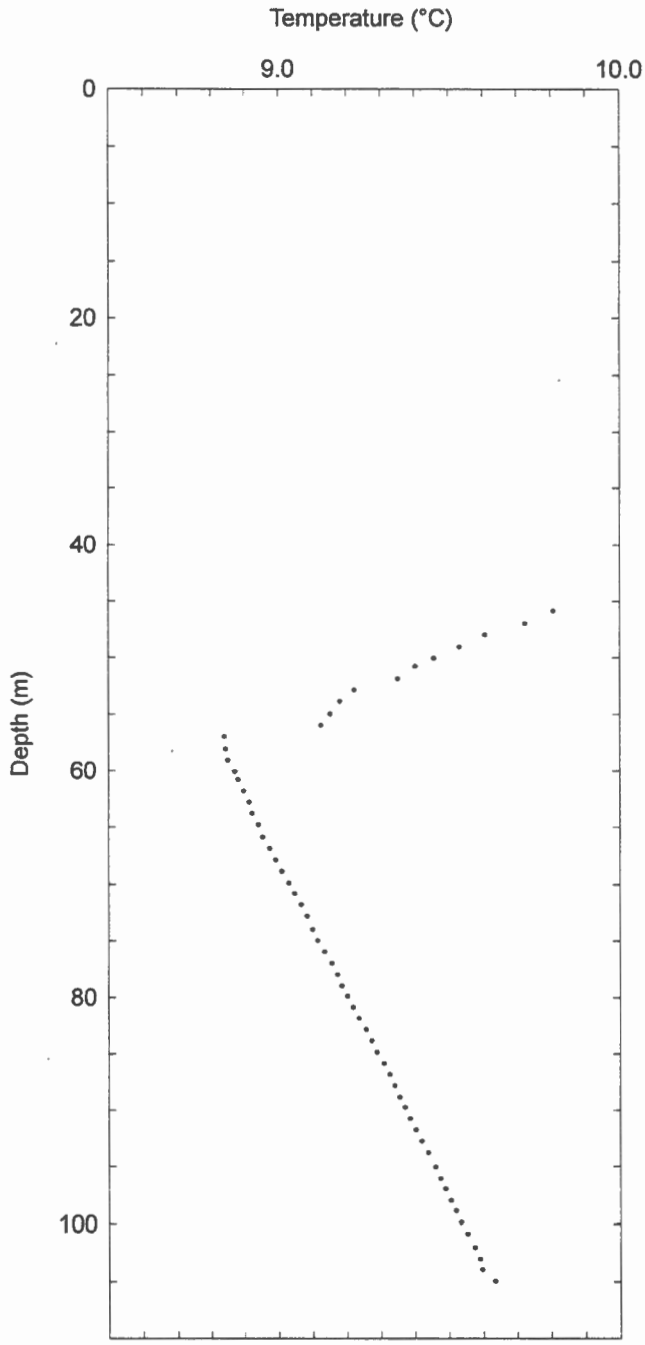

QUEENSVILLE #9
Test Well 1/91

• 28 July 1994

PEEL REGION WELLS

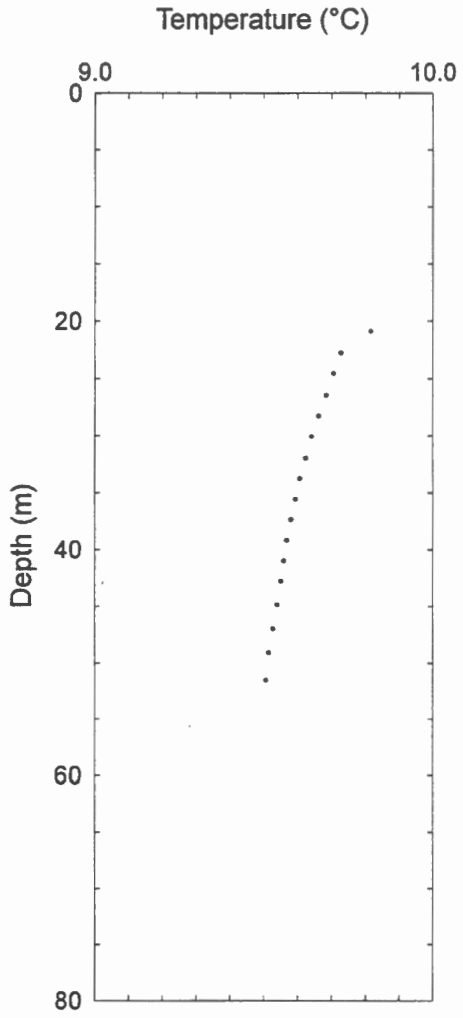

Bolton #4
TW2-72

• 4 August 1994

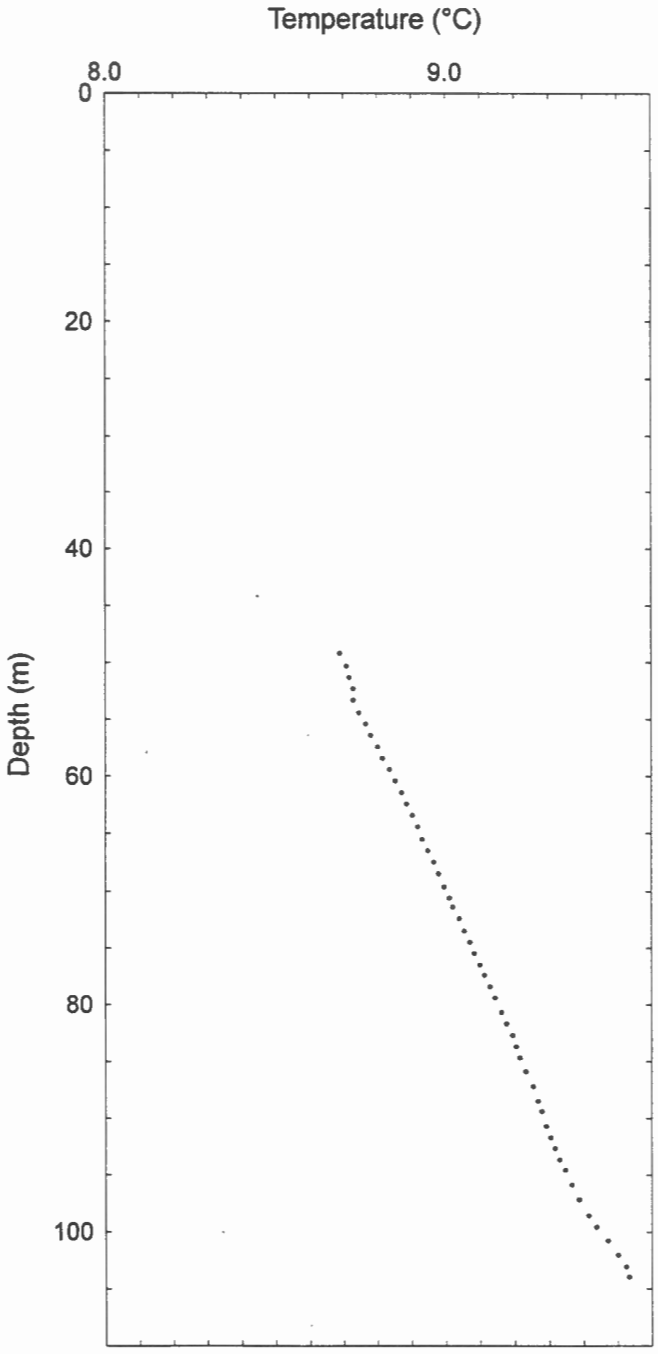

Bolton #6
TW1-88

• 3 August 1994

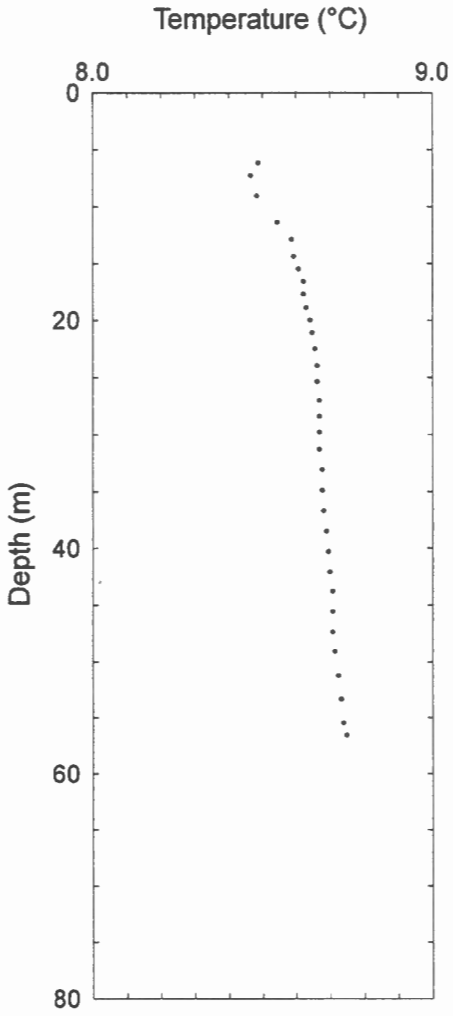

Caledon East #1
Granite Stones

• 3 August 1994

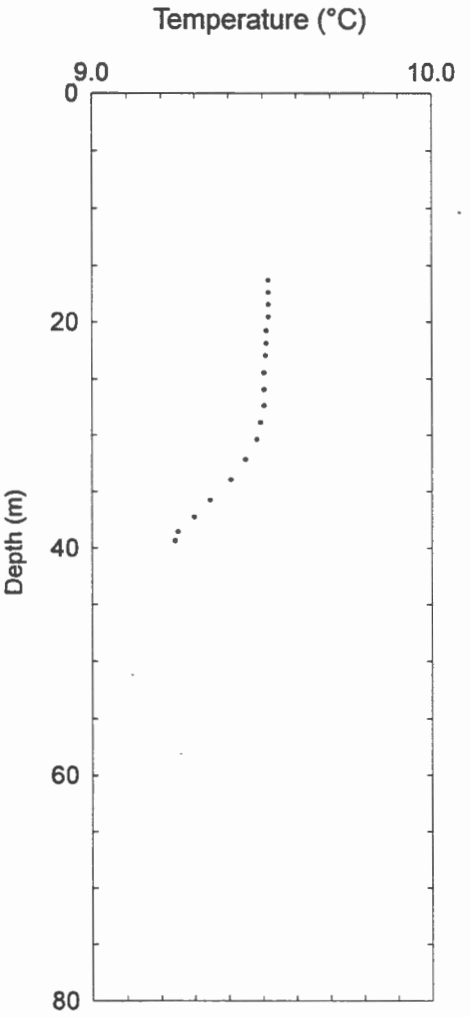

Caledon East #3
TW1-77B

• 4 August 1994

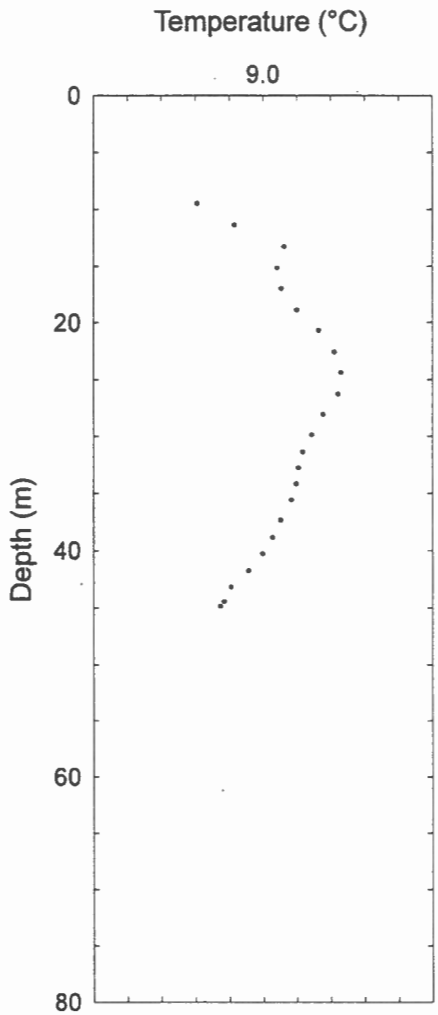

Caledon East #3
TW4-77

• 4 August 1994

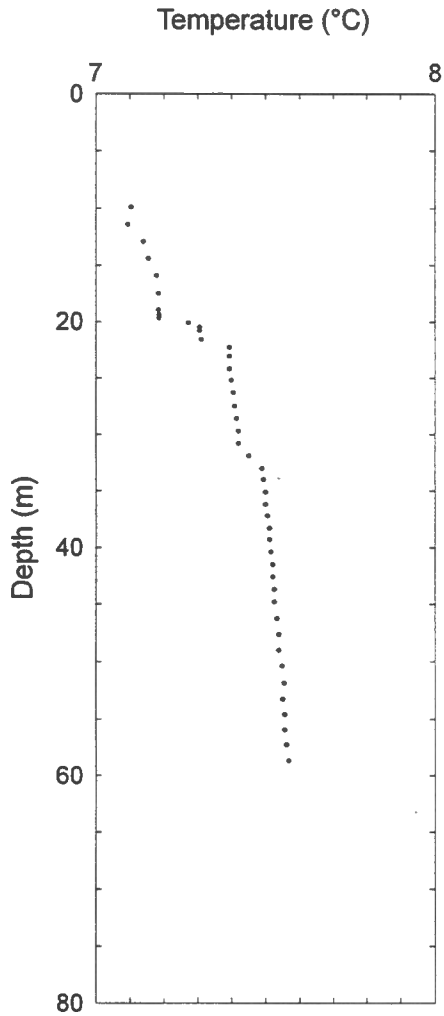

Caledon Well #4

- 5 August 1994

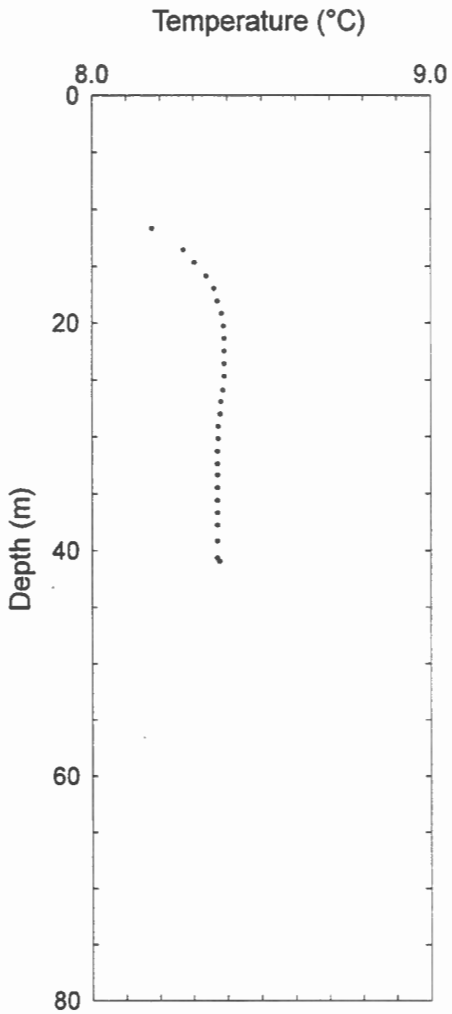

Centreville
Holly Park

• 5 August 1994

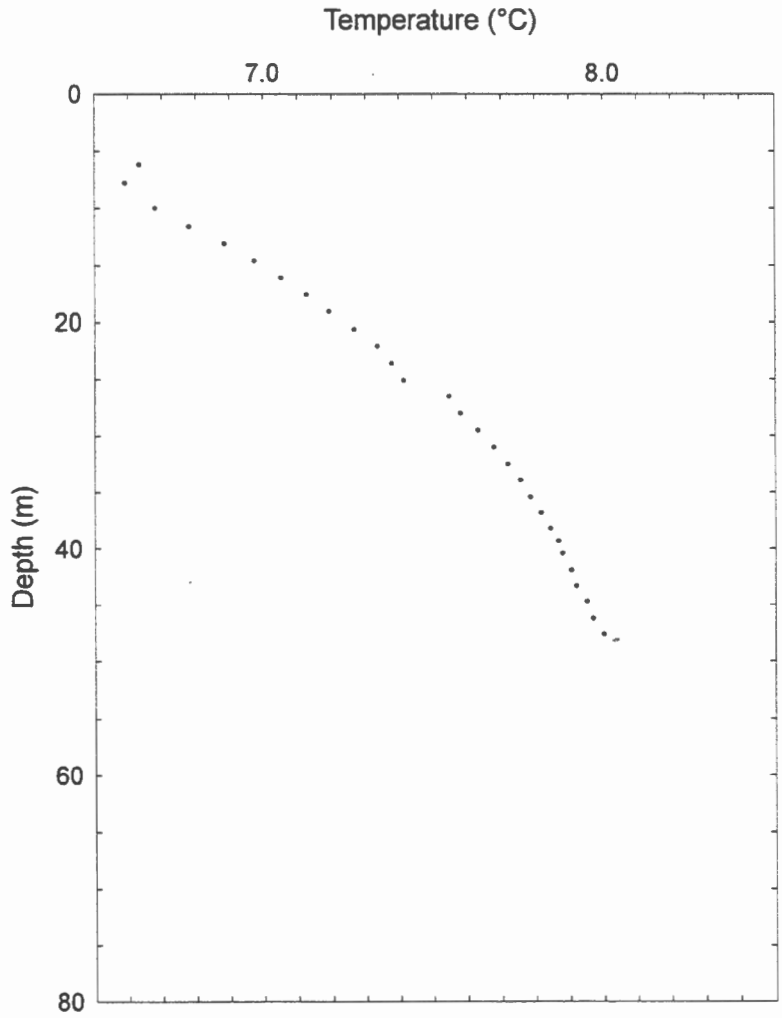

Mono Mills #6
TW2-90

• 5 August 1994

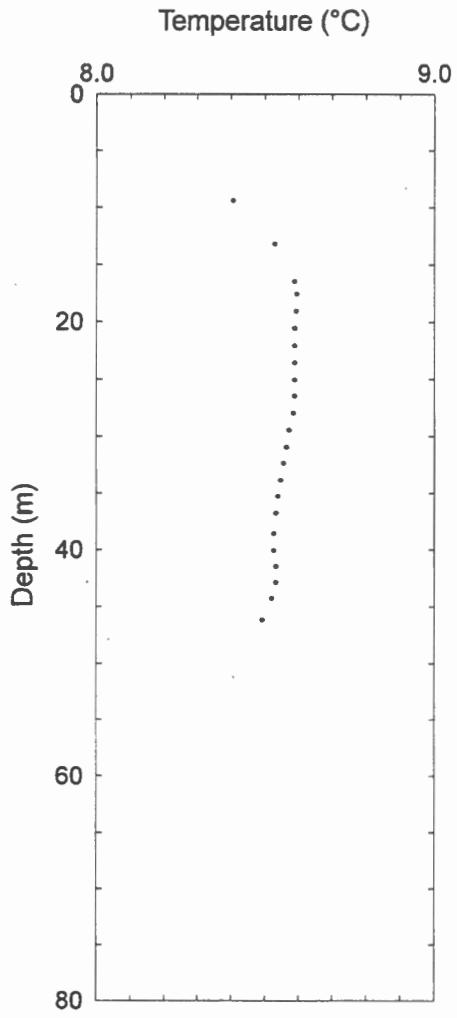

Palgrave #2
TW6-72

• 4 August 1994

DURHAM REGION WELLS

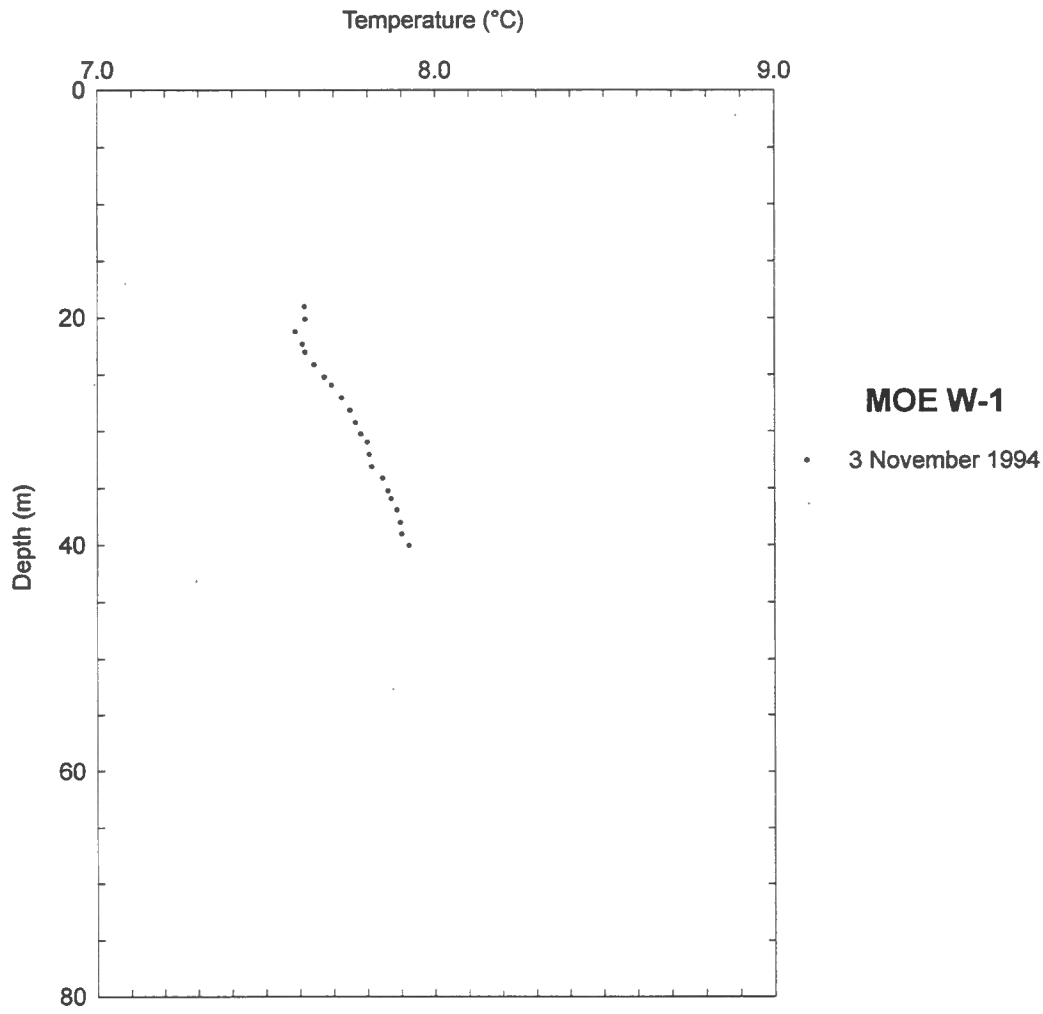
Temperature (°C)
7.0
8.0
9.0
0
20
40
60
80
Depth (m)
MOE W-1
3 November 1994

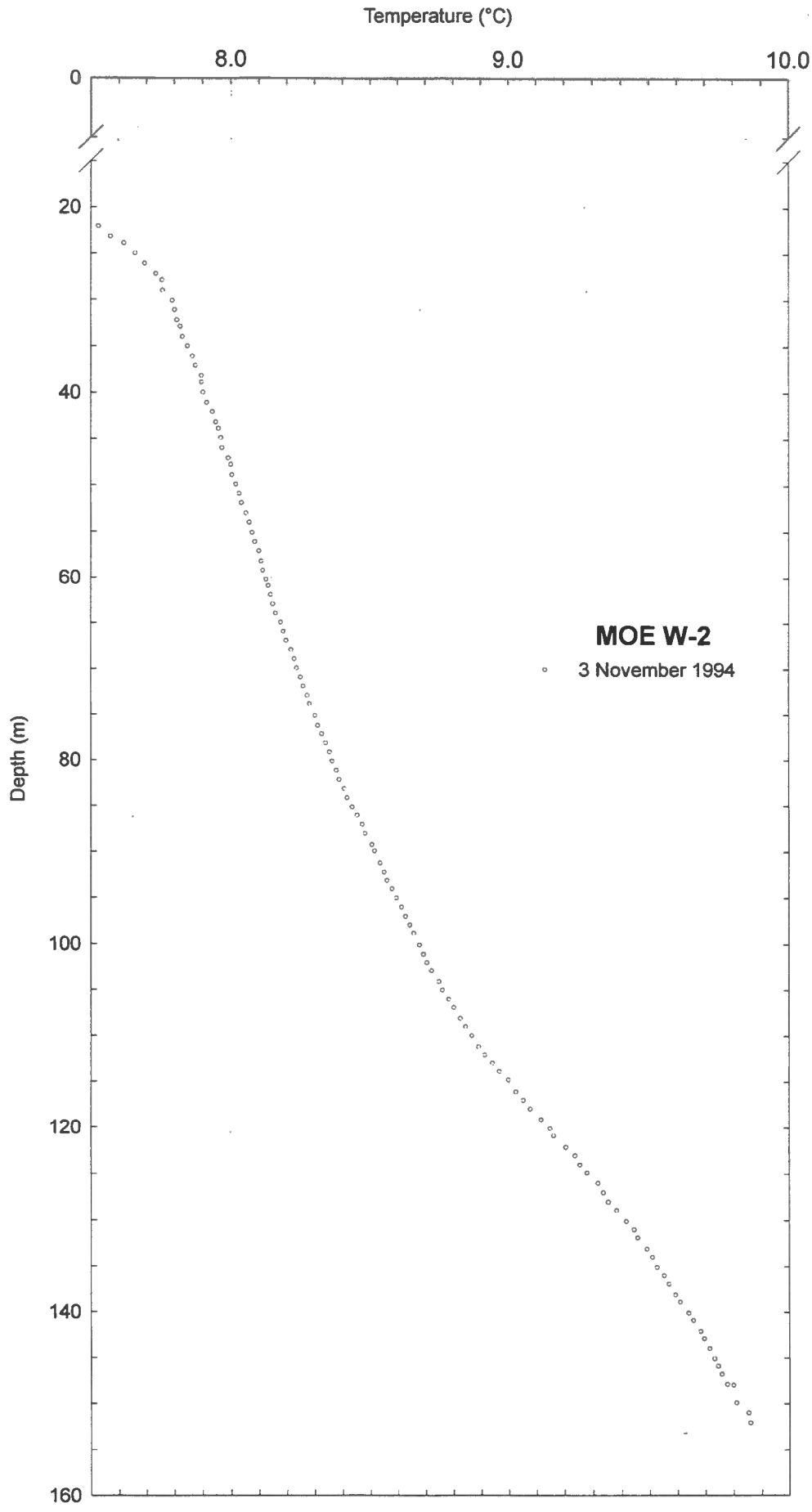
Temperature (°C)
8.0
9.0
10.0
0
20
40
60
80
100
120
140
160
Depth (m)
MOE W-2
3 November 1994

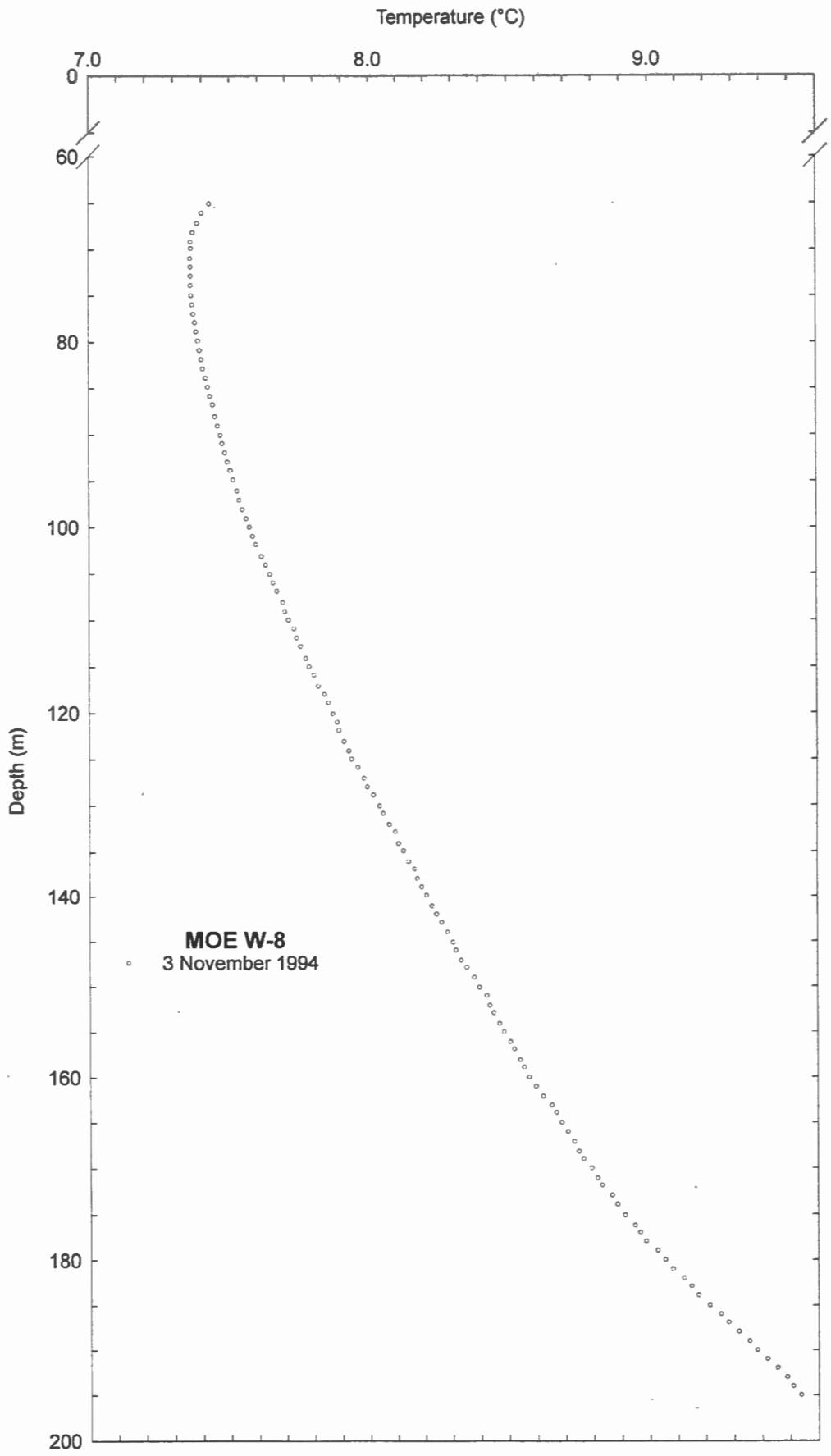
Temperature (°C)
7.0
8.0
9.0
0
60
80
100
120
140
160
180
200
Depth (m)
MOE W-8
3 November 1994

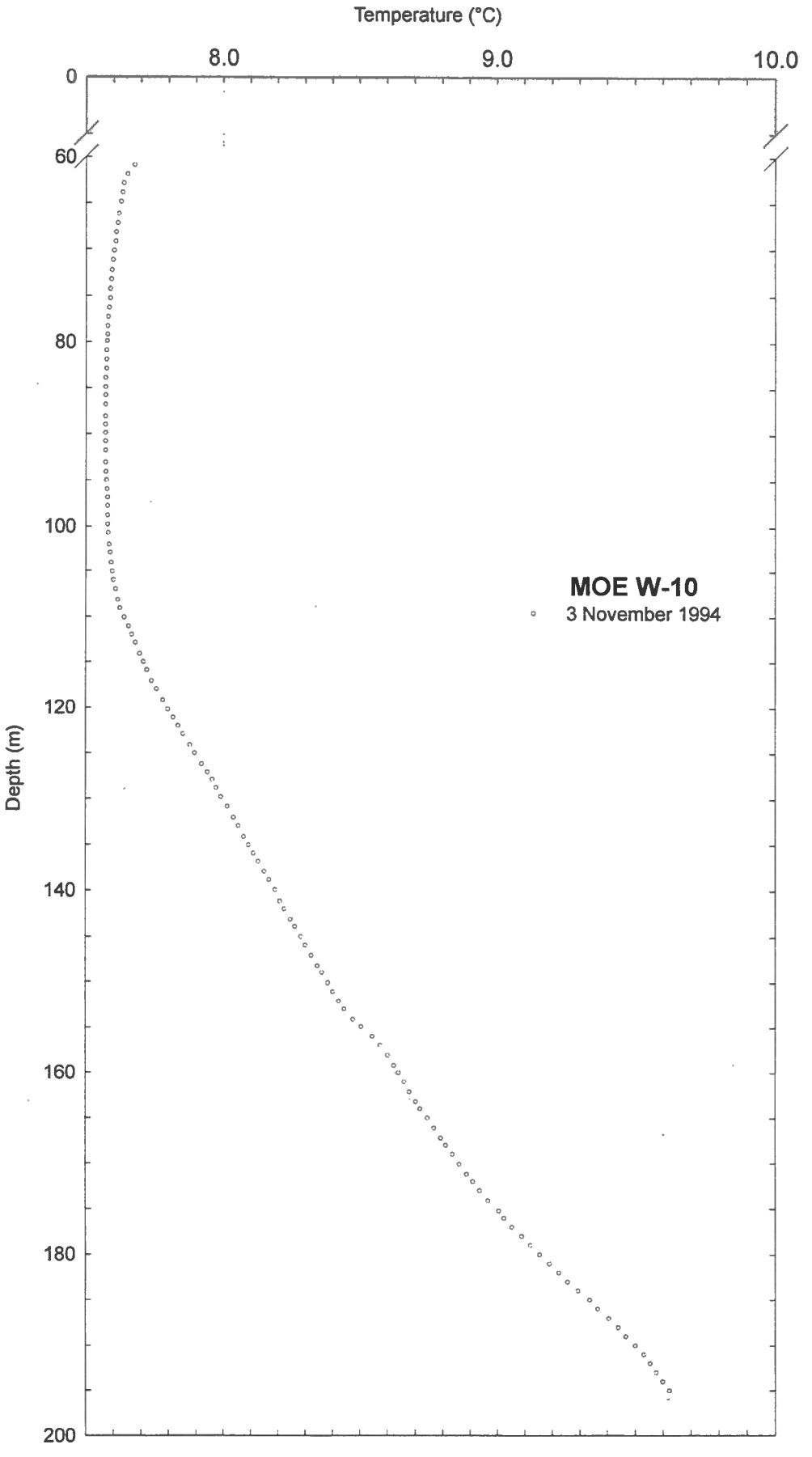
Temperature (°C)
8.0
9.0
10.0
0
60
80
100
120
140
160
180
200
Depth (m)
MOE W-10
3 November 1994

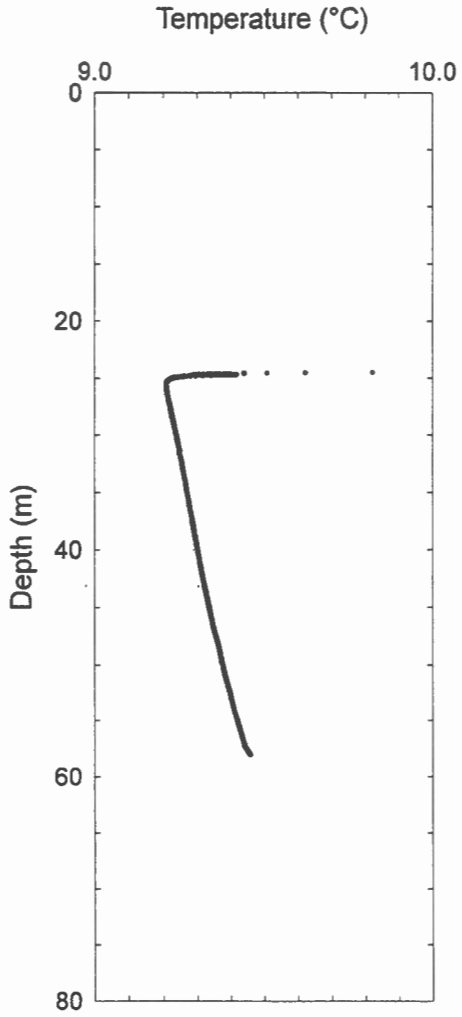

Whitevale
P1-16D

• 15 May 1995

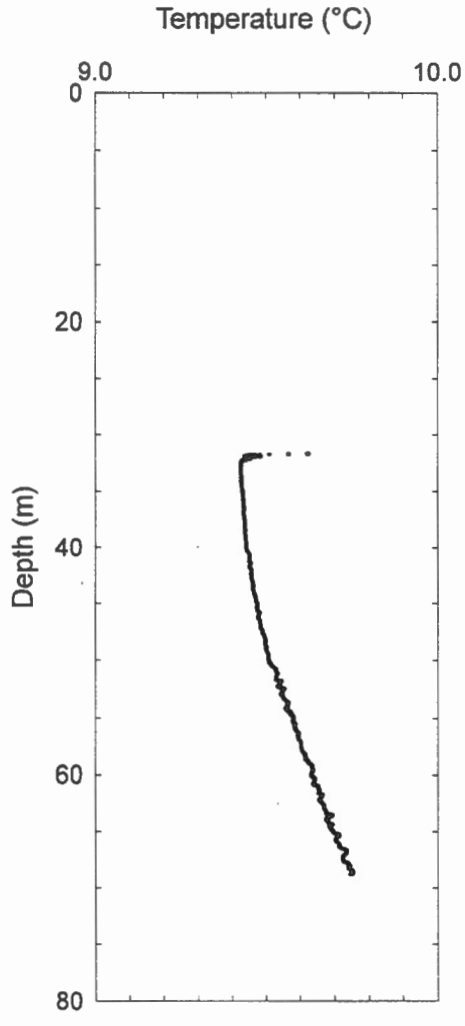

Whitevale
P1-26D

• 17 May 1995

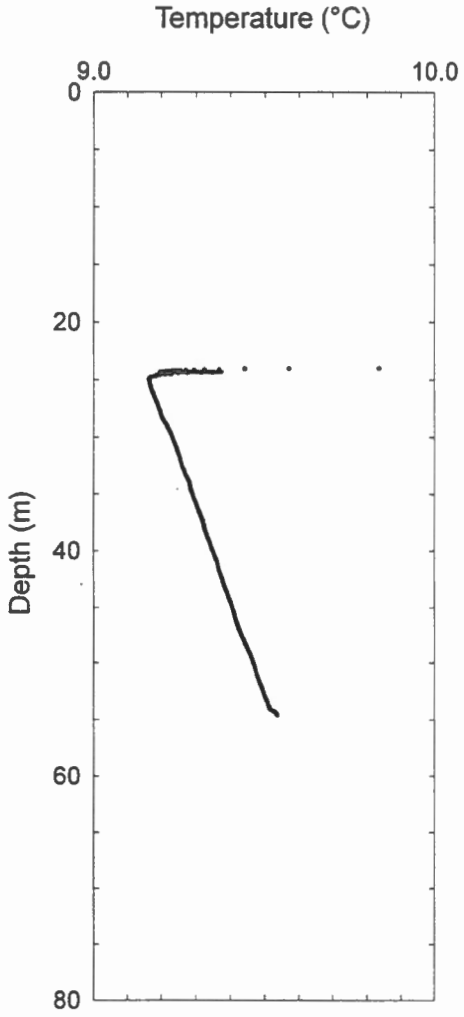

Whitevale
P1-29B

• 16 May 1995

Appendix C

Some examples on the application of temperature logs in hydrogeology

Compiled by Al Taylor

Completion of holes

In the literature, details of hole completion are frequently not explicitly stated but can sometimes be inferred from the effect described or the analysis technique used. Generally, holes can be described by three types of completion:

1. Grouted and cased hole through rock or unconsolidated material. Temperature profiles will detect vertical groundwater flow through the pore volume and flow in permeable beds or fractures. This is the ideal case. Theory assumes "cased hole".

2. Uncased hole through competent soils or rock. Temperature profile will detect flows in permeable beds and through fractures. Both may leak into the borehole and cause vertical flow within hole. The thermal signature of water flowing within the well is distinct from the thermal effect of water moving entirely within the formation, and theories have to consider the two components separately. Flow rate may interfere with lowering a temperature probe.

3. Grouted and cased hole with screens or leaking joints, or poorly grouted with flow outside casing.

Selected Bibliography

Andrews, C.B. (1978). The impact of the use of heat pumps on ground-water temperatures. Ground Water, 16, p. 437-443.

Andrews, C.B. and Anderson, M.P. (1979). Thermal alteration of groundwater caused by seepage from a cooling lake. Water Resources Research, 15, p. 595-602.

Andrews-Speed, C.P., Oxburgh, E.R., and Cooper, B.A. (1984). Temperatures and depth-dependent heat flow in western North Sea. American Association of Petroleum Geologists Bulletin, 68, p. 1764-1781.

Bair, E.S. and Parizek, R.R. (1978). Detection of permeability variations by a shallow geothermal technique. Ground Water, 16, p. 254-263.

Beck, A.E. and Shen, P.Y. (1985). Temperature distribution in flowing liquid wells. Geophysics, 50, p. 1113-1118.

Bodvarsson, G. (1973). Temperature inversions in geothermal systems. Geoexploration, 11, p. 141-149.

Boyle, J.M. and Saleem, Z.A. (1979). Determination of recharge rates using temperature-depth profiles in wells. Water Resources Research, 15, p. 1616-1622.

Bredehoeft, J.D. and Papadopulos, I.S. (1965). Rates of vertical groundwater movement estimated from the Earth's thermal profile. Water Resources Research, 1, p. 325-328.

Burgess, M.M. (1986). A discussion of non-linear temperature profiles at six closely spaced heat flow sites, southern Sohm Abyssal Plain, northwest Atlantic Ocean. Deep-Sea Research, 33, p. 1213-1224.

Cartwright, K. (1968). Thermal prospecting for ground water. Water Resources Research, 4, p. 395-401.

Cartwright, K. (1970). Groundwater discharge in the Illinois basin as suggested by temperature

anomalies. Water Resources Research, 6, p. 912-918.

Cartwright, K. (1971). Redistribution of geothermal heat by a shallow aquifer. Geological Society of America Bulletin, 82, p. 3197-3200.

Cartwright, K. (1974). Tracing shallow groundwater systems by soil temperatures. Water Resources Research, 10, p. 847-855.

Chapman, D.S., Kilty, K.T., and Mase, C.W. (1978). Temperatures and their dependence on groundwater flow in shallow geothermal systems. Geothermal Resources Council, Transactions, 2, p. 79-82.

Chen, C. and Reddell, D.L. (1983). Temperature distribution around a well during thermal injection and a graphical technique for evaluating aquifer thermal properties. Water Resources Research, 19, p. 351-363.

Domenico, P.A. and Palciauskas, V.V. (1973). Theoretical analysis of forced convective heat transfer in regional ground-water flow. Geological Society of America Bulletin, 84, p. 3803-3814.

Drury, M.J. (1984). Borehole temperature logging for the detection of water flow. Geoexploration, 22, p. 231-243.

Drury, M.J. (1984). Perturbations to temperature gradients by water flow in crystalline rock formations. Tectonophysics, 103, p. 19-32.

Drury, M.J. and Lewis, T.J. (1983). Water movement within Lac du Bonnet batholith as revealed by detailed thermal studies of three closely-spaced boreholes. Tectonophysics, 95, p. 337-351.

Drury, M.J., Jessop, A.M., and Lewis, T.J. (1984). The detection of groundwater flow by precise temperature measurements in boreholes. Geothermics, 13, p. 163-174.

Gosnold, W.D. (1985). Heat flow and ground water flow in the Great Plains of the United States. Journal of Geodynamics, 4, p. 247-264.

Jessop, A.M. (1987). Estimation of lateral water flow in an aquifer by thermal logging.

Geothermics, 16, p. 117-126.

Jessop, A.M., Lewis, T.J., Judge, A.S., Taylor, A.E., and Drury, M.J. (1984). Terrestrial heat flow in Canada. Tectonophysics, 103, p. 239-261.

Kayane, I., Taniguchi, M., and Kazuhiro, S. (1985). Alteration of the groundwater thermal regime caused by advection. Hydrological Sciences Journal, 30, p. 343-359.

Keys, W.S. and Brown, R.F. (1978). The use of temperature logs to trace the movement of injected water. Ground Water, 16, p. 32-48.

Kilty, K. and Chapman, D.S. (1980). Convective heat transfer in selected geologic situations. Ground Water, 18, p. 386-394.

Lu, N. and Ge, S. (1996). Effect of horizontal heat and fluid flow on the vertical temperature distribution in a semiconfining layer. Water Resources Research, 32, p. 1449-1453.

Mansure, A.J. and Reiter, M. (1979). A vertical groundwater movement correction for heat flow. Journal of Geophysical Research, 84, p. 3490-3496.

Noel, M. (1983). Origins and significance of non-linear temperature profiles in deep-sea sediments. Geophysical Journal of the Royal Astronomical Society, 76, p. 673-690.

Parson, M.L. (1970). Groundwater thermal regime in a glacial complex. Water Resources Research, 6, p. 1701-1720.

Ramey, H.J. (1962). Wellbore heat transmission. Journal of Petroleum Technology, 14, p. 427-435.

Reiter, M., Costain, J.K., and Minier, J. (1989). Heat flow data and vertical groundwater movement, examples from southwestern Virginia. Journal of Geophysical Research, 94, p. 12,423-12,431.

Smith, L. and Chapman, D.S. (1983). On the thermal effects of groundwater flow, 1. Regional scale systems. Journal of Geophysical Research, 88, p. 593-608.

Sorey, M.L. (1971). Measurement of vertical groundwater velocity from temperature profiles in wells. Water Resources Research, 7, p. 963-970.

Stallman, R.W. (1963). Computation of ground-water velocity from temperature data. USGS Water Supply Paper 1544-H, p. 36-46.

Stallman, R.W. (1965). Steady one-dimensional fluid flow in a semi-infinite porous medium with sinusoidal surface temperature. Journal of Geophysical Research, 70, p. 2821-2827.

Taniguchi, M. (1993). Evaluation of vertical groundwater fluxes and thermal properties of aquifers based on transient temperature-depth profiles. Water Resources Research, 29, p. 2021-2026.

Welch, L.R. (1997). Thermal monitoring of seepage at Fontenelle Dam. *in* Mahoney, Daniel J., ed., Waterpower '97, Proceedings of the International Conference on Hydropower, Atlanta, Georgia, Aug. 5-8, 1997. American Society of Civil Engineers, New York, v. 1, p. 786-795.

Woodbury, A.D. and Smith, L. (1985). On the thermal effects of three-dimensional groundwater flow. Journal of Geophysical Research, 90, p. 759-767.

Woodbury, A.D. and Smith, L. (1987). Simultaneous inversion of hydrogeologic and thermal data, 1. Theory and application using hydraulic head data. Water Resources Research, 23, p. 1586-1606.

Woodbury, A.D., Narod, B., Chandra, B., and Bennest, J.R. (1991). Temperature measurements in geotechnical studies using low-noise, high-resolution digital techniques. Canadian Geotechnical Journal, 28, p. 639-649.

Ziagos, J.P. and Blackwell, D.D. (1981). A model for the effect of horizontal fluid flow in a thin aquifer on temperature-depth profiles. Geothermal Resources Council, Transactions, 5, p. 221-223.

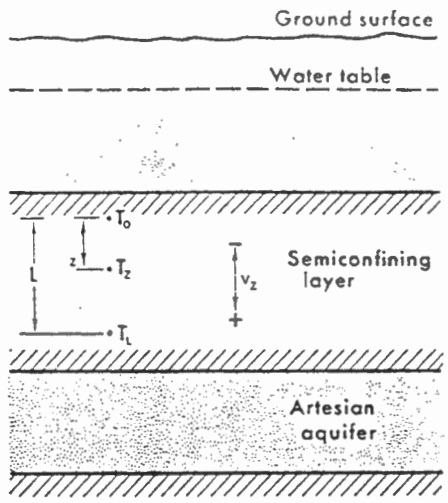

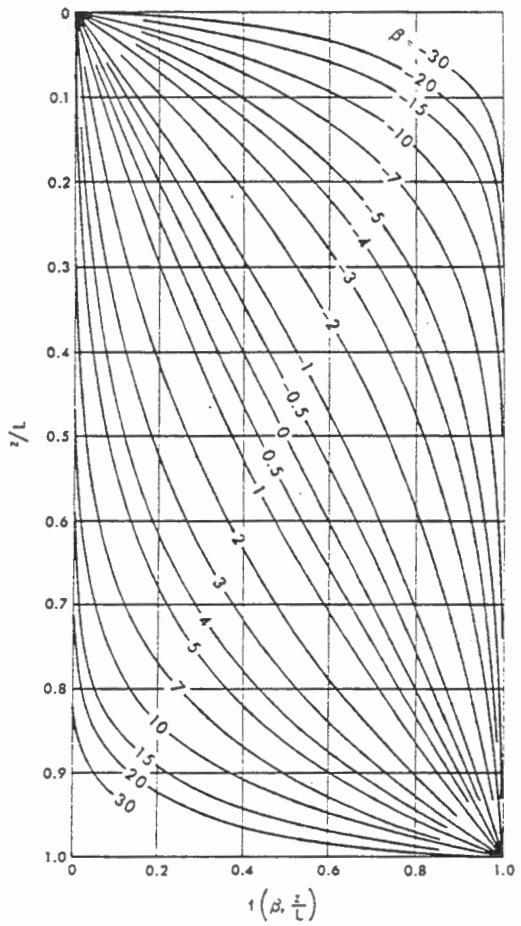

Fig. 2. Type curves of the function $f(\beta, z\ L)$.

Classic model of aquifer, leaky to surface through a semiconfining layer. Nomogram of type curves (essentially normalized depth-normalized temperature graph) for manually fitting ground temperatures. B=0, no vertical flow; B<0, flow upwards; B>0, flow downwards. (Fig. 1, 2; Bredehoeft and Papadopoulos, 1965).

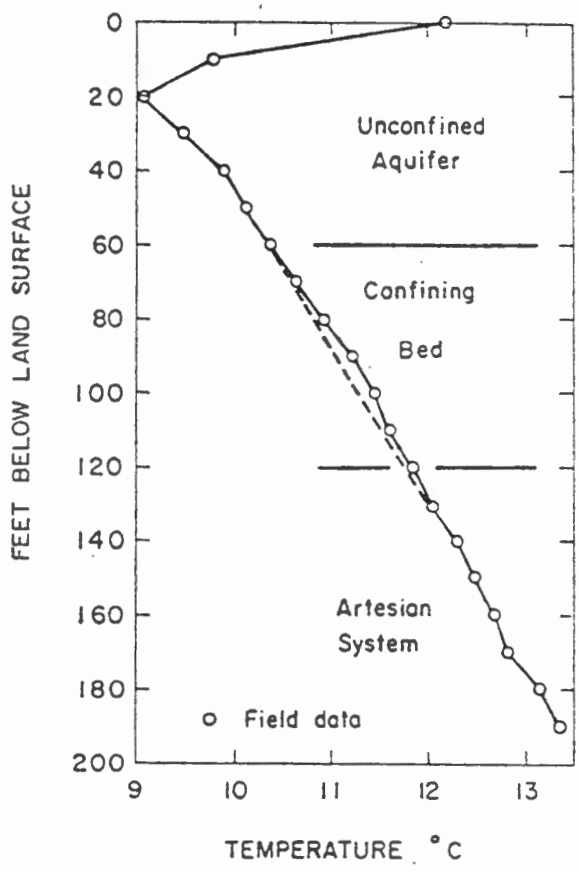

Fig. 3. Temperature profile and hydrologic section at site near Alamosa, Colorado, showing curvature for upward flow through the confining bed.

Thermal profile in 2" plastic, oil filled pipe in the San Luis Valley, Colorado. Aquifers consist of sand clay deposits, confining bed of clay with sand lenses. Profile exhibits downward concavity 60'-140' bridging the clay confining bed. This is interpreted in terms of upward flow of water between aquifers at a rate of 12 nm/s (0.4 m/year). A similar calculation was made at a well 60 km north and both rates agree well with a basin wide estimate. (Fig. 3; Sorey, 1971).

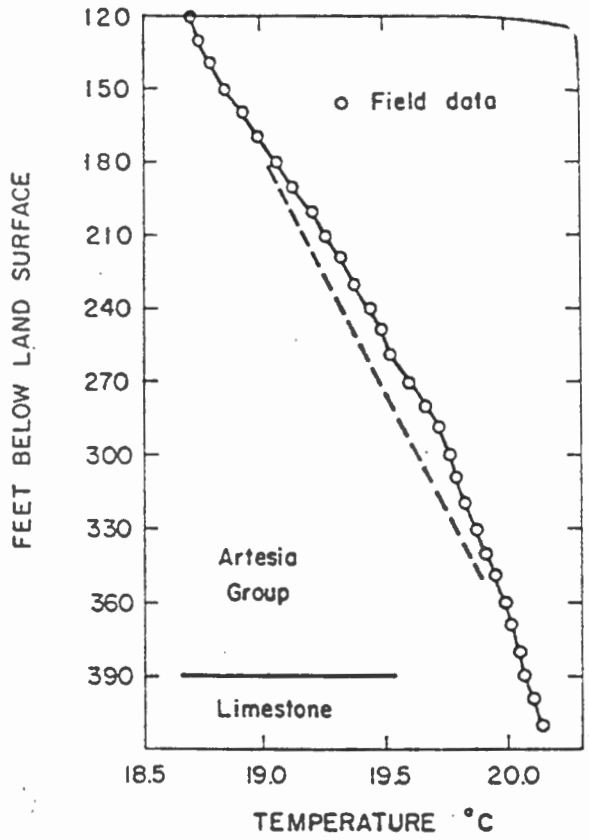

Fig. 5. Temperature profile in well PVACD 10 located 15 miles north of Roswell, New Mexico, showing curvature for upward flow through the Artesia group semiconfining bed.

Temperature profile in a well in New Mexico. The limestone aquifer is overlain by interbedded clay, silt, limestone and gypsum (Artesia group) that forms a semiconfining bed over most of the basin. Some of the curvature is due to the higher thermal conductivity of the limestone; however the downward concavity within the Artesia is interpreted in terms of upward leakage of water from the limestone aquifer at a rate of 8.2 nm/s (0.25 m/year). Pumping tests in the basin yield similar values. (Fig. 5; Sorey, 1971).

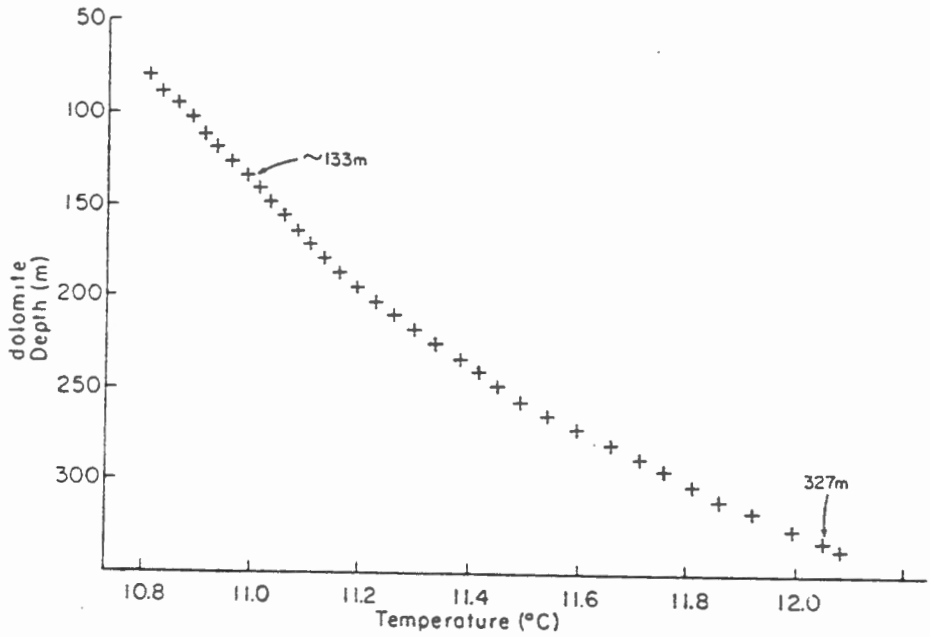

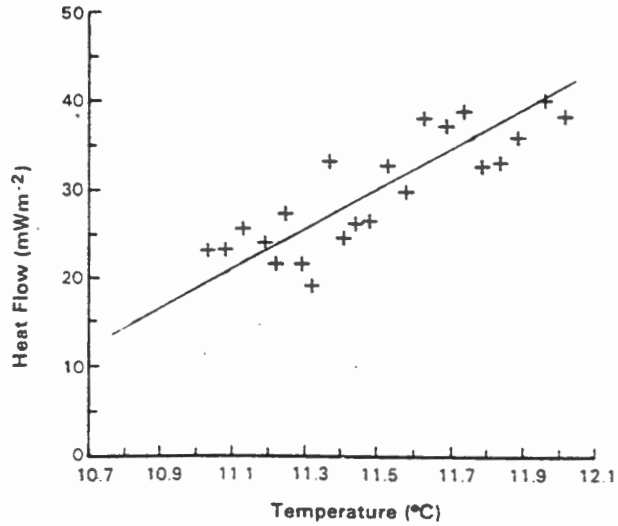

Fig. 3b. Well site B, heat flow temperature plot. Slope for all data is 19.1 ± 2.6 mW m^{-2} $^{o}C^{-1}$ (145-327 m).

Temperature profile from hilly terrane in dolomite of the Valley and Ridge province of southwest Virginia. Concave upward curvature below 133 m has been interpreted in terms of downward water movement of 4.6 nm/s (0.15 m/year). Vertical (upward) heat flow at bottom of hole is much greater than above 133 m (compare temperature-depth gradients); this excess is balanced by the heat carried by the downward flow of water. Theory indicates that in zone of flow, plot of temperature gradient (or heat flow) versus temperature is a straight line. (Fig. 3a,b; Reiter, Costain and Minier, 1989).

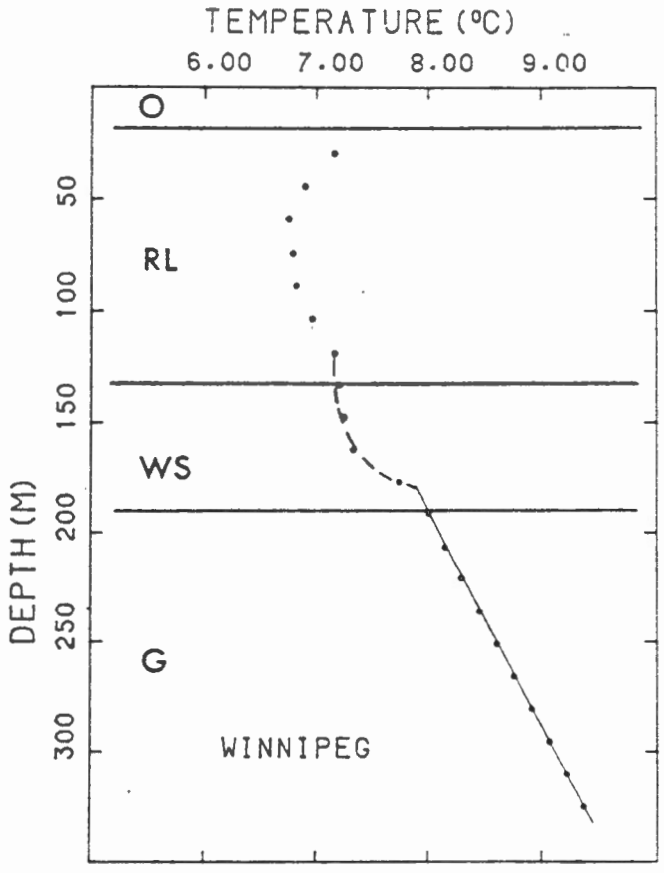

Downward flow of water at rate 120 nm/s (4 m/year) through a loose sand "WS"; water originates in the lower part of a limestone formation ("RL"). The temperature inversion above 100 m is due to climate warming over the past century. (Fig. 2; Drury et al., 1984).

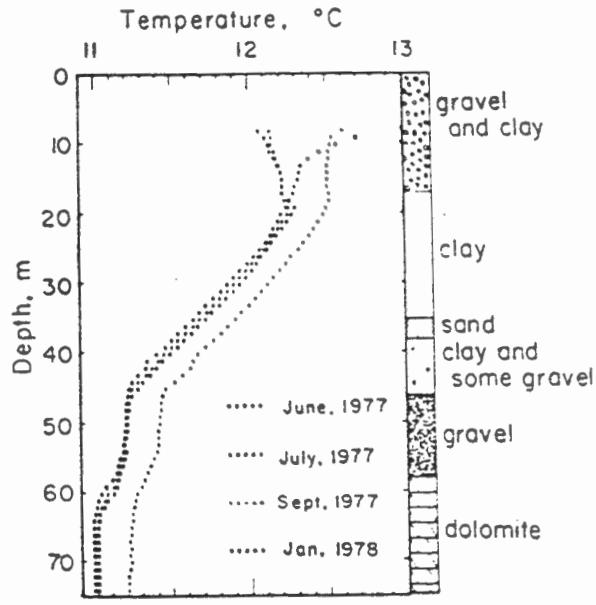

TABLE 2. Recharge Rates v_z for Various Thicknesses L Within the Aquitard as Determined by the Temperature Method

	v_z, $\times 10^{-9}$ m/s			
L, m*	June	July	Sept.	Jan.
16	7.50	8.96	6.08	9.86
19	6.39	7.43	5.57	7.88
27	3.10	3.18	2.47	2.90

*Extending downward from a point 19 m below the ground surface.

A concave-up character in a temperature profile through a clay aquitard from an abandoned water well in Illinois has been used to calculate seasonal changes in recharge rate of a lower aquifer. Rates were lowest in September (2.9 nm/s or 0.01 m/year) and highest in July and January. (Fig. 4 and Table 2; Boyle and Saleem, 1979).

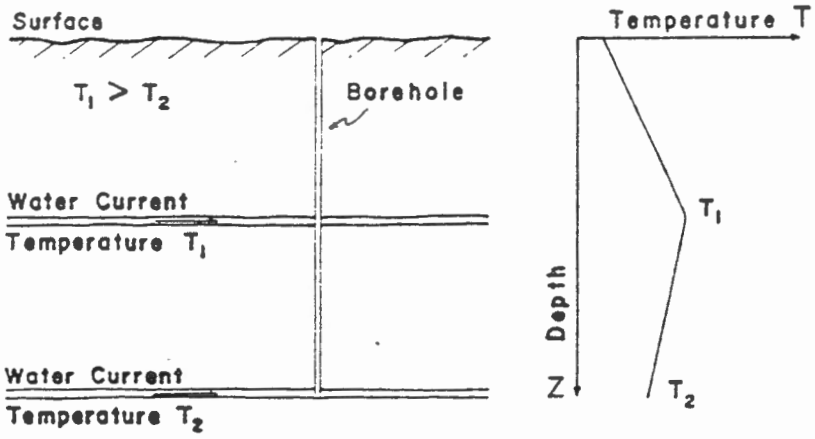

Fig.4. Sketch of model (1), two horizontal sheet-like currents of thermal water with different temperatures.

Model of borehole intersecting two aquifers or fractures carrying flowing water at temperatures T_1 and T_2. Flow assumed to have been occurring for a long enough period for equilibrium to be established. (Fig. 4; Bodvarsson, 1973).

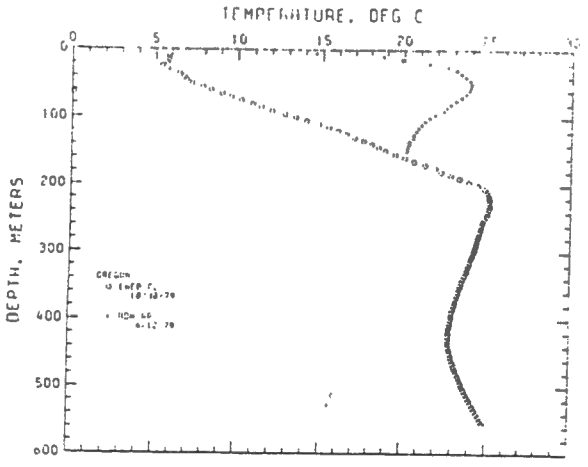

Figure 1a. Horizontal water flow effects on temperature-depth profiles measured in the northern Oregon Cascade Range.

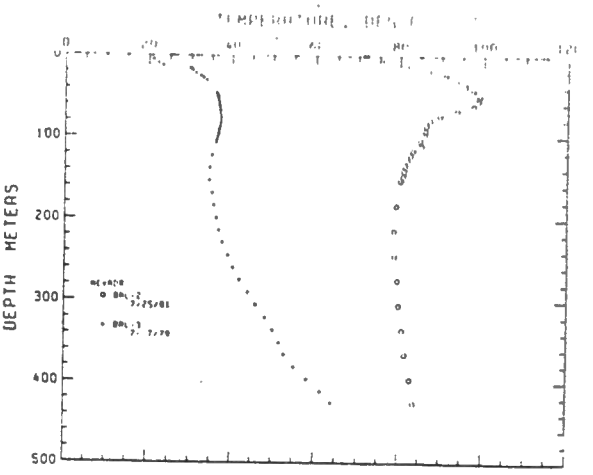

Figure 1b. Horizontal water flow effects on temperature-depth profiles measured in the Baltazar geothermal prospect in(Nevada Earth Power and Production Co).

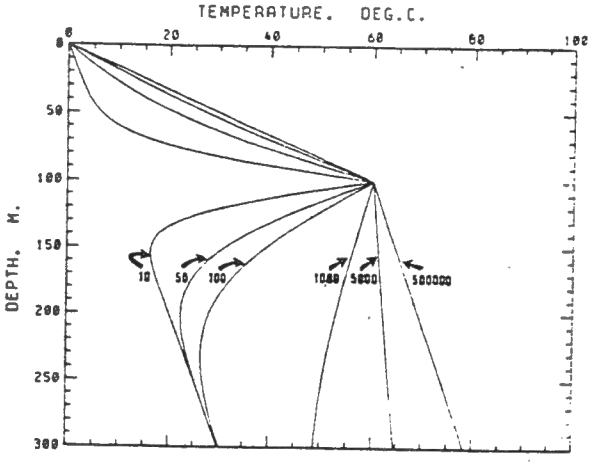

Figure 2. Theoretical temperature-depth profiles calculated at different times (in years) at x = 0; (α = .13).

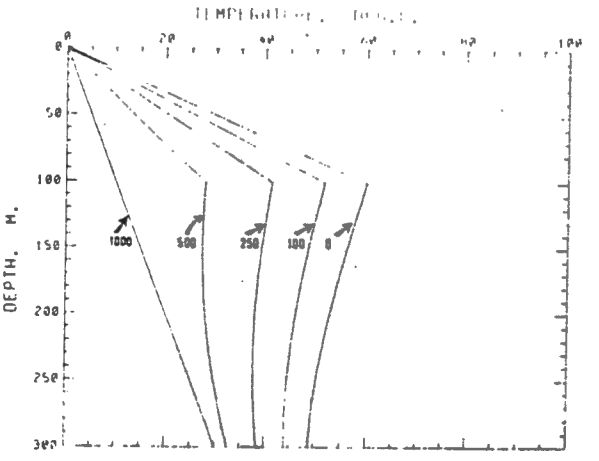

Figure 3. Theoretical temperature-depth profiles calculated at 1000 yrs. for different x-positions shown in meters from the source; (α = .13)

The temperature profile in Fig. 1a, b above has been interpreted in terms of water flow along a thin aquifer where temperatures are (in these cases) above rock temperatures. A simple analytic model by Ziagos and Blackwell (1981) shows the temporal development of such profiles in years after initiation of flow (Fig.2) and at different distances away from recharge point (Fig. 3). The "overturn" of the profile arises because the time constant in the layer above the aquifer is short compared to the time constant in the infinite half-space beneath the aquifer. (Figures from Ziagos and Blackwell, 1981; see also Bodvarsson, 1973).

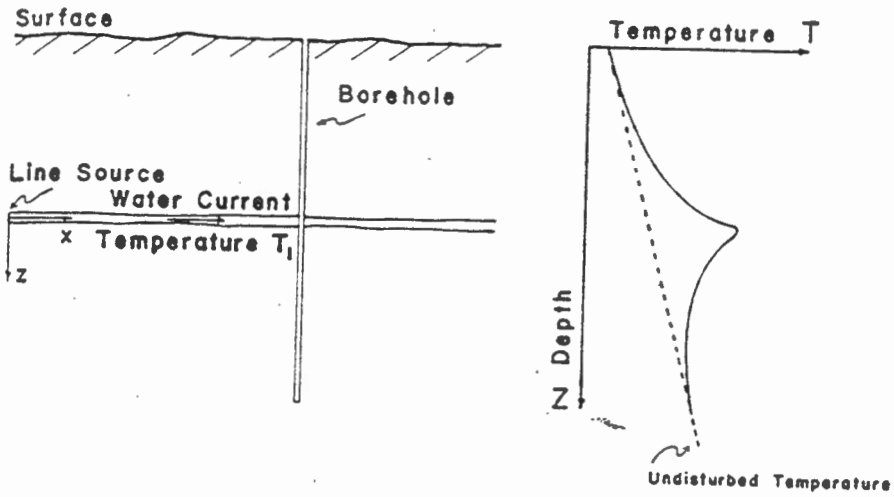

Fig. 6. A simple example of model (3), temperature disequilibrium adjacent to a sheet-like horizontal current of thermal water of recent origin.

Model of flow initiated recently along a single aquifer or fracture intersecting a borehole, such that thermal equilibrium is not established. In figure, aquifer temperature is shown greater than rock temperature at depth. (Fig. 6; Bodvarsson, 1973).

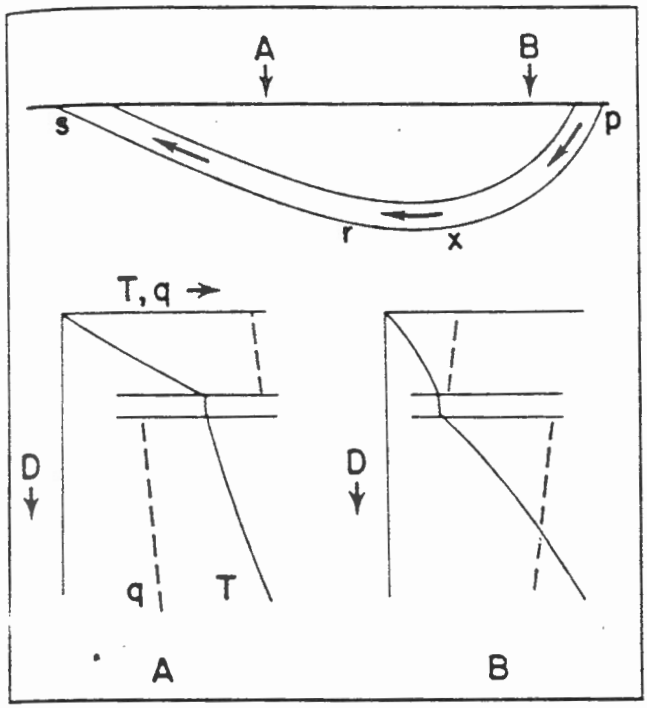

Figure 13—Top.—Possible transient circulation scheme in shallow aquifer. Aquifer carries flow from p to s. Bottom.—Temperature-depth profiles at A and B. Parallel lines indicate depth of aquifer; solid line is temperature; dashed line is heat flow.

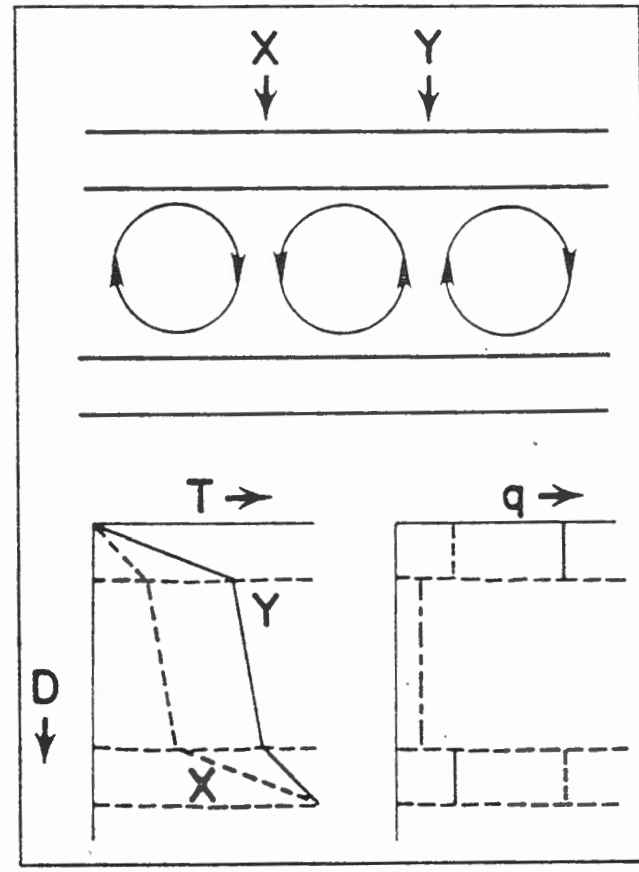

Figure 14—Top.—Possible circulation scheme where permeable zone with cellular convection of pore fluid is bounded above and below by impermeable strata. Bottom.—Temperature-depth profiles for temperature (left) and heat flow (right) show differences at X (dashes) and Y (solid).

Two examples of the effect on subsurface temperatures of water circulation (Fig. 13, 14; Andrews-Speed et al., 1984). In Fig. 13, water initially cooler than the ground descends but goes deep enough to be warmed above the temperature of the ground through which it ascends. In Fig. 14, circulation might be thermally driven and occur through joints and fractures or through natural porosity of the aquifer.

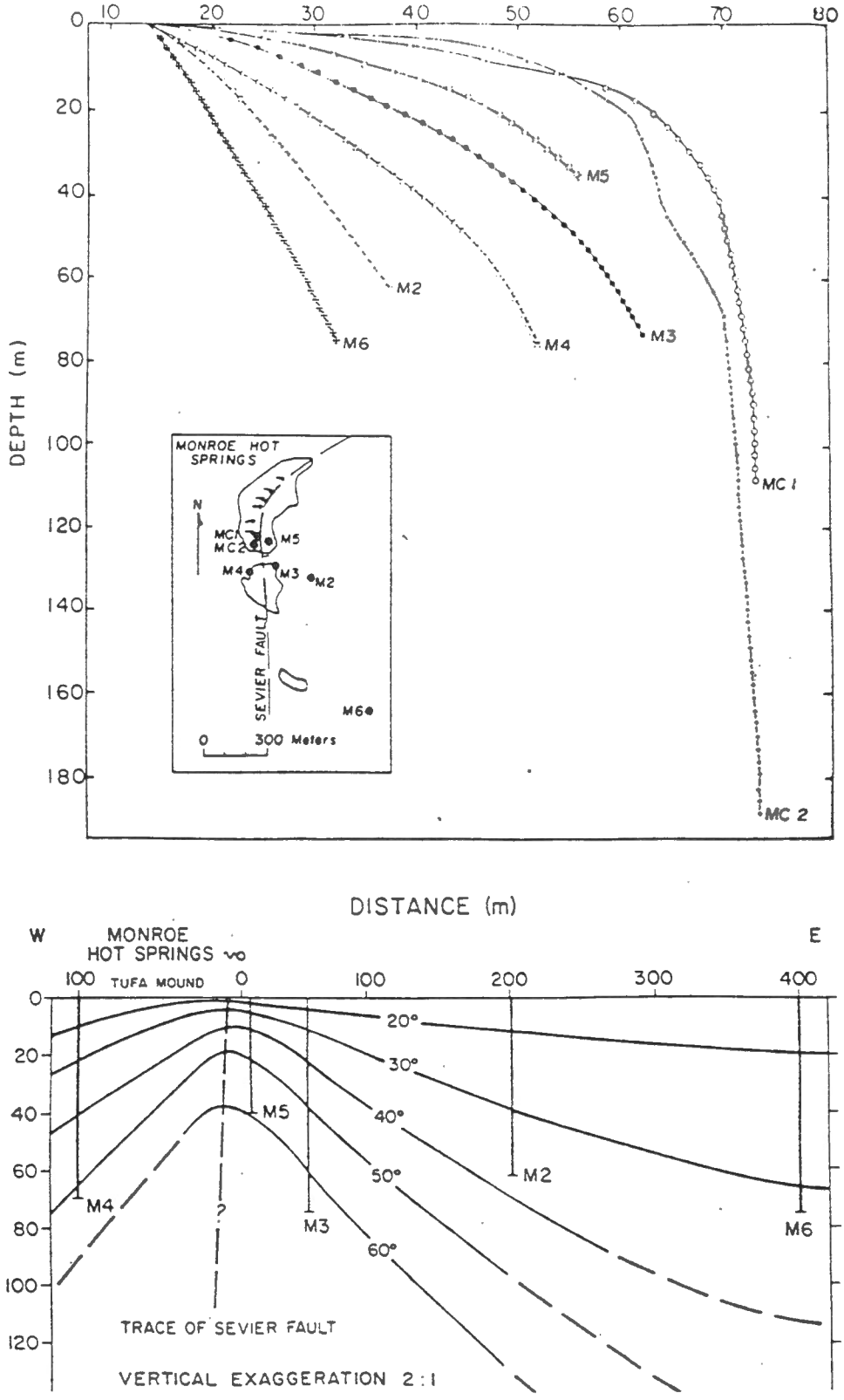

Temperature profiles in the Munroe geothermal resource area reflect the distortion of subsurface around a fault carrying geothermal waters at 69°C. Also shown is the model of the hot spring, based on the temperatures and other evidence. (Fig. 4, 5; Kilty and Chapman, 1980).

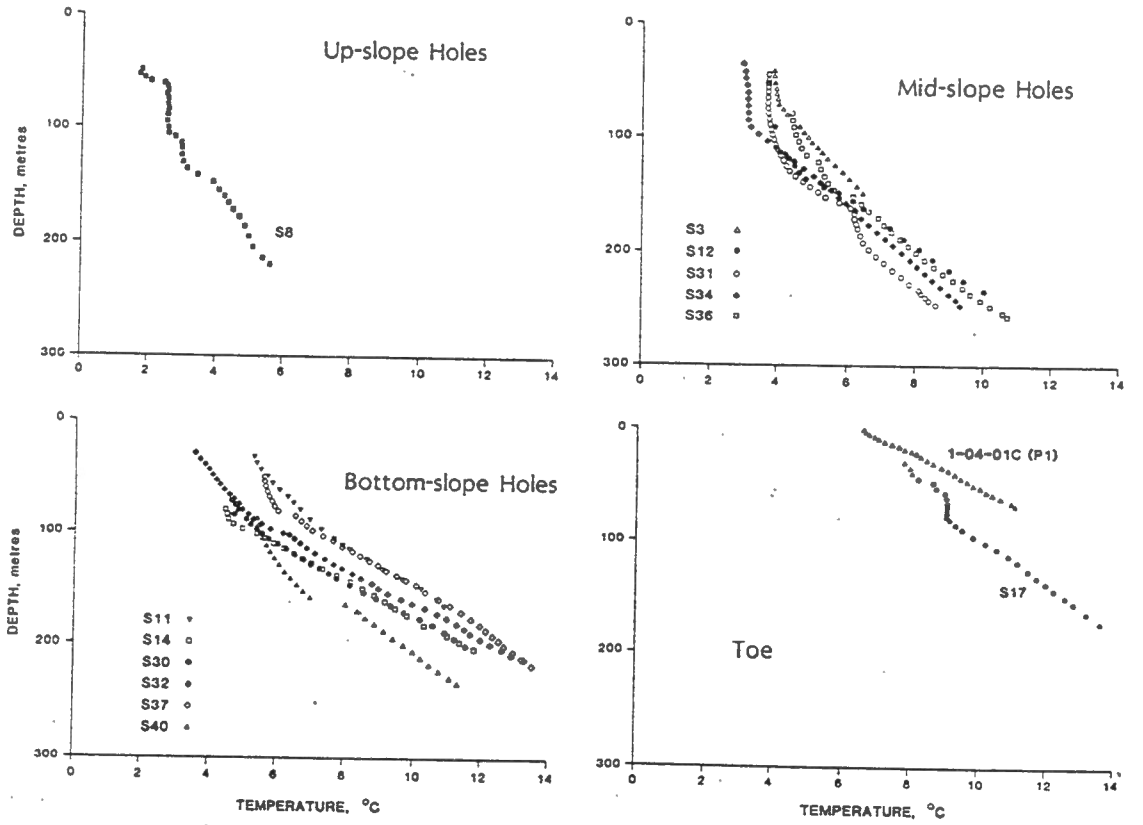

Fig. 12. Thermal profiles at Downie Slide: Upslope boreholes with surface elevations greater than 1200 m (top left); midslope boreholes with surface elevations between 800 and 1200 m (top right); bottom slope boreholes with surface elevations between 600 and 800 m (bottom left); toe boreholes with surface elevations below 600 m (bottom right).

Temperatures measured in PVC, ABS or aluminum cased holes in the Downie Slide, north of Revelstoke, BC. Upper portions of S8 and S17 reflect water flow in annulus around casing. Temperatures and hydraulic head data used in an inversion scheme to predict position of aquifer and hydraulic parameters. (Fig. 12, 8; Woodbury and Smith, 1988).

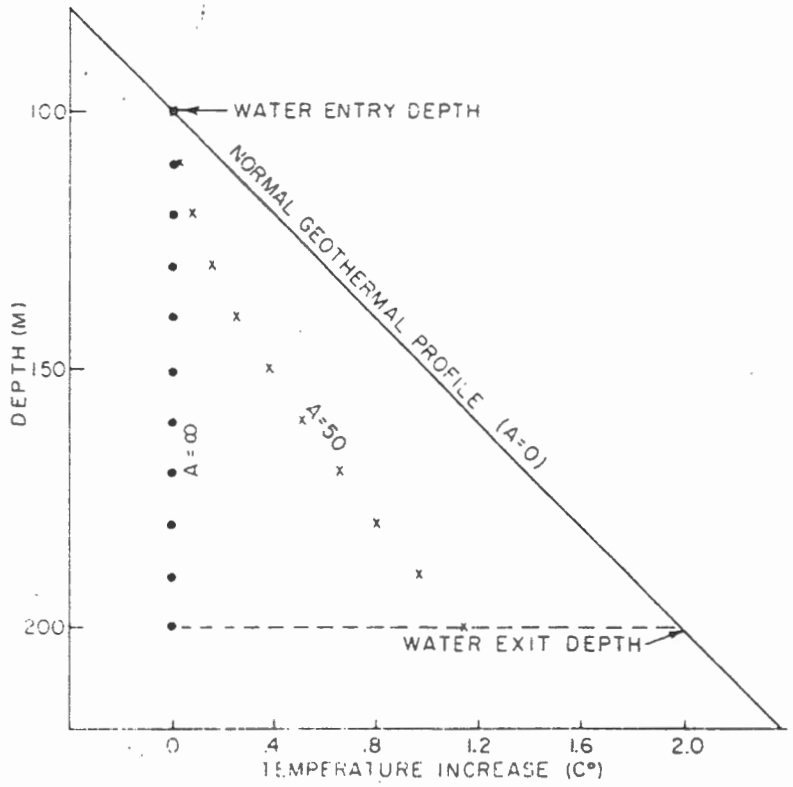

Fig. 6. Temperature versus depth profiles for fluid movement downward within the well bore.

Borehole temperatures also reflect movement of water within the borehole (e.g. entering at one depth, leaving at another in an uncased hole, or leakage at a plug or screen). The temperature disturbance has a different functional dependence from that due to water movement in the formation. Several orders of magnitude greater flows need to occur in the well to produce a similar curvature to that caused by water movement in the formation. In this example, the A=50 curve represents downward wellbore flow at 2×10^6 nm/s (63 km/year). (Fig. 6; Mansure and Reiter, 1979; see also Ramey, 1962).

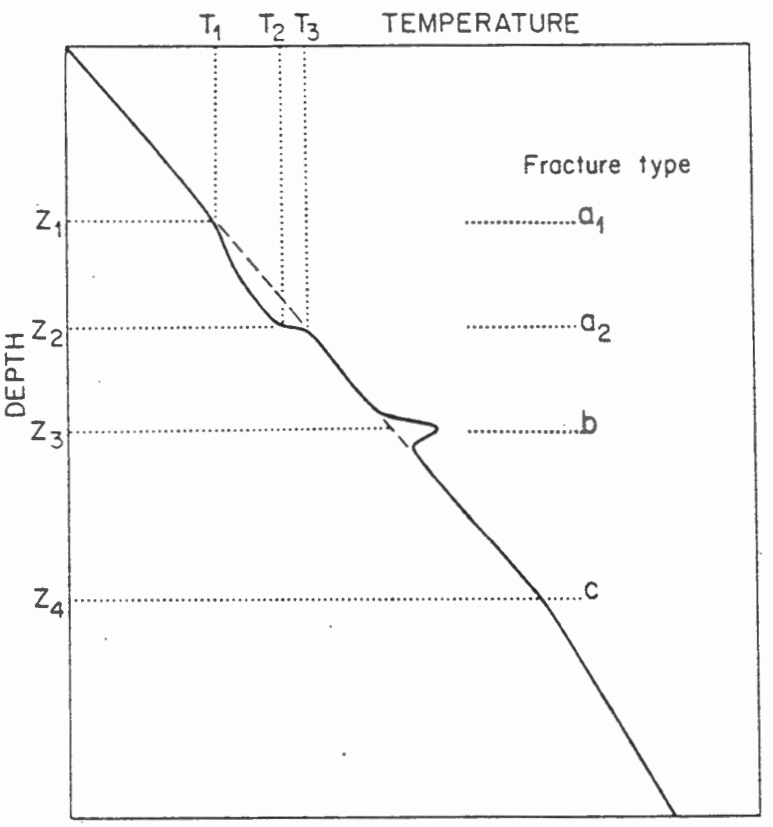

Thermal effects of various types of water flow from fractures as reflected in measurements in an uncased well (open hole).

-Type (a) fracture provide water flow to, or accept water flow from the borehole; in figure, water enters at z_1, flows down the borehole and exits at z_2.

-Type (b) fracture do not permit water flow before of after drilling but accept the storage of drilling fluid during drilling; in figure, warm fluid is trapped in fracture at z_3 and temperature will decay in time.

-Type (c) fracture do not permit water flow to the wellbore; in figure, water at a temperature higher than the rock temperature has been flowing for a long time at depth z_4.

-In all cases, fractures need not be horizontal. (Fig. 2; Drury, 1984).

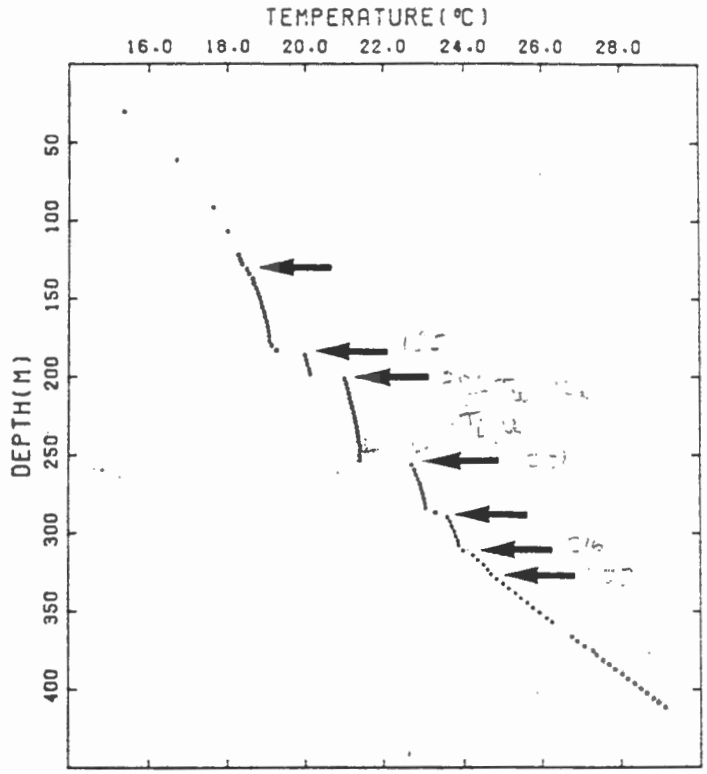

Table 2. Inlet temperatures at each water influx depth in the borehole

Mixing depth (m)	Velocity in (m s^{-1})	Temp. in (°C)	Velocity out (m s^{-1})	Temp. out (°C)	Calc. input temp. (°C)	Rock temp. (°C)
180	0.252	19.917	0.334	19.180	16.915	16.584
200	0.242	21.003	0.252	20.144	- 0.644	17.656
255	0.105	22.702	0.242	21.436	20.466	20.604
287	0.0408	23.527	0.105	23.067	22.775	22.318
311	0.0075	24.072	0.0408	23.889	23.848	23.604

Inlet temperatures at each influx depth calculated successively upwards from the lowest inlet, and calculated according to eq. (5). Temperatures below and above the inlet point are derived from the curves of Table 1. Undisturbed rock temperatures are given for comparison with the calculated water input temperature.

Example of an uncased well in a syenite batholith in southeastern British Columbia. Water is entering the borehole at depths marked by arrows and flowing up the borehole to the surface. At successively shallower depths, water entering the borehole is somewhat cooler than that already flowing up the borehole, producing the offsets measured. Curvature of temperature data between entry points is used to estimate flow rate in borehole (theory of Ramey, 1962); rates increase towards surface, where water velocity is 0.334 m/s (Table). (Fig. 4 and Table 1; Drury et al., 1984).

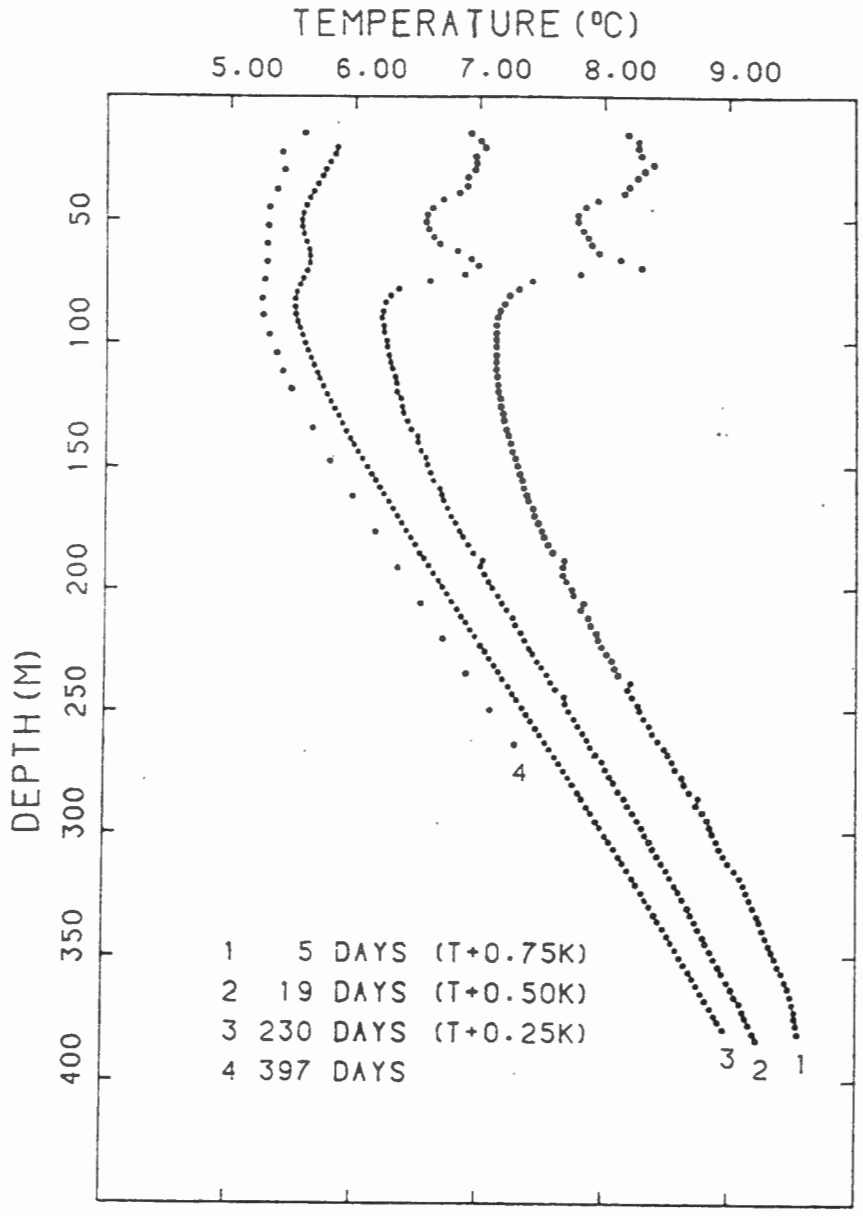

Temperature logs taken at weeks to a year after drilling a Northern Ontario hole in granite show the effect of storage of drilling fluid in a fracture (or permeable zone). Note temperature logs are displaced in temperature for clarity. Thermal spike at 69 m dissipates with time, and has largely disappeared after a year. (Fig. 5; Drury et al., 1984).

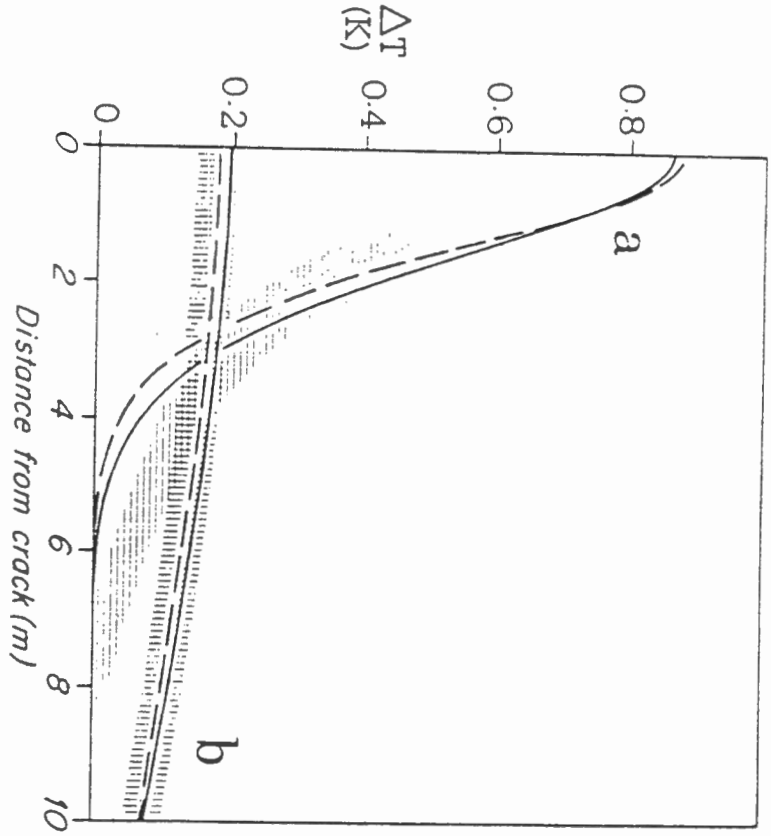

Shaded, spike anomalies resulting from storage of drilling fluid/heat in fracture at 69 m (see previous figure). Anomaly a (5 days after drilling) and b (230 days) are fitted by models that consider the source strength and size of the fractures. (Fig. 6, Drury, Jessop and Lewis, 1984).

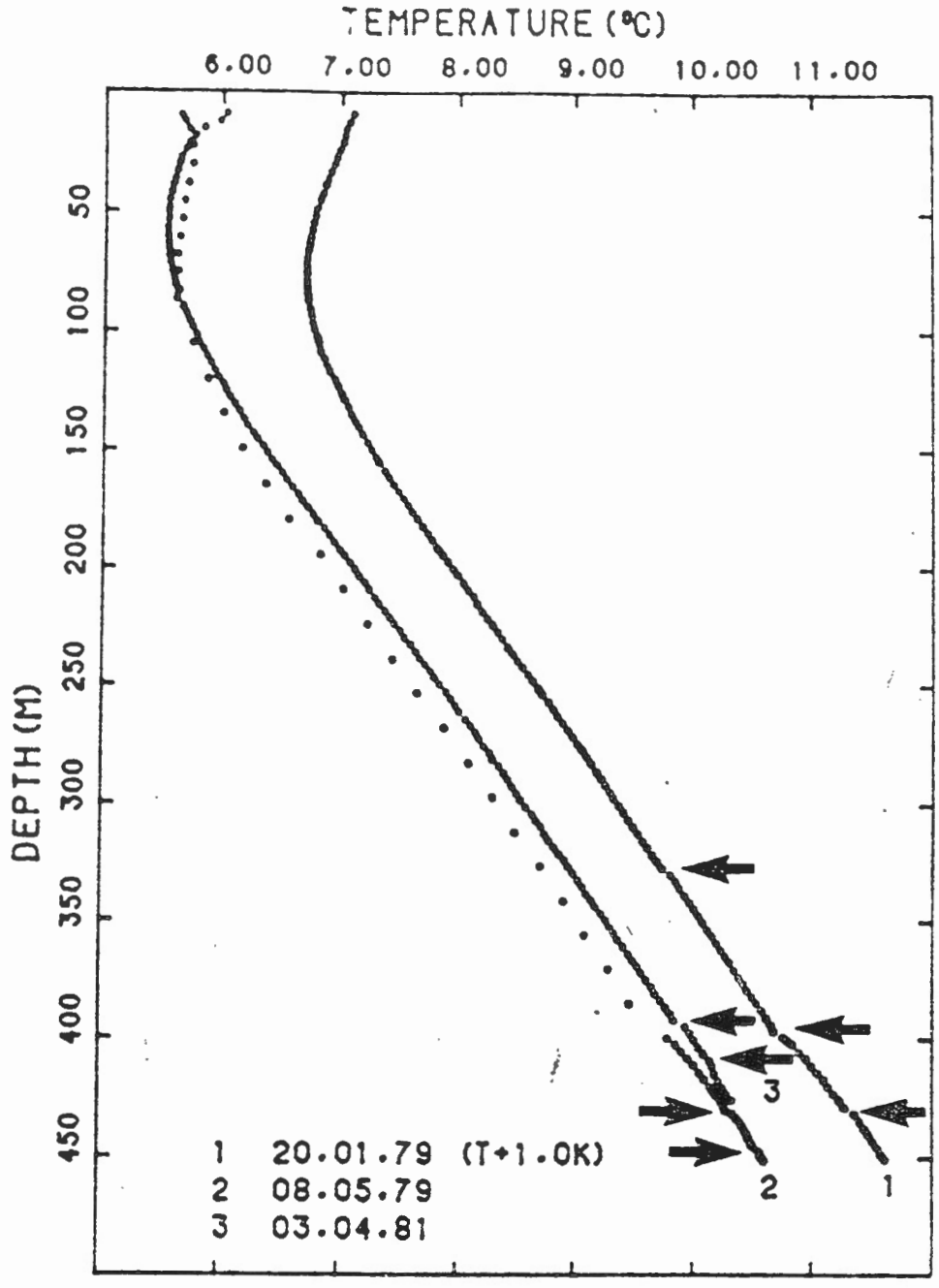

The first log is offset by 1 K along the temperature axis. In logs 1 and 2, water was flowing down the borehole from a perforated surface casing, and exiting at depths indicated by arrows. The casing was repaired and log 3, taken after the repair, shows possible zones of water flowing into the borehole. In comparing the log before (2) and after (3) the repair which eliminated the flow of colder water down the casing, we note that downhole temperatures are higher after the repair. Also, the reversal of temperature gradient in the upper 100 m is due probably to climate change of the past century; water flowing down the hole caused this reversal to appear deeper. (Drury and Lewis, 1983).

(NEW)

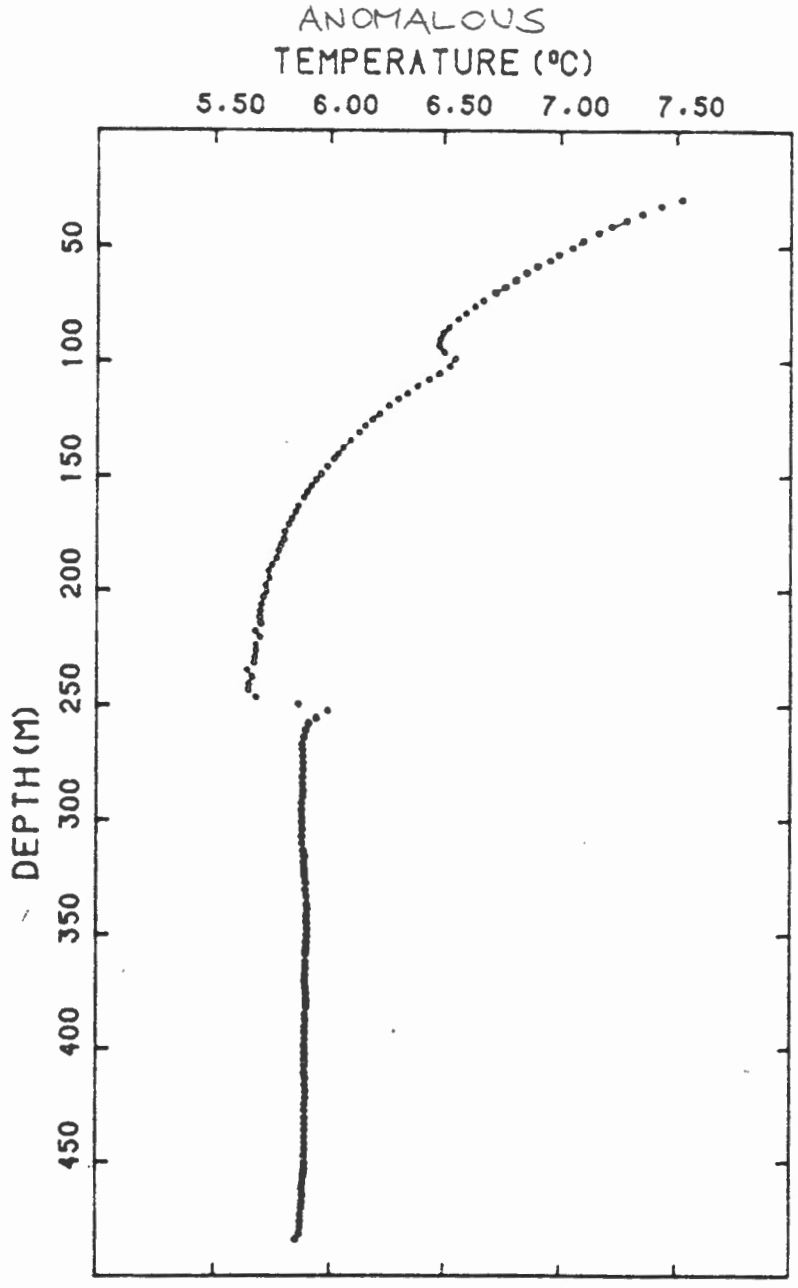

Temperature log in a hole in a granite batholith where two gently dipping fracture zones were encountered, at 100 m and 250 m. In the plot, the regional gradient has been subtracted to emphasize the temperature anomalies. It shows 3 types of temperature disturbances resulting from water flow. There is a "spike" at each depth; in logs shortly after drilling the spikes were larger, indicating the storage of drilling fluid and heat. At 250 m there is an offset in temperature, indicating water is flowing downhole (probably from near the surface) and exiting at that fracture. The change in temperature gradient at 250 m is not associated with a change in lithology, and arises from flow of water down the dip of this fracture. (Fig. 6, Drury, 1984).

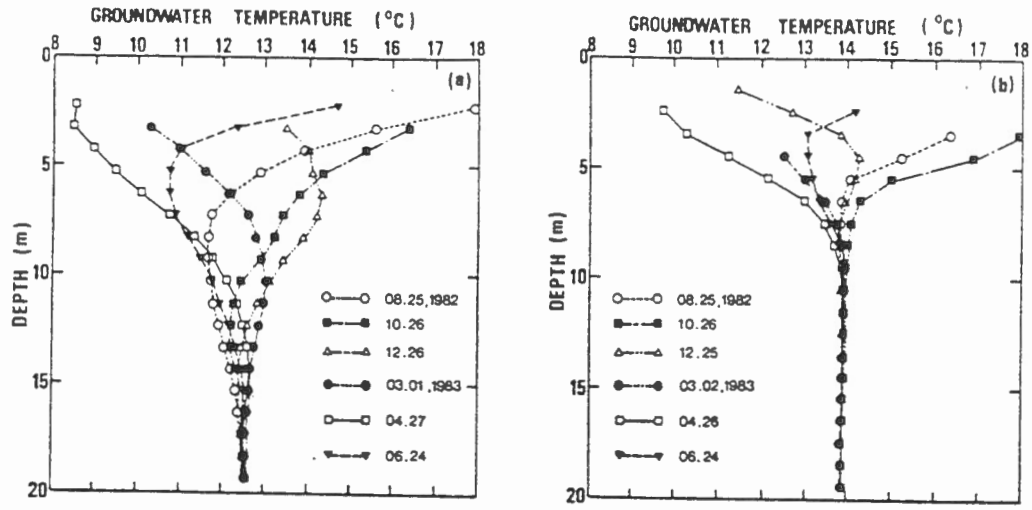

Fig. 3. Temperature-depth profiles at (*a*) well 15 in the recharge area and (*b*) well 18 in the discharge area.

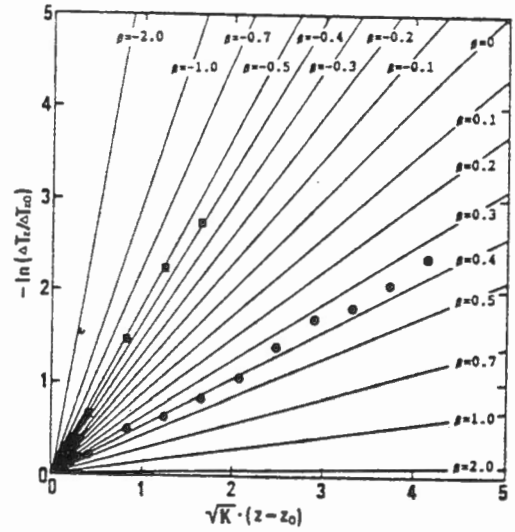

Fig. 7. Nondimensional plots of temperature data at well 15 (circles) and well 18 (squares).

Examples of shallow temperature profiles in the Nagaoka Plain, Japan. Infiltration of surface water throughout the year tends to deepen the depth to which seasonal variations would penetrate the ground with no water flow; surficial discharge reduces the depth of penetration of the seasonal variation. The nomogram is used to calculate the vertical flux of water, which also can be calculated from the amplitude decrement and phase lag of a time series (Stallman, 1965). Rates of 150 nm/s (recharge area; Fig. 3a) and 200 nm/s (discharge area, Fig. 3b) were thus calculated from the above temperature effect. These values are consistent with calculations based on aquifer test data on hydraulic gradients and conductivities. (Fig. 3a, b and Fig. 7, Taniguchi, 1993; see also Kayane et al., 1985 here).

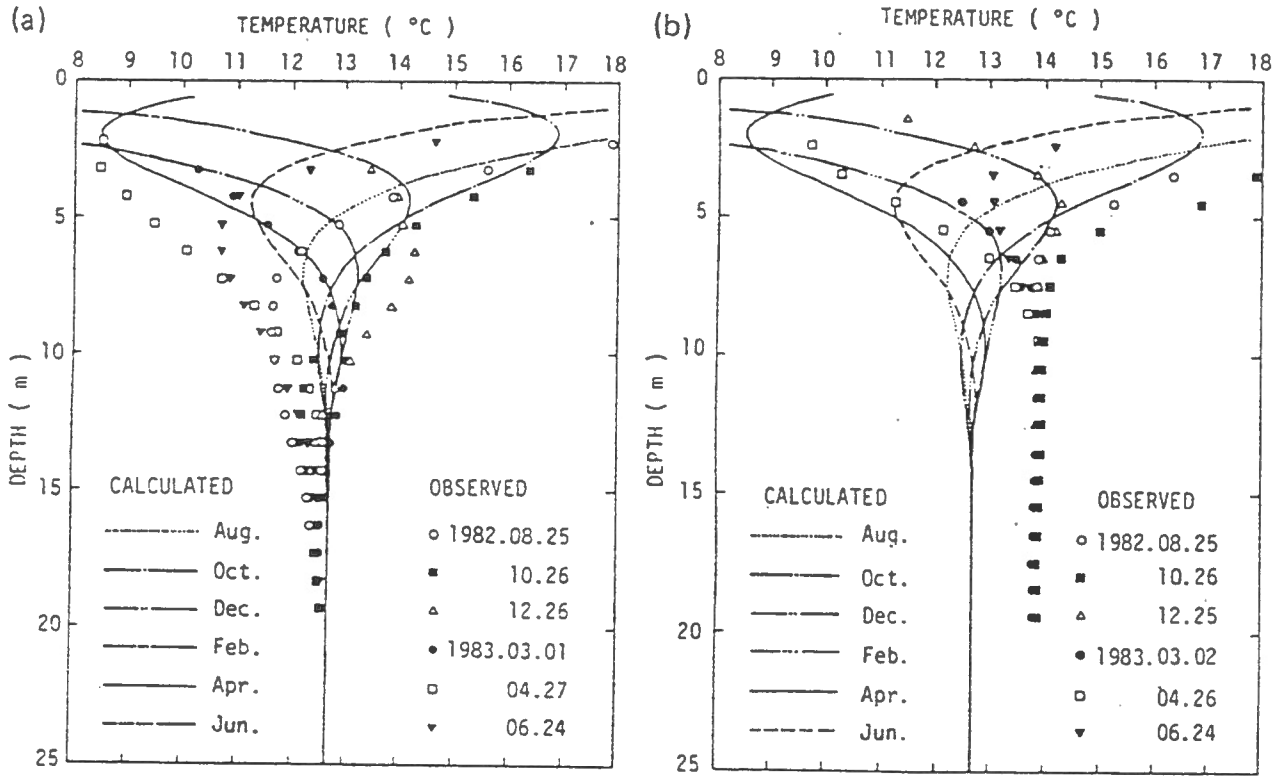

Fig. 7 Observed groundwater temperature depth profiles and calculated ones (based on one-dimensional heat conduction theory) for (a) W15, (b) W18.

Example of the effect on seasonal temperature variations of recharge or discharge at the surface. Solid curves represent possible seasonal variation with no vertical groundwater motion, symbols are measured data in a recharge (or infiltration, left diagram) and discharge (right) area. The temperature envelope of seasonal variation is deeper in recharge and more shallow in discharge, as water carries heat deeper or towards the surface.

(Fig. 7; Kayane et al., 1985). Rate of recharge or discharge may be calculated simply from the decrease of amplitude of the diurnal or seasonal variation with depth and the phase lag (Stallman, 1965).

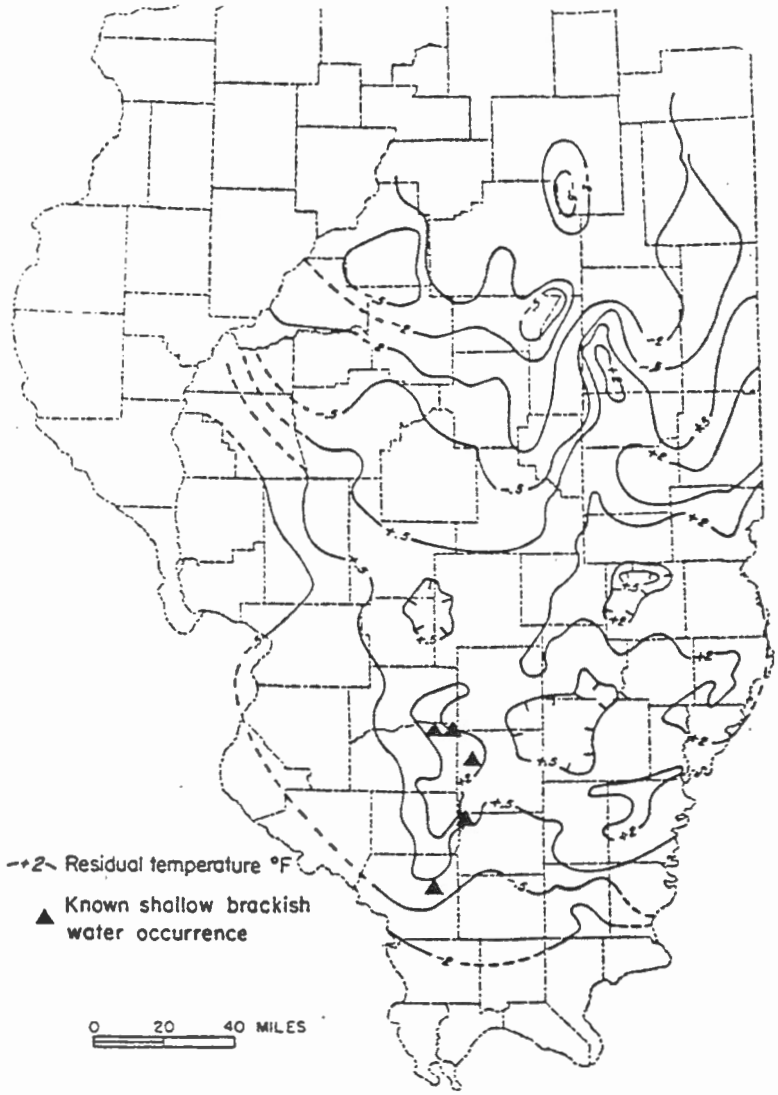

Fig. 4. Residual temperature map (calculated temperature minus observed temperature), showing anomalously warm (positive) and cool (negative) areas.

Subsurface temperature anomalies at 150 m depth in the Illinois Basin reconstruct the gross features of discharge (negative contours, above) and recharge (positive contours). Anomaly map made by subtracting observed well temperatures at 150 m depth from temperature calculated considering thermal properties of the rock and regional terrestrial heat flux. (Fig. 4; Cartwright, 1970).

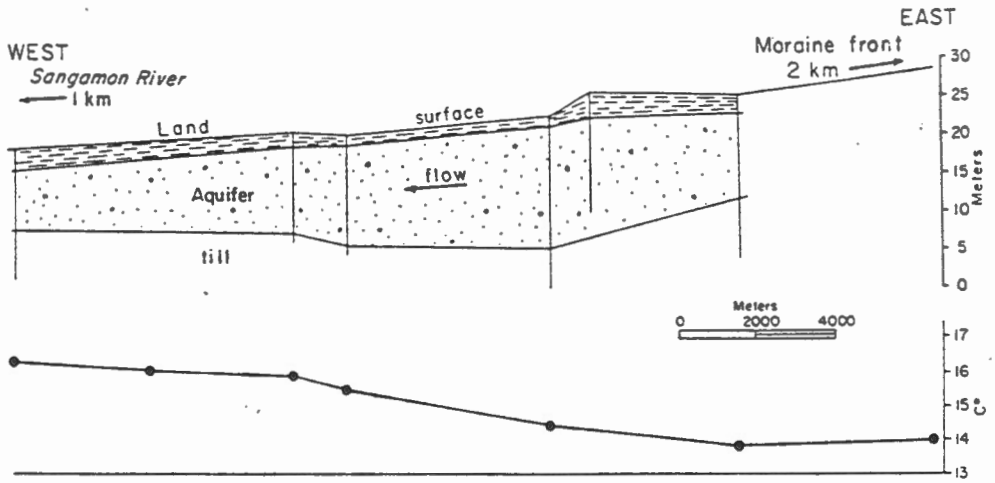

Figure 2. Longitudinal temperature profile and geologic cross section along the middle of the aquifer near Niantic, Illinois.

Temperatures measured at a depth of 0.5 m from surface in soil overlying a shallow aquifer in Illinois increased 2.4 K over 7 km.

A quantitative analysis shows that water flow in an aquifer absorbs some geothermal heat from below and carries it "downstream"; hence the water temperature increases in the downstream direction. (Fig. 2; Cartwright, 1971).

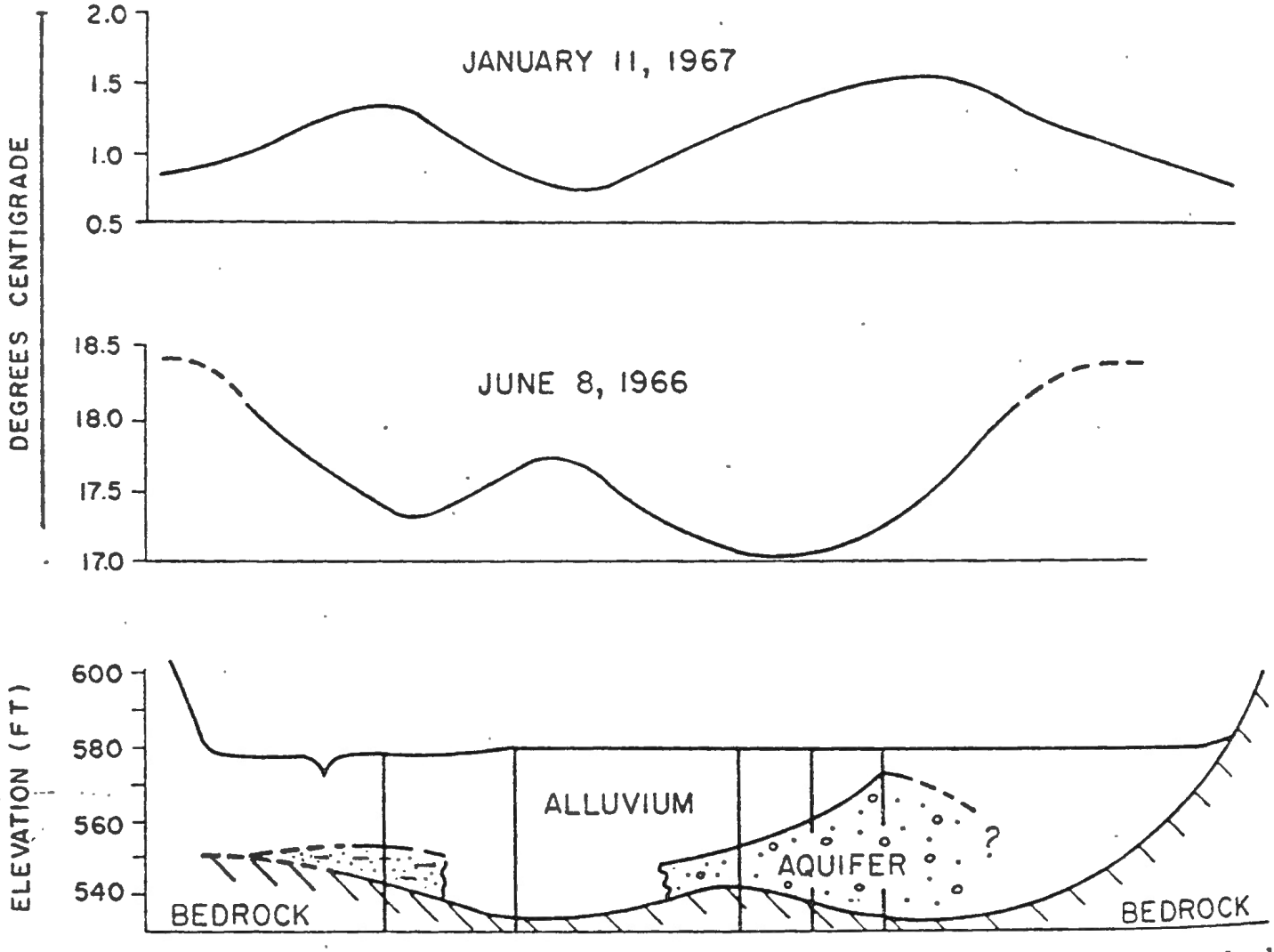

Fig. 5. Geologic cross section and thermal profile across Hurricane Creek Valley, Cumberland

Shallow, linear unconsolidated aquifers (<10 to 20 m) have been detected from anomalies in the shallow thermal regime obtained from temperature probing. Cartwright identified probing as an inexpensive tool especially during summer and winter months. (Fig. 5; Cartwright, 1968).

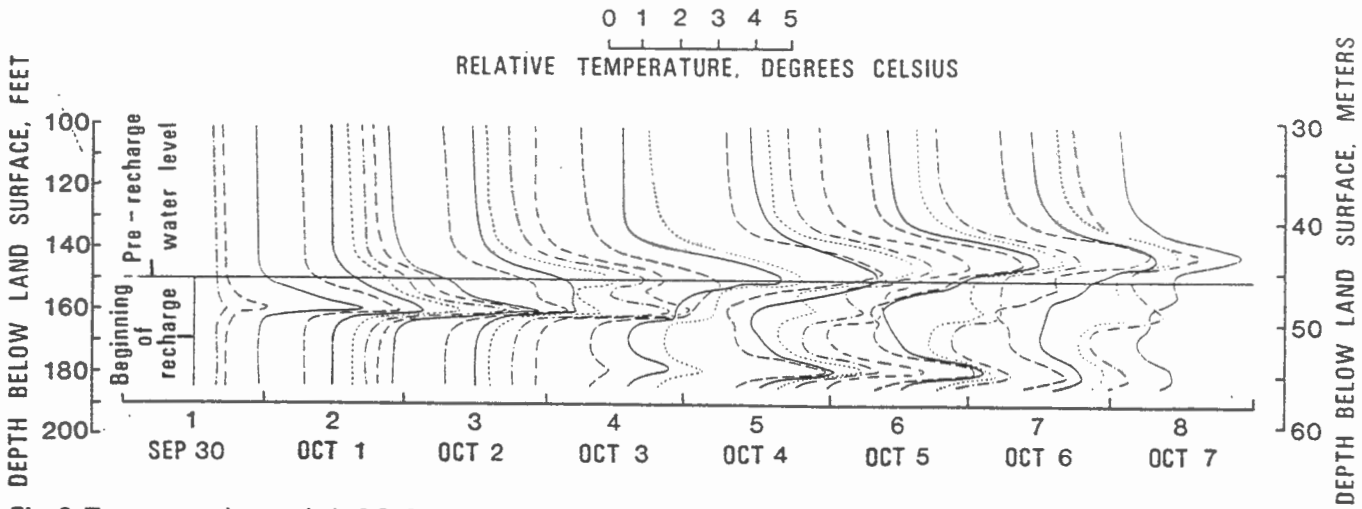

Fig. 2. Temperature logs on hole S-3, Stewart site. Relative temperature scale is the same for each log but displaced to show time. Bottom hole temperature approximately 15° C on each log.

In injection wells, tracing with temperature logs is useful in locating zones of high permeability and in detecting changes in flow as a function of time. In this example, water from a Texan playa lake at temperatures different from the aquifer was injected into wells that were perforated through part of the aquifer. Fig. 2 shows that water at 49 m depth reaches S-3, 12 m from the injection well, after 4 hours. The subsequent upward expansion of the thermal wave indicates the continuing injection and the rise of the "warm water table" by 6 m. Note that the thermal pulse took 3 days to reach S-3 at the 55 m level. Such transit times were used with head data to calculate hydraulic conductivities. (Fig. 2; Keys and Brown, 1978).

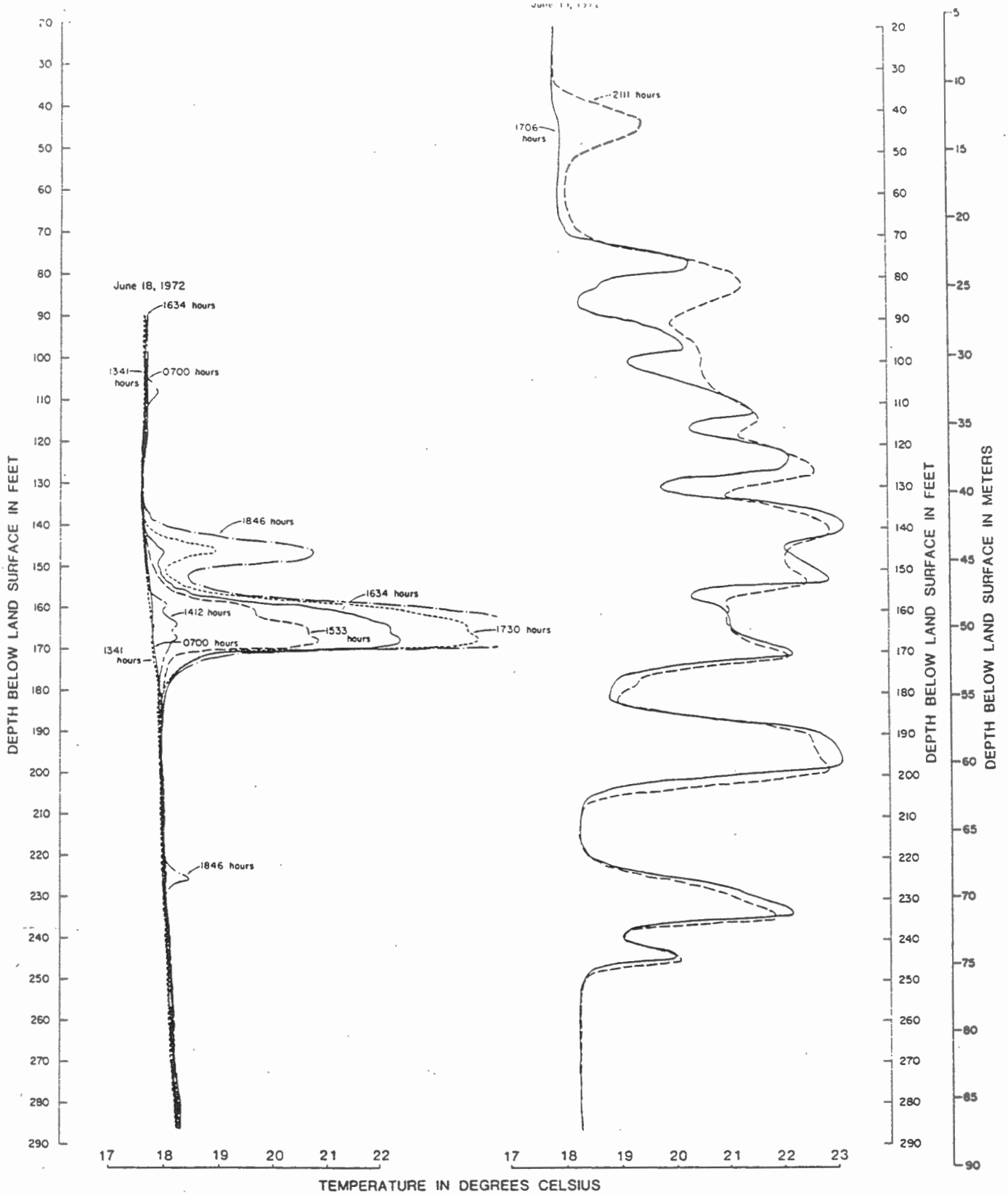

Water at a temperature different from the aquifer was pumped for 30 hours into an injection well ear Lubbock, Texas to determine zones of greater permeabilities. More permeable zones accepted a greater volume of water, leaving a thermal signature that was apparent later on temperature logs. The latter show that zones at 13 m and 24 m had to be saturated first. (Fig. 6; Keys and Brown, 1978).